Doctoral Dissertation

Synthesis of Cross-linked Multilayer Thin Films using Molecular Layer Deposition (MLD) Technique

MD. ABU RASHED

Supervisor: Assoc.Prof. Yuki Nagao

School of Materials Science

Japan Advanced Institute of Science and Technology

September, 2016

Table of Contents

PAGE

Chapter 3

Investigation of Surface Effect on Cross-linked Organic Multilayer Thin Film

LIST OF FIGURES

Figure Page

LIST OF TABLES

Table Page

LIST OF SCHEME

Scheme Page

LIST OF ABBREVIATIONS

PDI	1,3-Phenylene diisocyanate
TAPM	tetrakis(4-aminophenyl)methane
LbL	Layer-by-Layer
mLbL	Molecular Layer-by-Layer
SAMs	Self-assembled Monolayers
LB	Langmuir–Blodgett
ALD	Atomic Layer Deposition
MLD	Molecular Layer Deposition
APTMS	3-Aminopropyltrimethoxysilane
XPS	X-ray Photoelectron Spectroscopy
AFM	Atomic Force Microscopy
XRR	X-ray reflectivity
GI-SAXS	Grazing Incidence Small Angle X-ray Scattering
FTIR	Fourier Transform Infrared Spectroscopy
COFs	Covalent Organic Frameworks
POPs	Porous Organic Polymers
PPNs	Porous Polymer Networks
HCPs	Hyper-cross Linked Polymers
PIMs	Polymers of Intrinsic Microporosity
BOE	Buffered Oxide Etch

ABSTRACT

The research of cross-linked organic thin films garnered much attention for its many conventional applications like organic thin film transistors, purification membranes and so on. However, the synthesis of thin films with nanometer scale is very challenging. One of the simple and versatile techniques to prepare nanometer scale cross-linked multilayer thin films is solution based molecular layer deposition (MLD). However, to fabricate organic thin films with MLD technique need to deal with several parameters: solid surface properties, self-assembled monolayer, monomers symmetrical combination, as well as optimized reaction condition. Any of the above mentioned parameters can make significance influences of films physical and chemical properties. In this research, I focused a unique monomers combination on fabricating thin films with 3D molecular networks.

In this thesis, synthesis of urea (bonded) cross-linked multilayer thin film was demonstrated by sequential deposition of bifunctional 1,3-phenylene diisocyanate (PDI) and tetrafunctional tetrakis(4-aminophenyl)methane (TAPM) molecular building blocks over Si/SiO_2 surface. Multilayer growth as a function of deposition cycles was inspected using UV-vis absorption spectroscopy. From infrared spectroscopy results, three characteristic infrared bands confirmed the formation of polyurea networks. X-ray photoelectron studies also unveiled the formation of polyurea networks. From X-ray reflectivity (XRR) density investigation, constant mass density was not observed with a number of deposition cycles. This difference in packing density might derive from the different degrees of cross-linking among layers proximate to the substrate surface and extending away from the substrate surface. Moreover, grazing incidence small-angle X-ray scattering (GI−SAXS) studies demonstrated the improvement of structural ordering with deposition cycles or film thickness.

However, by changing Si substrate surface characteristic by chemical etching and followed by oxygen plasma activation, a significant variation was observed in polyurea films mass density property, even though films show non-linear mass density behavior. This may happen due to the formation of the dense packed amine-terminate self-assembled monolayer (SAM), which is formed prior to the layer deposition. This dense packed self-assembled monolayer, reduced the initial or buffer layers packing density by forming a significant number of double reactions between surface attached amine groups and initial deposited 1,3-phenylene diisocyanate (PDI) monomer. However, film mass density is successively increased with layers deposition. This phenomenon resulted due to the presence of multi-functional TAPM monomer, which can laterally extend the molecular networks using multiple reactive sites. This result suggests not only the degree of cross-linking but also particular monomer combination is responsible for getting variable density property in multilayer thin films.

Keywords: Polyurea, Covalent linkage, Self-assembled monolayer, Layer-by-Layer, Mass density

General Introduction

1.1 THIN FILMS: WHY?

With the development of civilization, the research of thin films is continuously progressing being used for the creation and development of radical devices or technologies to meet the challenge a wide range of applications in physics, chemistry, biology and medical science. Thin films deposited was carried out on different substrate materials including conducting metals, semiconductors, glass and porous polymers based on the demand of particular application. Furthermore, the chemical and physical properties of the thin film can be enriched and tailored by specific optimization of film growth technology and deposition material as well as the substrate materials. The physiochemical properties of a thin film which are based on surface/interface interactions among substrate or base material and the deposition materials show enhanced functionalities and properties compare to the corresponding bulk materials. This surface/interface interaction able to tailored the surface properties such as energy, polarity, charge, as well as roughness, morphology, topology etc. These tailored properties or functionalities have been acknowledged to determine a significant impact in a wide range of research fields such as biomaterials, energy, electronic, optics,

and biological and chemical sensors.[1-4]

Thin films have a significant advantage over bulk materials. The processability for devices application is regarding the main barrier for bulk materials. In addition, thin films offered enhancement of device performances over bulk materials for its structural diversity and orientation.[5-6]

1.2 RESEARCH TO DESIGN FUNCTIONAL THIN FILMS

During the past few decades, there has been enormous interest to fabricate solid support functional thin films with tunable chemical compositions and enhanced structural properties. The specific control of the properties of the substrate surface and deposited materials (e.g. organic and/or inorganic), demonstrated a dynamic role in the creation of nanostructured and nanocomposite functional assembly for biological, chemical, engineering and biotechnology applications. There are plenty of researches have been done to design functional thin films including techniques, Langmuir-Blodgett (LB),[7-10] polymer grafting,[11-12] chemical vapor depsoition[13-15] and others.[16-17] However, all these processes more or less biased with limitations, in term of expensive and specialized instrumentations. Moreover, the concern regarding the variation of deposited materials on the substrate surface as well as the stability and robustness of the fabricated nanostructured materials under open atmospheric conditions. Therefore, significant

efforts have been done to investigating a modest, inexpensive and flexible technique for fabricating thin films with numerous functionalities on practically any kind of the substrate surface as well as usage in unprecedented number and variation of deposition materials.

In this concern, a promising method has been developed by the alternating deposition of interacting species, namely, layer-by-layer (LbL) technique, which is an easy, reproducible, efficient, cost effective and versatile technique to fabricate functional multilayer thin films and nanocomposites.[4,18] LbL assembly formed by electrostatic[19-24] or nonelectrostatic interactions, i.e., hydrophobic interaction,[25-26] hydrogen bonding,[27-28] covalent and coordination interaction,[29-33] and others interaction.[34-36] In addition, multilayer thin films using LbL assembly technique can be performed on a variety of substrates materials of various shapes and sizes, for example, planar, colloidal, porous, cylindrical structures etc. Moreover, this LbL technique permits the incorporation of a wide range of materials such as polymers, carbon nanotubes, peptides, metal oxide, clays, dyes, as well as biological components including proteins, nucleic acids, enzymes and viruses into the multilayer assemblies to introduce new functionalities and proficiencies.[4,18] Figure 1.1 shows the conceptual

drawing of conventional layer-by-layer dipping cycles for polyelectrolyte thin film synthesis.

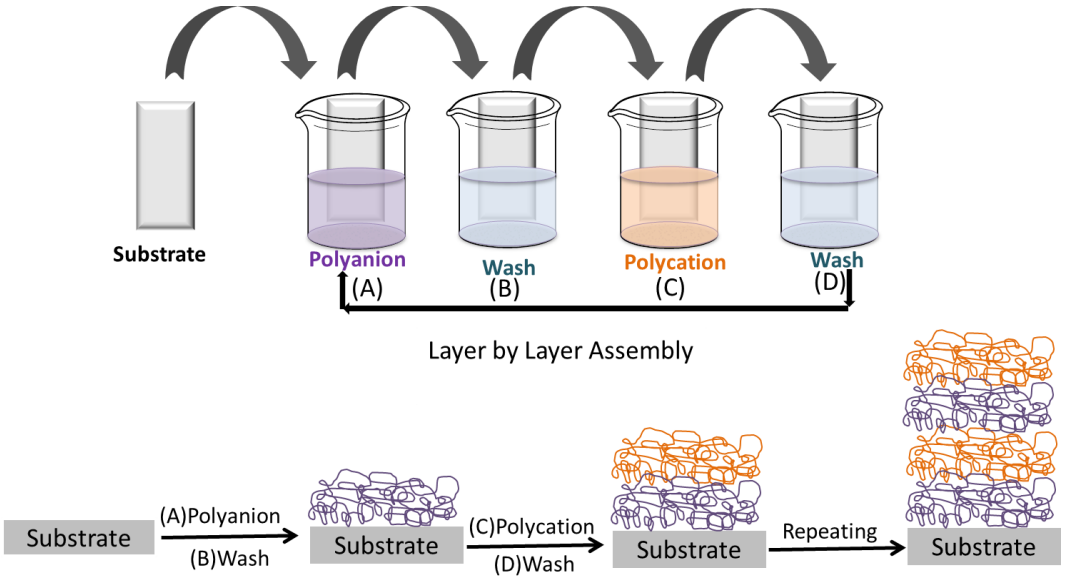

Figure 1.1. Conceptual drawing of polyelectrolyte multilayer thin film in layer-by-layer technique.

Even though those above discussed LbL processes showed better efficiencies to fabricate functional multilayer thin films. To achieve the well-controlled films composition, conformation, structure, smooth film morphology as well as precisely controlled of films thickness at atomic or molecular scale, relatively new developed multilayer growth techniques; vapor based LbL growth methods known as atomic layer deposition (ALD)[37-42] and molecular layer deposition (MLD)[43-48] have garnered much attention. Both ALD and MLD offers an efficient route to assemble multilayer thin films

have emerged for accurate control of film thickness at angstrom to nanoscale level, provide multilayer film with densely packed and well-ordered internal structure.[4,18] In atomic layer deposition, atoms are deposited one atomic layer at a time to grow a conformal film. In general ALD process has been used to the formation of inorganic thin films.[49] An analogy of the ALD, molecular layer deposition (MLD) provides high-quality organic multilayer thin films with self-limiting and surface terminating growth onto the substrate. In where a single layer of organic precursors deposited onto the substrate surface at a time.[50] MLD provides as powerful organic nanoscale thin film deposition technique and this technique establish a link between nanotechnology and polymer coating. In MLD process, an organic precursor interacts with another organic precursor which has previously deposited onto the substrate surface. This interaction is carried out via the reaction between functionalities of organic precursors based on the corresponding polymerization chemistry. After depositing the organic molecular layer on the surface, leave new surface functionality for deposition of an upcoming precursor. Due to the stepwise polymerization reaction, it is anticipated that the arrangement and orientation of the organic precursors tend to have less random distribution than interfacial polymerization or bulk polymeric materials. Moreover, as for surface terminating growth mechanism, desired chemical and physical properties can be

achieved by incorporation of new functionality into MLD films with tailoring the backbone of deposited organic precursors. The composition and positions of chemical functionalities can be eagerly tuned by appropriate selection of monomers and number of deposition cycles.[51] Schematic illustrations of ALD and MLD are shown in Figure 1.2 and Figure 1.3, respectively.

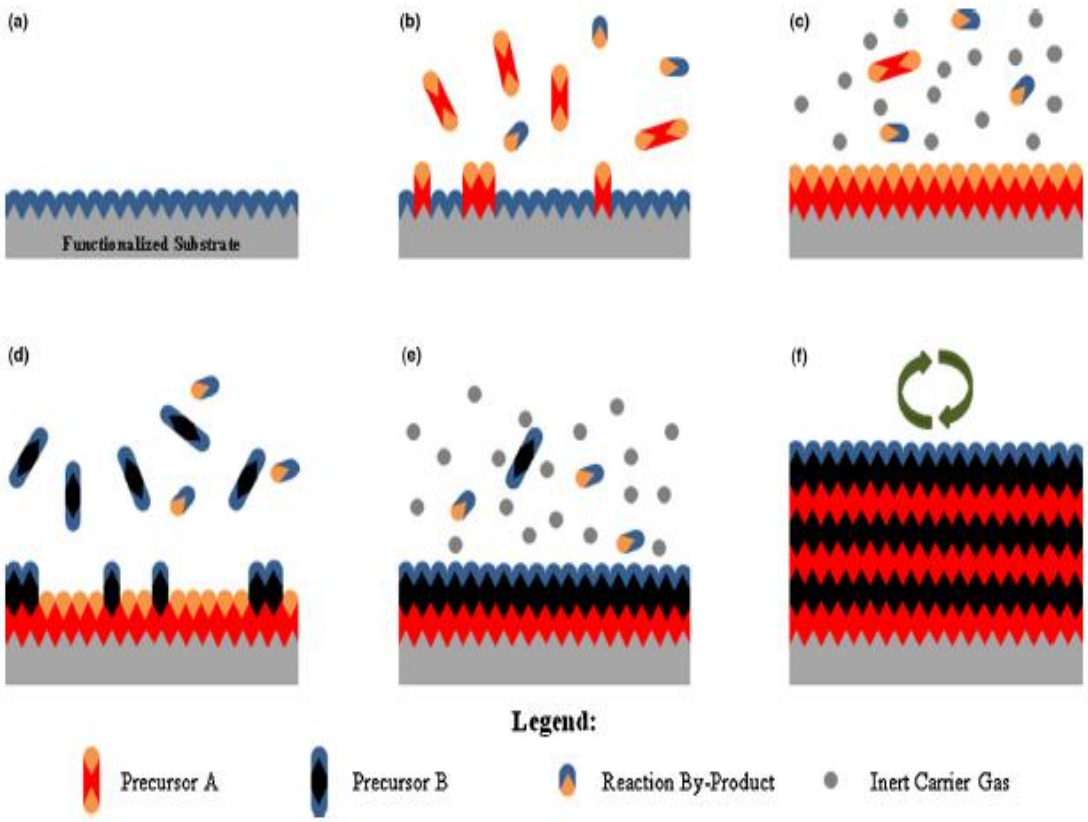

Figure 1.2. Schematic of ALD process (a) Substrate surface has natural functionalization or is treated to functionalize the surface. (b) Precursor A is pulsed and reacts with surface. (c) Excess precursor and reaction by-products are purged with inert

carrier gas. (d) Precursor B is pulsed and reacts with surface. (e) Excess precursor and reaction by-products are purged with inert carrier gas. (f) Steps 2–5 are repeated until the desired material thickness is achieved (Adapted from ref. 39).

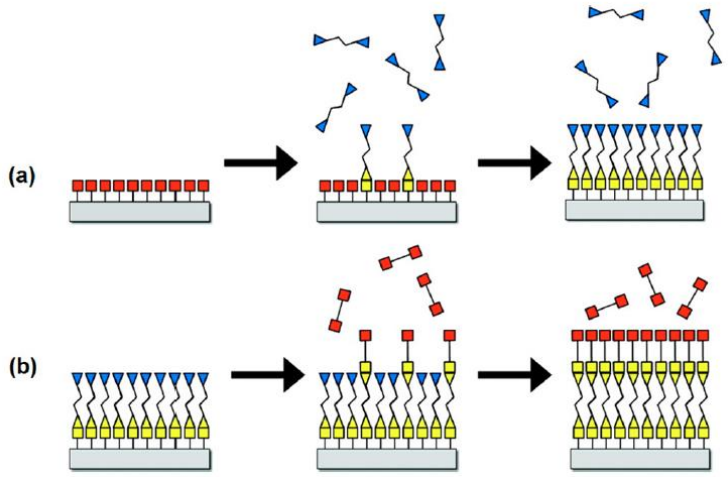

Figure 1.3. A cartoon illustrating the vacuum based MLD process using bifunctional precursor's combination (Adapted from ref. 44).

1.3 ORGANIC THIN FILMS WITH MOLECULAR NETWORKS

Molecular-scale organic network materials[52] have become an interesting research topic for applications such as molecular storage / separation, delivery, catalyst or catalyst support.[53-56] Polymerization reaction of rigid organic monomers with multiple functional groups yields organic molecular networks via the strong covalent interaction. In this aspect, covalent organic frameworks (COFs), which have demonstrated crystallinity and permanent porosity,[57-61] would be a most suitable

candidate to fabricate organic thin film with molecular networks. However, COFs are generally formed in harsh reaction conditions with thermodynamic control of the reversible condensation reaction.[60] In addition, several amorphous organic networks such as porous organic polymers (POPs),[62] porous polymer networks (PPNs),[63] hyper-cross linked polymers (HCPs),[64] polymers of intrinsic microporosity (PIMs)[65] are well-known. Even though those materials have unique structural properties either crystalline or amorphous, because of their inherent insoluble and indefeasible behavior these networks materials used mainly as gas or liquid adsorbents in their powdery form. Moreover, due to the complex or thermal assist synthesis route, direct synthesis of these polymeric networks on solid surface is still a great challenge. Therefore, most researches of above mentioned polymers confined only in bulk state.

In contrast, molecular layer deposition provides a systematic route to synthesize molecular networks based organic thin films within nanometer-scale thickness. This thin film with organic molecular networks synthesis was carried out via the cross-linking polymerization reaction using layer-by-layer sequential assembly of multifunctional organic molecular building blocks.[66] MLD thin films with molecular networks would provide higher thermal and chemical stability due to the cross-linked polymeric networks. This cross-linked phenomenon has been appeared without any

post-treatment approach such as thermal treatment, expose to UV radiation or using reactive cross-linking agents.

Though MLD technique was introduced earlier in 1990s, the MLD method reported to date has been limited to the surface grafting chain polymerization reaction using bi-functional monomers combination under vacuum deposition techniques. However, synthesis of molecular networks with aromatic compounds contains multifunctional groups, having high molar mass and boiling point. Therefore, for these monomers it is incredible to apply vacuum based MLD techniques. The major difficulty is removing physio-absorb monomers after each cycle of vapor deposition using inert carrier gas.

The solution based MLD may offer an effective route to overcome some of these problems.[66-67] This approach consists of a series of dipping steps in solution contained multifunctional reactant species in mild reaction condition and excess absorb monomers can be removed easily by rinsing in organic solvents. This solution based approach can offer molecular networks instead of surface-grafted polymeric chain. The practical advantage of covalently bonded thin films with multifunction monomers is they provide multilayer film with remaining reactive groups, as buried inside or residing at the surface. These unreacted functionalities can be used as a platform for further

functionalize of the films. Figure 1.4 shows the organic molecular networks using bifunctional and tetrafunctional precursors on solid surface.

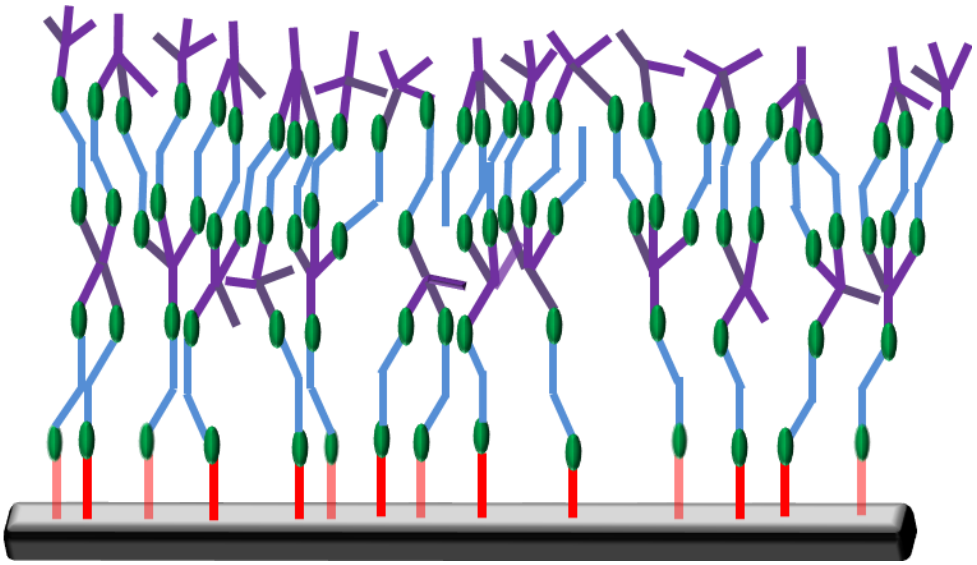

Figure 1.4. Schematic illustration of cross-linked organic molecular networks on solid surface using molecular layer deposition technique.

1.4 SELF-ASSEMBLED MONOLAYER

A self-assembled monolayer (SAMs) on solid surface was needed prior to multilayer film growth using MLD technique. SAMs are ordered molecular assemblies formed by the adsorption of active precursor molecules on a solid surface which have been commonly used to achieve the surface modification.[68]SAMs played a significant role to fabricate multilayer thin film with organic molecular networks on surface normal direction. In general thiol derivatives and organosilicon derivatives (silane coupling

agent) were used for self-assembly monolayer formation. SAMs formation using alkanethiol on gold surface was focused great attention in 1990s.[32] However, latterly it has become exposure that this alkanothiol/gold system suffered serval limitations; such as lack of driving force of monolayer formation, leading to labile structure, the thiol head groups are sensitive to oxidation degradation.[69,70] In contrast, organosilane precursors are typically chosen for SAMs formation on –OH terminated silicon surface due to the primarily strong covalent interaction between the alkoxy group (−OR) of agent molecules and surface silanol (Si−OH) group via Si−O−Si bond.[51] Organosilane SAMs are well-established surface modification agent to synthesis covalent bonded multilayer films over silicon surface via MLD process.[51, 65-66, 71-73] However, differences can be induced in the surface characteristics of the substrate, for example, the surface concentration of OH groups by oxidation treatment may affect the SAMs nucleation density. And, thus this change may be directly influenced films physical and chemical properties, even though MLD process was carried out with same monomers combination and identical experimental conditions. Film growth with variation of surface OH concentrated has readily been examined in ALD process.[74,75]

Figure 1.5 demonstrated the formation of self-assemblies monolayer on solid surface using amine-substituted alkyl silane. In where, the alkoxy group (−OR) of the

organosilane precursors hydrolyzed and then react with the active group on the silicon surface (e.g., −OH) as well as interact with others precursors.

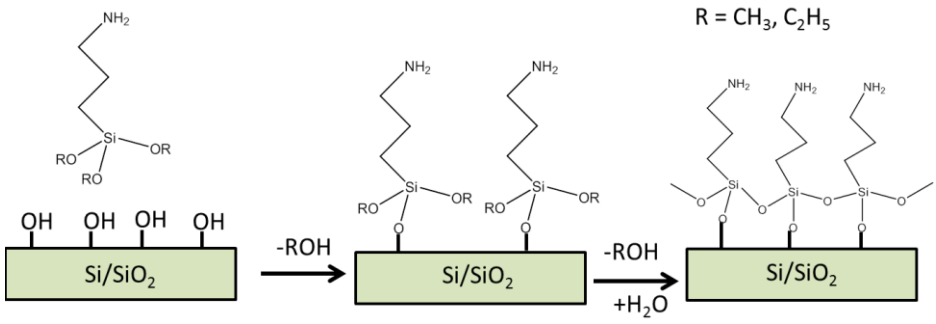

Figure 1.5. Self-assemblies monolayer on solid surface using amine−substituted alkyl silane precursors.

1.5 PRESENT ISSUES AND FINDINGS

Upto date most of the reported organic thin films, synthesis in MLD technique (both vacuum and solution based MLD) employed same symmetrical pairs of monomers combination (both bifunctional or both tetrafunctional). Until now the MLD thin films research have been focused only in the investigation of chemical bonding, chemical composition, orthogonally film growth to the surface, films surface morphology and so on. Although the conformity and controlling the deposition of ultrathin polymer films bare very important phenomena, only a few investigations have done to explore the details of MLD thin films' surface and interfacial properties.

In this thesis, the author has paid attention to synthesize urea linked covalent bonded molecular networks via solution based MLD technique using bifunctional and tetrafunctional monomers combination and investigate the surface/interface properties of the thin films. The driving force induced by the covalent bonding interaction significantly increases the durability and creditable performance of the laminated multilayer thin films. Due to the presence of tetrahedral arms precursor the resulting networks are linked three-dimensionally (3D) via urea linkage, $-NHCONH-$. Polyurea networks have been chosen because of its higher thermal and chemical stability. Urea coupling is a well-recognized chemical reaction, where the interaction between amine and isocyanate functionalities is carried out by the nucleophilic interaction from the electron-rich nitrogen of amine to the carbon of isocyanate functional group. This polymerization reaction can be performed at room temperature without producing any byproduct molecular that may be trapped inside the molecular networks or introduce impurities into thin film. In general, polyurea is synthesized industrially via a simple additional polymerization reaction between diisocyanate and diamine monomers, mainly used as fiber and coating polymers. Recently, the chemistry of urea bonds demonstrated molecularly cross-linked covalent networks, which could be rearranged to form stiff urea-bonded molecular networks while producing reticulated

micropores.[76] This reticulated micropores through covalent networks have explored to fabricate nanocomposite membrane for selective separation of carbon dioxide.[77]

In this present study, the author has synthesized cross-linked polyurea molecular networks based multilayer thin films using MLD technique. In where, it was observed that the sequential deposition of different symmetrical monomers, such as bifunctional and tetrafunctional was influenced in films physical properties within number of laminating cycles, especially, films mass density. This phenomenon may directly relate with degrees of cross-linking within layer deposition cycles. This mass density phenomenon also correlated with substrate surface OH group concentration. The author also paid much attention regarding the investigation of chemical bonding as well as film morphology. This finding can contribute a brief understanding in the surface/interfacial phenomena in organic multilayer thin films.

1.6 SURVEY OF THIS THESIS

The objective of this thesis is to synthesis and characterization a new class of cross-linked multilayer thin film using solution based molecular layer deposition technique. The specific chemical system is reported in this study form covalent bonded polyurea networks based on the additional polymerization reaction of amine and isocyanate functionalities. Various experimental techniques were used to investigate films physical and chemical properties, and the experiments were systematically performed.

In chapter 2, the non-linear mass density of the thin films was observed within number of layer deposition. This is the first report is to synthesize variable densities organic thin film using layer assembled technique. In chapter 3, the effect of substrate surface OH concentration in layer growth has been studied. This study revealed that change of surface characteristic has significant influenced in film properties. The author also provided a significant attention regarding the chemical bonding and atomic environments into molecular networks as well as surface morphology of film and SAMs modified substrate.

This research investigates the surface/interfacial phenomena in cross-linked multilayer thin film using unique monomers combination in solution processable MLD technique. In detail of research will address the following aspects (scheme 1).

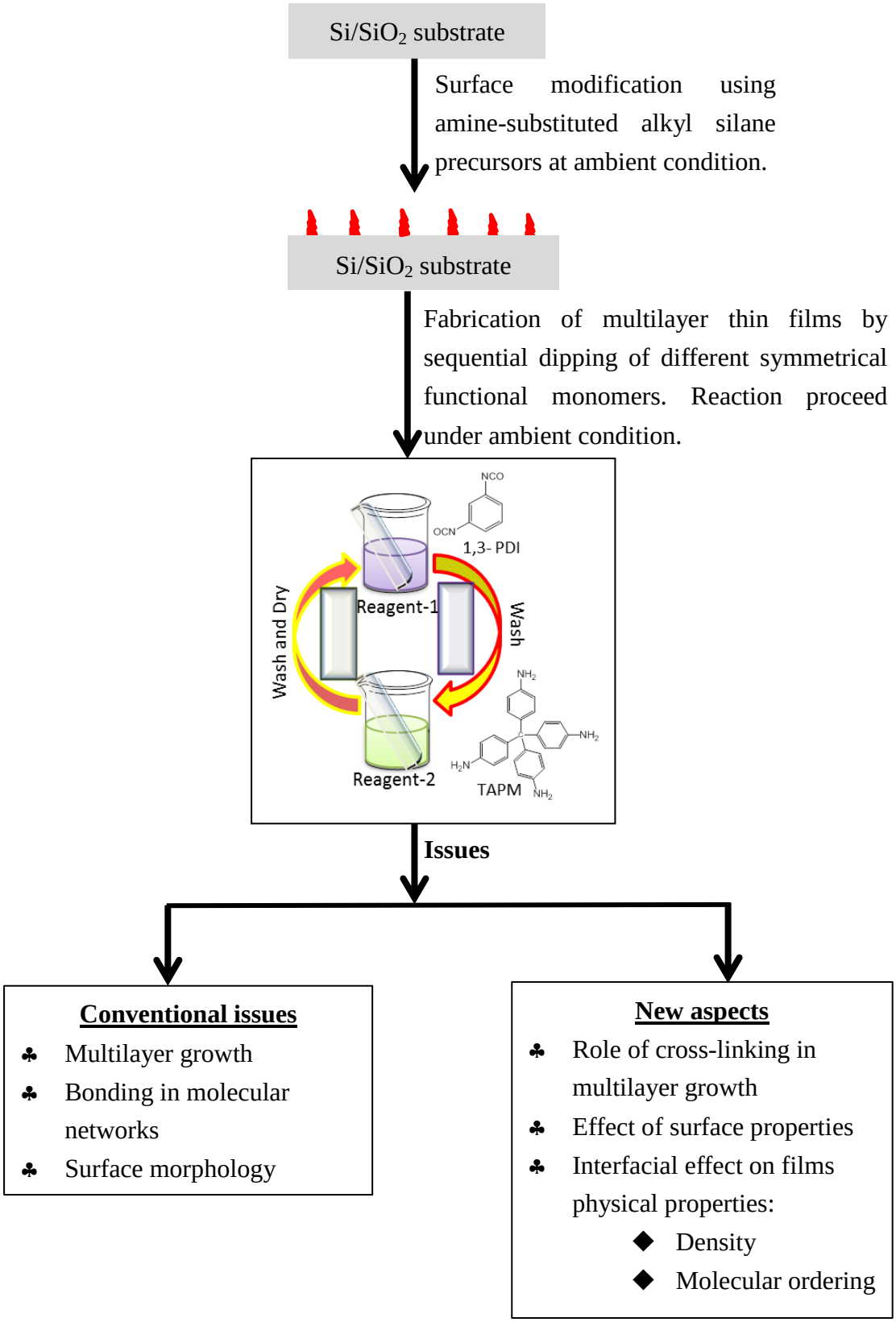

Scheme 1.1. Schematic illustration of the issues and research objectives.

REFERENCES

(1) Castner, D. G.; Ratner, B. D. Biomedical Surface Science: Foundations to Frontiers. *Surf. Sci.* **2002**, *500*, 28-60.

(2) Lord, M. S.; Foss , M.; Besenbacher, F. Influence of Nanoscale Surface Topography on Protein Adsorption and Cellular Response, *Nano Today* **2010**, *5*, 66-78.

(3) Koegler, P.; Clayton, A.; Thisen, H.; Santos, G. N. C.; Kingshott, P. The Influence of Nanostructured Materials on Biointerfacial Interactions. *Adv. Drug Delivery rev.* **2012**, *64*, 1820-1939.

(4) Xiao, F.-X.; Pagliaro, M.; Xu, Y.-J.; Liu, B. Layer-by-Layer Assembly of Versatile Nanoarchitectures with Diverse Dimensionality: a new Perspective for Rational Construction of Multilayer Assemblies. *Chem. Soc. Rev.* DOI: 10.1039/c5cs00781j (**2016**).

(5) Krishnan, K.; Iwatsuki, H.; Hara, M.; Nagano, S.; Nagao, Y.; Proton Conductivity Enhancement in Oriented, Sulfonated Polyimide Thin Films. *J. Mater. Chem. A*, **2014**, *2*, 6895-6903.

(6) Ichiki, I.; Maeda, R.; Morikawa, Y.; Mabune, Y.; Nakada, T.; Momaka, K. Photovoltaic Effect of Lead Lanthanum Zirconate Titanate in a Layered Film Structure Design. *Appl. Phys. Lett.* **2004**, *84*, 395-397.

(7) Blodgett. K. B. Films Built by Depositing Successive Monomolecular Layers on a Solid Surface. *J. Am. Chem. Soc.* **1935**, *57*, 1007-1022.

(8) Langmuir, I.; Schaefer, V. J. Monolayers and Multilayers of Chlorophyll. *J. Am. Chem. Soc.* **1937**, *59*, 2075-2076.

(9) Talham, D. R. Conducting and Magnetic Langmuir−Blodgett Films. *Chem. Rev.* **2004**, *104*, 5479-5502.

(10) Ariga, K.; Yamauchi, Y. Mori, T.; Hill, J. P. 25th Anniversary Article: What Can Be Done with the Langmuir-Blodgett Method? Recent Developments and its Critical Role in Materials Science. *Adv. Mater*, **2013**, *25*, 6477-6512.

(11) Edmondson, S.; Osborne, V. L.; Huck, W. T. S. Polymer Brushes via Surface-initiated Polymerizations. *Chem. Soc. Rev.* **2004**, *33*, 14-22.

(12) Bhattacharya, A.; Misra, B. N. Grafting: a Versatile Means to Modify Polymers: Techniques, Factors and Applications. *Prog. Polymer. Sci.* **2004**, *29*, 767-814.

(13) Ozaydin-Ince, G.; Coclite, A. M.; Gleason, K. K. CVD of Polymeric Thin Films: Applications in Sensors, Biotechnology, Microelectronics/Organic Electronics, Microfluidics, MEMS, Composites and Membranes. *Rep. Prog. Phys.* **2012**, *75*, 016501.

(14) Malik, M. A.; Afzaal, M.; O'Brien, P. Precursor Chemistry for Main Group Elements in Semiconducting Materials, *Chem Rev.* **2010**, *110*, 4417-4446.

(15) Baxamusa, S. H.; Gleason, K. K. Initiated Chemical Vapor Deposition of Polymer Films on Nonplanar Substrates. *Thin Solid Films* **2009**, *517*, 3536-3538.

(16) Ashfold, M. N. R.; Claeyssens, F.; Fuge, G. M.; Henley, S. J. Pulsed Laser Ablation and Deposition of Thin Films. *Chem. Soc. Rev.* **2004**, *33*, 23-31.

(17) Chan, K.; Gleason, K. K. Initiated Chemical Vapor Deposition of Linear and Cross-linked Poly(2-hydroxyethyl methacrylate) for Use as Thin-Film Hydrogels. *Langmuir* **2005**, *21*, 8930-8939.

(18) Borges, J.; Mano, J. F. Molecular Interactions Driving the Layer-by-Layer Assembly of Multilayers. *Chem. Rev.* **2014**, *114*, 8883-8942.

(19) Dubas, S. T.; Schlenoff, J. B. Factors Controlling the Growth of Polyelectrolyte Multilayers. *Macromolecules* **1999**, *32*, 8153-8160.

(20) Dubas, S. T.; Schlenoff, J. B. Swelling and Smoothing of Polyelectrolyte Multilayers by Salt. *Langmuir* **2001**, *17*, 7725-7727.

(21) Hammond, P. T. Form and Function in Multilayer Assembly: New Applications at the Nanoscale. *Adv. Mater.* **2004**, *16*, 1271-1293.

(22) Hammond, P. T. Recent Explorations in Electrostatic Multilayer Thin Film Assembly. *Curr. Opin. Colloid Interface Sci.* **2000**, *4*, 430-442.

(23) Hammond, P. T. Engineering Materials Layer-by-Layer: Challenges and Opportunities in Multilayer Assembly. *AIChE J.* **2011**, *57*, 2928-2940.

(24) Schoeler, B.; Kumaraswamy, G.; Caruso, F. Investigation of the Influence of Polyelectrolyte Charge Density on the Growth of Multilayer Thin Films Prepared by the Layer-by-Layer Technique. *Macromolecules* **2002**, *35*, 889-897.

(25) Shimazaki, Y.; Mitsuishi, M.; Ito, S.; Yamamoto, M.; Inaki, Y. Preparation of the Nucleoside-containing Nanolayered Film by the Layer-by-Layer Deposition Technique. *Thin Solid Films* **1998**, *333*, 5-8.

(26) Serizawa, T.; Yamamoto, K.; Akashi, M. A Novel Fabrication of Ultrathin Poly(vinylamine) Films with a Molecularly Smooth Surface. *Langmuir* **1999**, *15*, 4682-4684.

(27) Zelikin, A. N.; Li, Q.; Caruso, F. Disulfide-Stabilized Poly(methacrylic acid) Capsules: Formation, Cross-Linking, and Degradation Behavior. *Chem. Mater.* **2008**, *20*, 2655-2661.

(28) Stockton, W. B.; Rubner, M. F. Molecular-Level Processing of Conjugated Polymers. 4. Layer-by-Layer Manipulation of Polyaniline via Hydrogen-Bonding Interactions. *Macromolecules* **1997**, *30*, 2717-2725.

(29) Wang, X.; Jiang, Z.; Shi, J.; Liang, Y.; Zhang, C.; Wu, H. Metal–Organic Coordination-Enabled Layer-by-Layer Self-Assembly to Prepare Hybrid Microcapsules for Efficient Enzyme Immobilization. *ACS Appl. Mater. Interfaces* **2012**, *4*, 3476-3483.

(30) Lee, H.; Kepley, L. J.; Hong, H.-G.; Mallouk, T. E. Adsorption of Ordered Zirconium Phosphonate Multilayer films on silicon and gold surfaces. *J. Phys. Chem.* **1988**, *92*, 2597-2601.

(31) Hanke, M.; Arslan, H. K.; Bauer, S.; Zybaylo, O.; Christophis, C.; Gliemann, H.; Rosenhahn, A.; Wöll, C. The Biocompatibility of Metal–Organic Framework Coatings: An Investigation on the Stability of SURMOFs with Regard to Water and Selected Cell Culture Media. *Langmuir* **2012**, *28*, 6877-6884.

(32) Kohli, P.; Blanchard, G. J. Applying Polymer Chemistry to Interfaces: Layer-by-Layer and Spontaneous Growth of Covalently Bound Multilayers. *Langmuir* **2000**, *16*, 4655-4661.

(33) Zhang, Y.; Yang, S.; Guan, Y.; Cao, W.; Xu, J. Fabrication of Stable Hollow Capsules by Covalent Layer-by-Layer Self-Assembly. *Macromolecules* **2003**, *36*, 4238-4240.

(34) Zhang, Y.; Cao, W. Stable Self-Assembled Multilayer Films of Diazo Resin and Poly(maleic anhydride-*co*-styrene) Based on Charge-Transfer Interaction. *Langmuir* **2001**, *17*, 5021-5024.

(35) Crespo-Biel, O.; Dordi, B.; Reinhoudt, D. N.; Huskens, J. Supramolecular Layer-by-Layer Assembly: Alternating Adsorptions of Guest- and Host-Functionalized Molecules and Particles Using Multivalent Supramolecular Interactions. *J. Am. Chem. Soc.* **2005**, *127*, 7594-7600.

(36) Yao, H.; Hu, N. pH-Switchable Bioelectrocatalysis of Hydrogen Peroxide on Layer-by-Layer Films Assembled by Concanavalin A and Horseradish Peroxidase with Electroactive Mediator in Solution. *J. Phys. Chem. B* **2010**, *114*, 3380-3386.

(37) George, S. M. Atomic Layer Deposition: An Overview. *Chem. Rev*. **2009**, *110*, 111-131.

(38) Ritala, M.; Leskela, M. Atomic Layer Deposition. In Handbook of Thin Film Materials. Nalwa, H. S., Ed.; Academic Press; San Diego, **2002**; Vol.1.

(39) Johnson, R. W.; Hultqvist, A.; Bent, S. F. A Brief Review of Atomic layer Deposition: from Fundamental to Applications. *Mater. Today*, **2014**, *17 (5)*, 236-246.

(40) Chan, R.; Bent, S. F. Chemistry for Positive Pattern Transfer Using Area-Selective Atomic Layer Deposition. *Adv. Mater.* **2006**, *18*, 1086-1090.

(41) Jiang, X.; Bent, S. F. Area-Selective ALD with Soft Lithographic Methods: Using Self-Assembled Monolayers to Direct Film Deposition. *J. Phys. Chem. C* **2009**, *113*, 17613-17625.

(42) Jiang, X.; Huang, H.; Prinz, F. B.; Bent, S. F. Application of Atomic Layer Deposition of Platinum to Solid Oxide Fuel Cells. *Chem. Mater*. **2008**, *20*, 3897-3905.

(43) Kubono, A.; Yuasa, N; Shao, H.-L.; Umemoto, S.; Okui, N. In-situ Study on Alternating Vapor Deposition Polymerization of Alkyl Polyamide with Normal Molecular Orientation. *Thin Solid Films* **1996**, *289*, 107-111.

(44) Du, Y.; George, S. M. Molecular Layer Deposition of Nylon 66 Films Examined Using in situ FTIR Spectroscopy. *J. Phys. Chem. C* **2007**, *111*, 8509-8517.

(45) Kim, A.; Filler, M. A.; Kim, S.; Bent, S. F. Layer-by-Layer Growth on Ge (100) via Spontaneous Urea Coupling Reactions. *J. Am. Chem. Soc.* **2005**, *127*, 6123-6132.

(46) Loscutoff, P. W.; Zhou, H.; Clendenning, S. B.; Bent, S. F. Formation of Organic Nanoscale Laminates and Blends by Molecular Layer Deposition. *ACS Nano* **2010**, *4*, 331-341.

(47) Yoshida, S.; Ono, T.; Esashi, M. Deposition of Conductivity-Switching Polyimide Film by Molecular Layer Deposition and Electrical Modification using Scanning Probe Microscope. *Micro. Nano Lett.* **2010**, *5*, 321-323.

(48) Loscutoff, P. W.; Lee, H. B. R.; Bent S. F. Deposition of Ultrathin Polythiourea Films by Molecular Layer Deposition. *Chem. Mater*. **2010**, *22*, 5563-5569.

(49) Sundberg, P.; Karppine, M. Inorganic–Organic Thin Film Structures by Molecular Layer Deposition: A review. *Beilstein J. Nanotechnol.* **2014**, *5*, 1104-1136.

(50) Zhou, H.; Bent, S. F. Febrication of Organic Interfacial Layers by Molecular Layer Deposition: Present Status and Future Opportunities. *J. Vac. Sci. Technol. A* **2013**, *31(4)*, 040801-(1)-(18).

(51) Prasittichai, C.; Zhou, H.; Bent, S. F. Area Selective Molecular Layer Deposition of Polyurea Films. *ACS Appl. Mater. Interfaces* **2013**, *5*, 13391-13396.

(52) Jeon, E.; Moon, S.-U.; Bae, J.-S.; Park, J.-W. In situ Generation of Reticulate Micropores though Covalent Network/Polymer Nanocomposite Membranes for Reverse-Selective Separation of Carbon Dioxide. *Angew. Chem. Int. Ed.* **2016**, *55*, 1318-1323.

(53) Sekizkardes, A. K.; İslamoğlu, T.; Kahveci, Z.; El-Kaderi, H. M. Application of Pyrene-derived Benzimidazole-linked Polymers to CO_2 Separation under Pressure and Vacuum Swing Adsorption Settings. *J. Chem. Mater A* **2014**, *2*, 12492-12500.

(54) Zhang, Y.; Riduan, S. N. Functional Porous Organic Polymers for Heterogeneous Catalysis. *Chem. Soc. rev.* **2012**, *41*, 2083-2094.

(55) Chan-Thaw, C. E.; Villa, A.; Katekomol, P.; Su, D.; Thomas, A.; Prati, L. Covalent Triazine Framework as Catalytic Support for Liquid Phase Reaction. *Nano Lett.*, **2010**, *10* (2), 537–541.

(56) Pachfule, P.; Kandambeth, S.; Díaz, D. D.; Banerjee, R. Highly Stable Covalent Organic Framework–Au Nanoparticles Hybrids for Enhanced Activity for Nitrophenol Reduction. *Chem. Commun.*, **2014**, *50*, 3169-3172.

(57) Uribe-Romo, F. J.; Hunt, J. R.; Furukawa, H.; Klöck, C.; O'Keeffe, M.; Yaghi, O. M. A Crystalline Imine-Linked 3-D Porous Covalent Organic Framework. *J. Am. Chem. Soc.*, **2009**, *131* (13), 4570–4571.

(58) Ding, S.-Y.; Wang, W.; Covalent Organic Frameworks (COFs): from Design to Applications. *Chem. Soc. Rev.* **2013**, *42*, 548-568.

(59) Feng, X.; Ding, X.; Jiang, D. Covalent Organic Frameworks. *Chem. Soc. Rev.*, **2012,** *41*, 6010-6022.

(60) Zeng, Y.; Zou, R.; Luo, Z.; Zhang, H.; Yao, X.; Ma, X.; Zou, R.; Zhao, Y. Covalent Organic Frameworks Formed with Two Types of Covalent Bonds Based on Orthogonal Reactions. *J. Am. Chem. Soc.* **2015**, *137*, 1020-1023.

(61) Shinde, D. B.; Kandambeth, S.; Pachfule, P.; Kumar, R. R.; Banerjee, R. Bifunctional Covalent Organic Frameworks with Two Dimensional Organocatalytic Micropores. *Chem. Commun.*, **2015**, *51*, 310-313.

(62) Farha, O. K.; Bae, Y.-S.; Hauser, B. G.; Spokoyny, A. M.; Randall Q. Snurr, R. Q.; Mirkin, C. A.; Hupp, J. T. Chemical Reduction of a Diimide based Porous Polymer for Selective Uptake of Carbon Dioxide versus Methane. *Chem. Commun.*, **2010**, *46*, 1056–1058.

(63) Yuan, D.; Lu, W.; Zhao, D.; Zhou, H.-C. Highly Stable Porous Polymer Networks with Exceptionally High Gas-Uptake Capacities. *Adv. Mater.* **2011**, *23*, 3723–3725.

(64) Yao, S.; Yang, X. Yu, M.; Zhang, Y.; Jiang, J.-X. High Surface area Hypercrosslinked Microporous Organic Polymer Networks based on Tetraphenylethylene for CO_2 Capture. *Mater. Chem. A* **2014**, *2*, 8054-8059.

(65) Budd, P. M.; Ghanem, B. S.; Makhseed, S.; McKeown, N. B.; Msayib, K. J.; Tattershall, C. E. Polymers of Intrinsic Microporosity (PIMs): Robust, Solution-processable, Organic Nanoporous Materials. *Chem. Commun.* **2004**, 203-231.

(66) Kim, M.; Byeon, M.; Bae, J-S.; Moon, S. Y.; Yu, G.; Shin. K.; Basarir, F.; Yoon, T. H.; Park, J-W. Preparation of Ultrathin Films of Molecular Networks

through Layer-by-Layer Cross-Linking Polymerization of Tetrafunctional Monomers. *Macromolecules* **2011**, *44*, 7092-7095.

(67) Qian, H.; Li, S.; Zheng, J.; Zhang, S. Ultrathin Films of Organic Networks as Nanofiltration Membranes via Solution-Based Molecular Layer Deposition. *Langmuir* **2012**, *28*, 17803-17810.

(68) Ulman, A. Formation and Structure of Self-Assembled Monolayer, *Chem. Rev.* **1996**, *96*, 1533-1554.

(69) Karpovich, D. S.; Blanchard, G. C. Direct Measurement of the Adsorption Kinetics of Alkanethiolate Self-Assembled Monolayers on a Microcrystalline Gold Surface. *Langmuir* **1994**, *10*, 3315-3322.

(70) Kohli , P.; Taylor, K. K.; Harris, J. J.; Blanchard, G. J. Assembly of Covalently-Coupled Disulfide Multilayers on Gold. *J. Am. Chem. Soc.*, **1998**, *120 (46)*, 11962–11968.

(71) Zhou, H.; Blackwell, J. M.; Lee, H.-B.-R., Bent, S. F. Highly Sensetive, Patternable Organic Films at the Nanoscale made by Bottom-Up Assembly, *ACS Appl. Mater. Interfaces* **2013**, *5*, 3691-3696.

(72) Zhou, H.; Bent. S. F. Molecular Layer Deposition of Functional Thin Films for Advanced Lithographic Patterning. *ACS Appl. Mater. Interfaces* **2011**, *3*, 505-511.

(73) Zhou, H.; Toney, M. F.; Bent, S. F. Cross-Linked Ultrathin Polyurea Films via Molecular Layer Deposition. *Macromolecules* **2013**, *46*, 5638-5643.

(74) Puuruuen, R. L. Correlation between the Growth-per-cycle and the Surface Hydroxyl Group Concentration in the Atomic Layer Deposition of Aluminum Oxide from Trimethylaluminum and Water. *Appl. Sur. Sci.* **2005**, *245*, 6-10.

(75) Puuruuen, R. L. Surface Chemistry of Atomic Layer Deposition: A case Study for the Trimethylaluminum/Water Process. *J. Appl. Phys.* **2005**, *97*, 121301-121352.

(76) Moon, S.-Y.; Jeon, E.; Bae, J.-S.; Park, M.-K.; Kim, C.; Noh, D. Y.; Lee, E.; Park, J.-W. Thermo-processable Covalent Scaffolds with Reticular Hierarchical Porosity and Their High Efficiency Capture of Carbon Dioxide *J. Mater. Chem. A* **2015**, *3*, 14871-14875.

(77) Jeon, E.; Moon, S.-Y.; Bae, J.-S.; Park, J.-W. In situ Generation of Reticulate Microspores though Covalent Networks/Polymer Nanocomposite Membranes for Reverse-Selective Separation of Carbon Dioxide. *Angew. Chem. Int. Ed.* **2016**, *55*, 1318-1323.

Fabrication and Characterization of Cross-linked Organic Thin Films with Nonlinear Mass Densities

The preparation of urea (bonded) cross−linked multilayer thin film by sequential deposition of bifunctional and tetrafunctional molecular building block was demonstrated. Multilayer growth as a function of deposition cycles was inspected using UV−vis absorption spectroscopy. From infrared spectroscopy results, three characteristic infrared bands of amide I, amide II, and asymmetric ν_a (N−C−N) stretching band confirmed the formation of polyurea networks by alternate dipping into a solution of amine and isocyanate functionality monomers. The deconvoluted component of the C 1s and N 1s spectra obtained by X−ray photoelectron spectroscopy (XPS) shows clear evidence of stable polyurea networks. Thickness of the multilayer films was investigated using AFM and XRR techniques. From XRR density investigation, constant mass density was not observed with deposition cycles. The mass density increased up to 16% within deposited layers from proximate layers to those extending away from the substrate surface. This difference in packing density might derive from the different degrees of cross-linking among layers proximate to the substrate surface and extending away from the surface. Enhancement of structural periodicity with film growth was demonstrated by grazing incidence small angle X-ray

scattering (GI-SAXS) measurements. The thin film near the substrate surface seems to have an amorphous structure. However, molecular ordering improves in the surface normal direction of the substrate with a certain number of deposited layers.

2.1 INTRODUCTION

Cross-linked organic thin films have garnered much attention recently for their higher density,[1] better mechanical strength,[2] and chemical stability.[3,4] Demand for cross-linked nanoscale organic thin films has increased rapidly for conventional applications such as organic thin film transistors[5,6], purification membranes[7] etc. However, the synthesis of thin films with sub-nanometer scale is still challenging. For the synthesis of organic thin films, spin-coating[8] and Langmuir–Blodgett (LB)[9] are well-known and useful techniques. Another simple and versatile technique to prepare multilayer organic thin films is molecular layer deposition (MLD),[10–12] which deposits films in a layer-by-layer (LbL)[13,14] fashion to prepare multilayer thin films with a sub-nanometer scale. Molecular layer deposition is an analogy of atomic layer deposition (ALD).[15-17] In MLD process, organic monomer deposited in a molecular level through the reaction of alternating pendent functional groups. Therefore, MLD provides opportunity to fabricate ultrathin film in molecular level thickness. To date, most MLD processes have been conducted with polymerization reaction of volatile bifunctional monomers under vacuum conditions. Polymeric thin films such as polyamides,[18–20] polyimides,[21–25] polyurethane,[26] polyureas,[1, 27–30] polythiourea,[31] and polyester[32] have been reported. However, this vapor-based MLD technique is inapplicable for monomers with high molar mass and low vapor pressure.[33] Because of

the high boiling point of monomers, excess adsorbed monomers onto the substrate surface by vapor deposition cannot be removed completely, which hinders single molecular layer deposition. Moreover, with vacuum−based reaction system, it is difficult to use a catalyst or pH change in the reaction media to make a non-spontaneous reaction a spontaneous one.[29] Solution-based MLD offers an exclusive route to overcoming these problems. Stafford and co-workers reported multilayer cross-linked polyamide thin film using solution-based molecular layer-by-layer (mLbL) synthesis. They used bifunctional m-phenylene diamine and trifunctional trimesoyl chloride monomers to fabricate organic multilayer thin films.[34,35] Recent reports by Qian *et al.* and Kim *et al.* show cross-linked polyamide and polyurea thin films by polymerization of the same symmetrical tetrafunctional monomers to produce three-dimensional (3D) covalent bonded molecular networks via LbL dipping technique.[33, 36]

My approach to fabrication of 3D covalent bonded multilayer thin films is based on sequential deposition of different symmetrical monomers, such as bifunctional 1,3-phenylene diisocyanate (PDI) and tetrafunctional tetrakis(4−aminophenyl)methane (TAPM), on a 3-aminopropyltrimethoxysilane (APTMS) modified amine−terminated surface. The longer urea chains with combinations of different symmetrical monomers lead to different cross-linking states within multilayer growth. This different degree of

cross-linking might be facilitated by changing the molecule–molecule interaction proximate to the substrate surface and extending away from the substrate surface. It is reasonable to consider that intermolecular interaction apart from the substrate surface is considerably higher than the intermolecular interactions among monomers near the surface. It is also rational to infer that molecular networks extending away from the substrate surface exhibit higher cross-linking than molecular networks located near the substrate surface. Presumably, this different degree of cross-linking provides films with variable densities among layers (with a certain thickness) proximate to the substrate surface and extending away from the substrate surface (Figure 2.1).

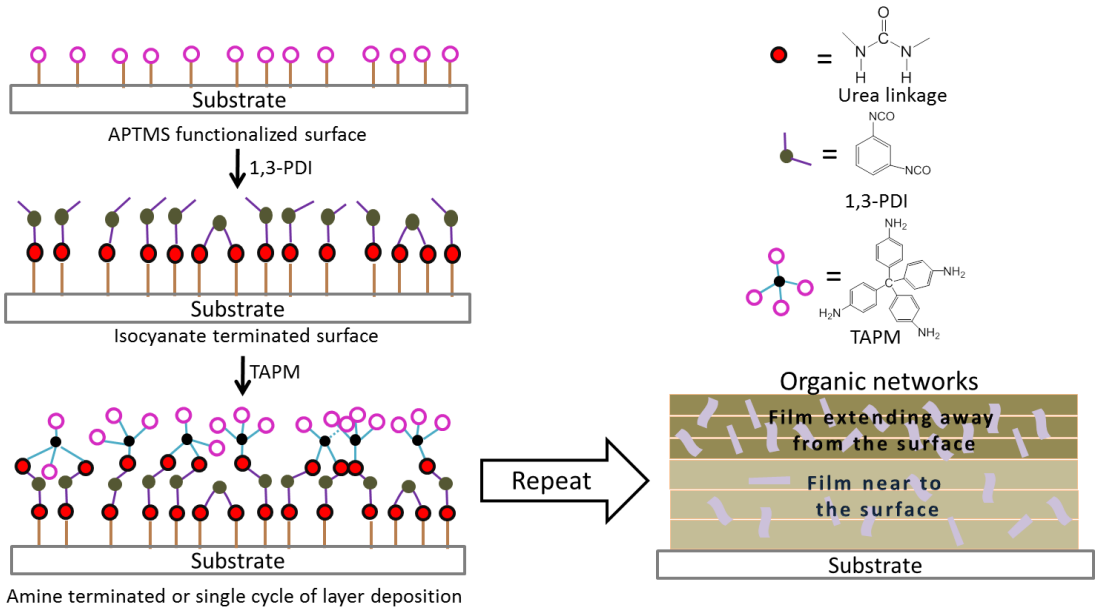

Figure 2.1. Schematic illustration of molecular layer deposition (MLD) process on a solid surface and the chemical structure of 1,3−PDI and TAPM monomers.

This work shows the synthesis and characterization of a new class of cross−linked multilayer polyurea thin films using 3D covalent bonded molecular networks with nonlinear mass densities via solution-based MLD technique. Infrared (IR) spectroscopy and X-ray photoelectron spectroscopy (XPS) confirmed the formation of a urea bond between the reaction of amine and isocyanate functionalities. UV−vis absorption spectroscopy demonstrated multilayer growth. The thickness of multilayer polyurea films on the silicon substrate was measured using atomic force microscopy (AFM) and X−ray reflective (XRR) techniques. The mass density and degree of molecular ordering with film growth were examined, using X-ray reflectivity (XRR) analysis and grazing incidence small angle X-ray scattering (GI-SAXS) measurements, respectively.

2.2 EXPERIMENTAL SECTION

2.2.1 Materials

As molecular building blocks, tetrakis(4-aminophenyl)methane (TAPM) and 1,3-phenylene diisocyanate (PDI) were purchased from Aldrich Chemical Co. Inc., USA and Tokyo Chemical Industry Co. Ltd., Japan, respectively. Using recrystallization technique, 98% pure commercial PDI was purified further. 3-Aminopropyltrimethoxysilane (APTMS, >96%) was purchased from Tokyo Chemical Industry Co. Ltd., Japan, and was used as received. All solvents (super-dehydrated and AR grade) were purchased from Wako Pure Chemical Industries Ltd., Japan and were used without further purification.

2.2.2 Surface Cleaning

Multilayer thin films were synthesized onto quartz substrates (25 × 15 mm^2, t = 0.5 mm) and silicon wafers (30 × 20 mm^2, t = 0.525 mm) of p-type silicon (p-Si(100), 5 - 20 Ω-cm with boron doped). Substrates were cleaned using 2-propanol with sonication (three times each, 15 min duration), and were then dried and kept in the clean bench.

2.2.3 Self-assembled Monolayer (SAM) Formation

After cleaning the substrate, the cleaned substrates were immersed into 10 mM amine−functionalized 3-aminopropyltrimethoxysilane (APTMS) in ethanol solution at room temperature for 1 hr under Ar atmosphere with constant stirring. After taking out from the APTMS solution, substrates were cleaned using ethanol (twice) and 2-propanol (twice) consecutively with sonication and finally rinsed with 2-propanol and dried. Finally, APTMS modified substrates kept in a clean bench for multilayer film formation within 24 hours.

2.2.4 Multilayer Thin Film Formation

These modified substrates were used for the formation of a multilayer thin film using an automatic layer-by-layer (LbL) system. Layer deposition was carried out in the following procedures: (i) amine-functionalized substrate was immersed into 17.6 mM 1,3−PDI in 1,4−dioxane and toluene (3:1, v/v) solution for 5 min. Then, the substrate was rinsed in five separate containers: two beakers of 1,4−dioxane and toluene mixture at the previously described ratios, two beakers of dry THF, and finally one beaker of chloroform. (ii) After washing, the isocyanate−terminated substrate was immersed into 3.78 mM TAPM in 1,4-dioxane and toluene (3:1, v/v) solution for 5 min, followed by rinsing successively in two beakers with 3:1 (v/v) ratio of 1, 4−dioxane and toluene

mixture, and two beakers of THF. The deposited substrate was dried under an Ar atmosphere. This bilayer deposition process described above (steps (i) and (ii)) was designated as a single cycle of molecular layer deposition (MLD). Multilayer thin films were formed by repeating the procedure described above in a desired number of cycles. In every cycle, the amine−terminated surface is regarded as a top surface.

2.2.5 Characterization Techniques

Several analytical techniques have been used to investigate multilayer growth, explore the physical and chemical properties of the polyurea thin films, and elucidate the films surface morphology.

2.2.5.1 X-ray Photoelectron Spectroscopy (XPS)

XPS study was performed using a DLD spectrometer (Kratos Axis−Ultra; Kratos Analytical Ltd.) with an Al Kα radiation source (1486.6 eV). Spectra were taken at 90° normal to the specimen surface. A neutralizer gun was used to reduce charging of the samples. Energy calibration and component separation were conducted using the bundled software with pure Gaussian profiles and a Shirley background (otherwise it will be mentioned). Binding energy correction was made by taking reference spectra of C 1s peak at 284.5 eV.

2.2.5.2 UV−vis Absorption Spectroscopy

UV−vis absorption spectra of the molecular networks fabricated on quartz substrates were obtained using a UV−vis spectrometer (Jasco V−630BIO−IM; Jasco Corp. Japan). The APTMS−modified quartz substrate was used as a background.

2.2.5.3 Atomic Force Microscopy (AFM)

Films thickness and surface morphology were measured by atomic force microscopy (AFM), respectively, VN–8000; Keyence Co. and AFM, Nanoscope IIIa; Veeco Instruments under following experimental conditions. Film thickness was measured using an AFM (VN–8000; Keyence Co.) equipped with a DFM/SS mode cantilever (OP-75041; Keyence Co.). For thickness measurements, films were partly scratched and height difference was evaluated for film thickness. Thickness was measured at four positions at least on each sample and an average (mean) value was obtained.

For surface morphology investigation, an atomic force microscopy (AFM, Nanoscope IIIa; Veeco Instruments) with tapping mode was used. Silicon cantilevers (SI−DF3FM; Nanosensors Corp.) with a spring constant between 2.8 Nm^{-1} and 4.4 Nm^{-1} and resonance frequency of 79–89 kHz were used. The measurements were taken, respectively, under an air atmosphere with a scan rate of 0.4 Hz and scan size of 5 × 5 μm^2 and 0.5 × 0.5 μm^2.

2.2.5.4 IR Spectra

Fourier−transform infrared (FTIR) spectroscopy was used to investigate the urea bond formation of the thin film on the substrate. Infrared spectra were collected

using an FTIR spectrometer (Nicolet 6700; Thermo Fisher Scientific Inc.) equipped with a mercury cadmium telluride (MCT) detector. An APTMS-modified Si wafer was used as a background. Spectra were taken at 8° from the surface normal. All measurement was carried out by flowing dry nitrogen gas (in avg. 90 min) to improve signal to noise ratio.

2.2.5.5 X-ray Reflectivity (XRR)

To investigate changes of internal properties of multilayer films in respect with layer growth X-ray reflectivity (XRR) analysis was performed using a high-resolution diffractometer (ATX/G; Rigaku Corp., Japan) with an R−AXIS IV two-dimensional (2D) detector. The diffractometer was equipped with Cu Kα radiation (λ= 0.1542 nm) and divergence of 0.01°. The reflective oscillation curves were fitted using software (GIXRR; Rigaku Corp., Japan). Curve fitting areas were chosen between 0.3° to 3°. During XRR investigation, the thickness of native oxide layer was estimated 0.6 nm. This thin native oxide layer did not affect to the XRR fitting process.

2.2.5.6 Grazing Incidence Small Angle X-ray Scattering (GI-SAXS)

Grazing incidence small angle X-ray scattering (GI-SAXS) analysis was performed using a diffractometer (FR−E; Rigaku Corp., Japan) with beam size of approximately 300 × 300 μm^2. The camera length was 300 mm. The sample stage was

composed of the goniometer and a vertical stage (ATS-C316-EM/ALV-300-HM; Chuo Precision Industrial Co. Ltd.). The X-ray incidence angle varied between 0.21° and 0.22°. The X-ray exposure time was fixed for 4 hours for every measurement.

2.3 RESULTS AND DISCUSSION

2.3.1 Investigation of Self-Assembled Monolayer

Prior to multilayer growth, a self-assembled monolayer was formed on solid surface using amine−terminated organosilane precursor (APTMS). Self-assembled monolayer was investigated using X-ray photoelectron spectroscopy (XPS). Figure 2.2 (A) demonstrates XPS fine scan spectra of Si 2p for bare Si wafer. Peaks at 99.0 eV and 100.0 eV represent the Si-bulk (Si $2p_{3/2}$ and Si $2p_{1/2}$). Higher binding energy peak at 102.8 eV attributed for native oxide layer on Si surface. After modification with aminosilane precursors (APTMS), Si $2p_{3/2}$ and Si $2p_{1/2}$ peaks were shifted towards lower binding energy (ca. 0.3 eV) (Figure 2.2 (B)). This shifting might be occurred due to the chemisorption of APTMS on Si surface. In addition, a new peak appeared at intermediate binding energy position for aminosilane attribution at 101.7 eV.

In addition, N 1s XPS fine scan spectra of APTMS modified surface provided two peaks at 399.1 eV and 401.2 eV, respectively (Figure 2.2 (C)). These peaks are assigned for terminated free amine and hydrogen bonded/protonated amine.[37] This hydrogen bonded/protonated amine (N 1s) peak might arise due to the acid-base interaction between chain terminal amine groups with surface silanol group (Si-OH).[38]

This discussion confirmed the successful formation of self-assembled monolayer (SAM) on Si surface using covalent interaction between the alkoxy group (−OR) in amine−terminated organosilane precursors and surface silanol (Si−OH) group via Si−O−Si bond.[27] This SAM surface creates a preferred route to synthesis multilayer films by coupling reaction.

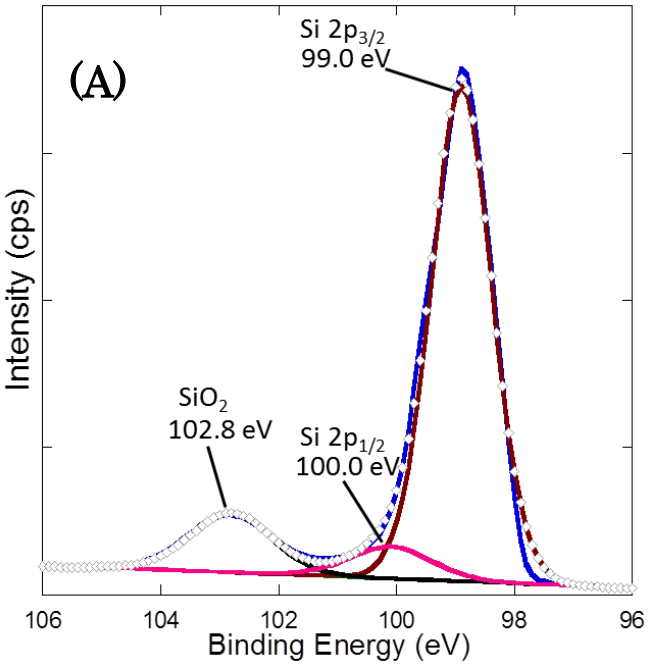

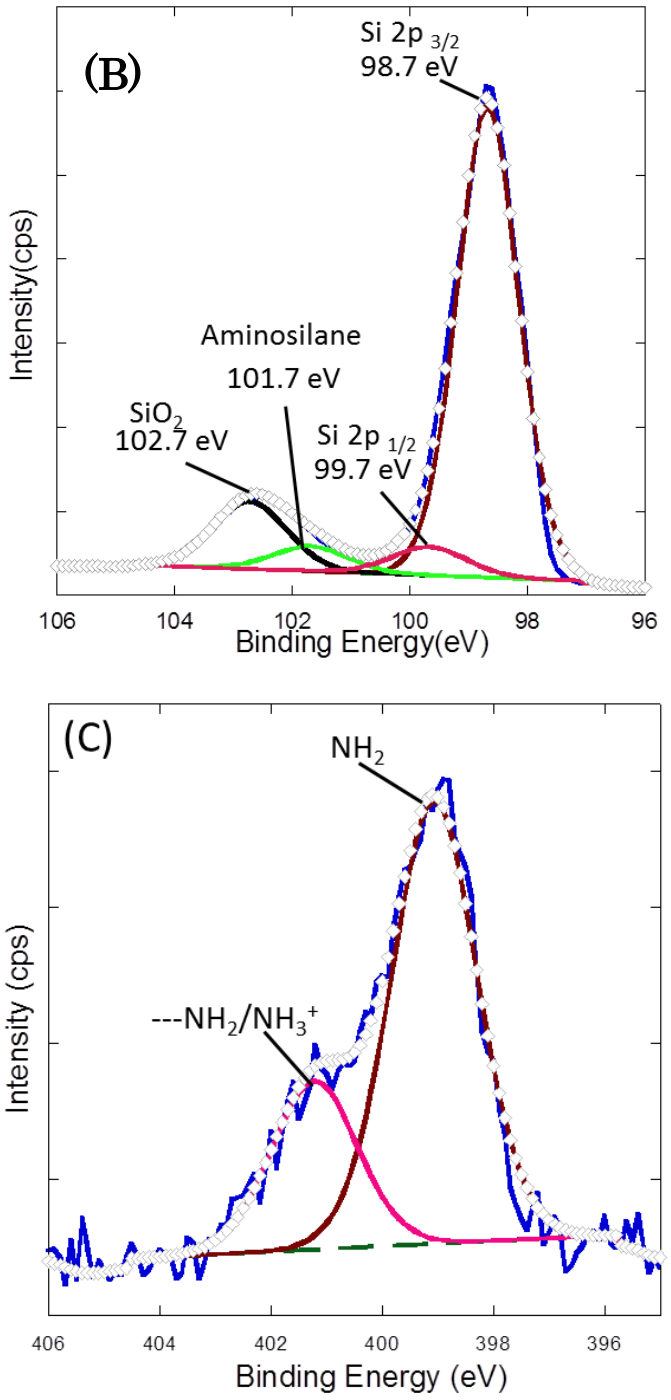

Figure 2.2. XPS fine scan spectra of (A) Si 2p of bare Si wafer, (B) Si 2p of APTMS modified Si wafer, (C) N 1s of APTMS modified Si wafer.[a]

[a]Linear background were used for N 1s spectra deconvolution.

2.3.2 Investigation of Multilayer Growth

To confirm the multilayer growth of the MLD process, transparent UV−vis spectra of thin films were measured as a function of the MLD cycles (Figure 2.3). The absorption maxima were centered at 268 nm. The absorbance intensities continuously increased within deposition cycles represents the multilayer growth carried out. The inset of Figure 2.3 shows the layer growth near the substrate up to 10 MLD cycles and extending away layer growth above 10 MLD cycles followed two distinctive linear trends. This results suggested non-linear growth for MLD cycles.

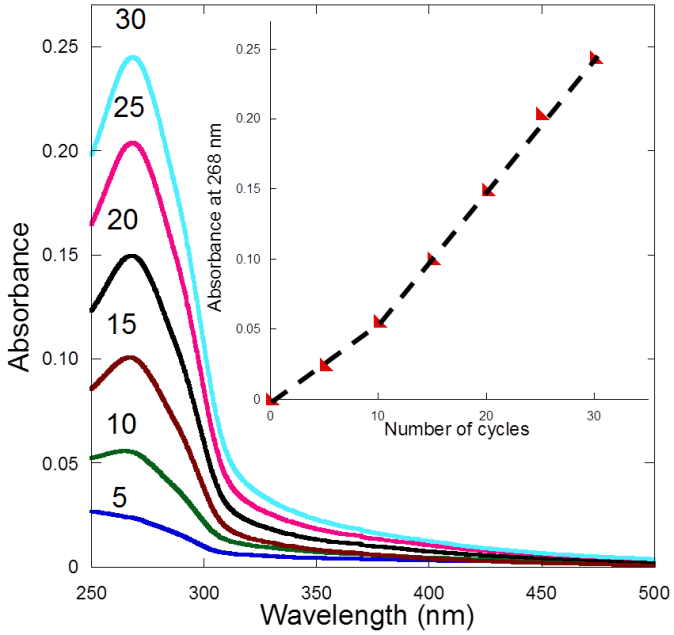

Figure 2.3. UV−vis spectra of multilayer thin film as the number of deposition cycles on quartz substrate. Inset: absorption peak intensity at 268 nm as a function of 0–30 deposition cycles.

2.3.3 Film Thickness Measurement

Film thickness was investigated using AFM and XRR techniques. For AFM thickness measurements, films were partly scratched and the height difference was evaluated for film thickness. Thicknesses of the 10, 20, and 30 MLD cycle films were 4.34 ± 0.29, 6.82 ± 0.40, and 9.33 ± 0.59 nm thick, respectively (error bars based on standard deviation). These results show growth rates (avg.) of 0.434 nm / cycle, 0.341 nm / cycle and 0.311 nm / cycle for 10, 20, and 30 MLD cycle films, respectively. The thickness of AFM results is well−matched to the XRR results, as shown in Figure 2.4. Results of XRR data are discussed later. The non−uniform growth rate (avg.) per cycle in 10, 20, and 30 MLD cycle films might be attributed to different packing conformations (loose/dense) per unit volume (cm^3) of different depth into the films. This density (g/cm^3) change phenomenon will be discussed next. Moreover, this thickness value is lower than the combined molecular length of 1,3-PDI and TAPM, which is estimated to be approximately 1.44–1.61 nm / cycle. Some reports have described that growth rates are much less than the ideal repeating unit length for thin films deposited by MLD.[1,11,12] This deviation can be explained with several reasons. Thinner growth could be observed because of the tilting of organic molecular networks. In “double” reactions, the bifunctional monomer stops the layer growth by forming a

"capped" region on the reactive film surface.[10,11] Finally, steric hindrance because of a bulky precursor may also affect the accessibility of surrounding reactive sites and cause submonolayer coverage.[1] Although, the growth rate of the polyurea thin film is lower than expected, the film thickness increased with MLD cycles, indicating multilayer deposition. This phenomenon is consistent with the UV−vis results discussed above. It is noted that MLD thin films with 1,4-PDI also faced "double" or "capped" reactions problem. Therefore, the experimental growth per layer shows much lower than the expected growth per layer with MLD cycles.[11,12]

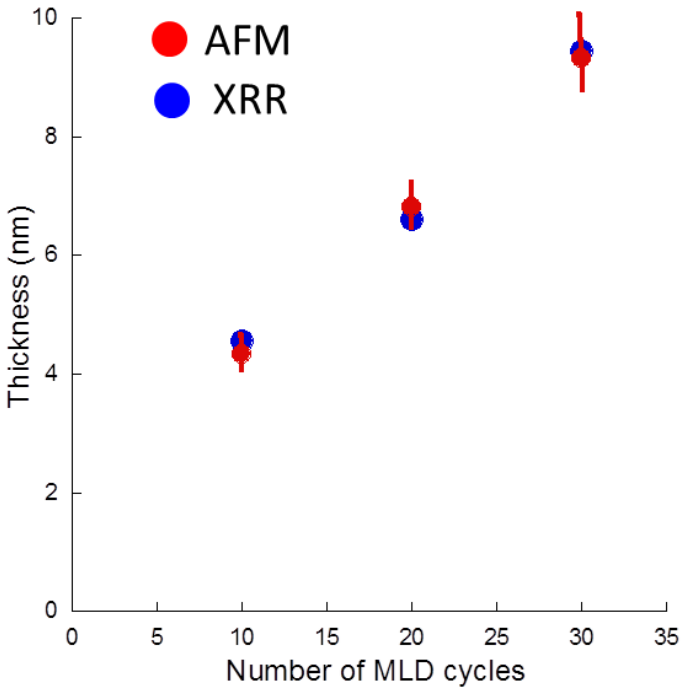

Figure 2.4. Thickness profiles of 10, 20, and 30 MLD cycle films by AFM (red circle) and XRR (blue circle).[a]

[a] Reported error bars for thickness results from AFM.

2.3.4 Determination of Chemical Bond using FT-IR

Polyurea networks formation through reaction between amine and isocyanate functionalities was inspected with infrared (IR) spectroscopy. Figure 2.5 presents IR spectra of 10, 20, and 30 MLD cycle thin films. Several characteristic peaks were observed in the region of 1200–1800 cm^{-1}. Peaks around 1650–1690 cm^{-1} can be assigned to the amide I band with the ν(C=O) stretching vibration mode of the urea group. The band at 1510 cm^{-1} can be assigned to the amide II band with (N–H) bending vibration. These two bands and the ν_a(N−C−N) asymmetric stretching band at 1300 cm^{-1} suggest the formation of urea linkage. The wavenumbers of these characteristic peaks are consistent with others reported in the literature of polyurea linkage,[29,30,39,40] and assist to confirm polyurea networks in as-synthesized thin films. In addition, a shoulder-type band near 1535 cm^{-1} and a sharp band near 1603 cm^{-1} are attributable to aromatic ring breathing and aromatic ring stretching, respectively.

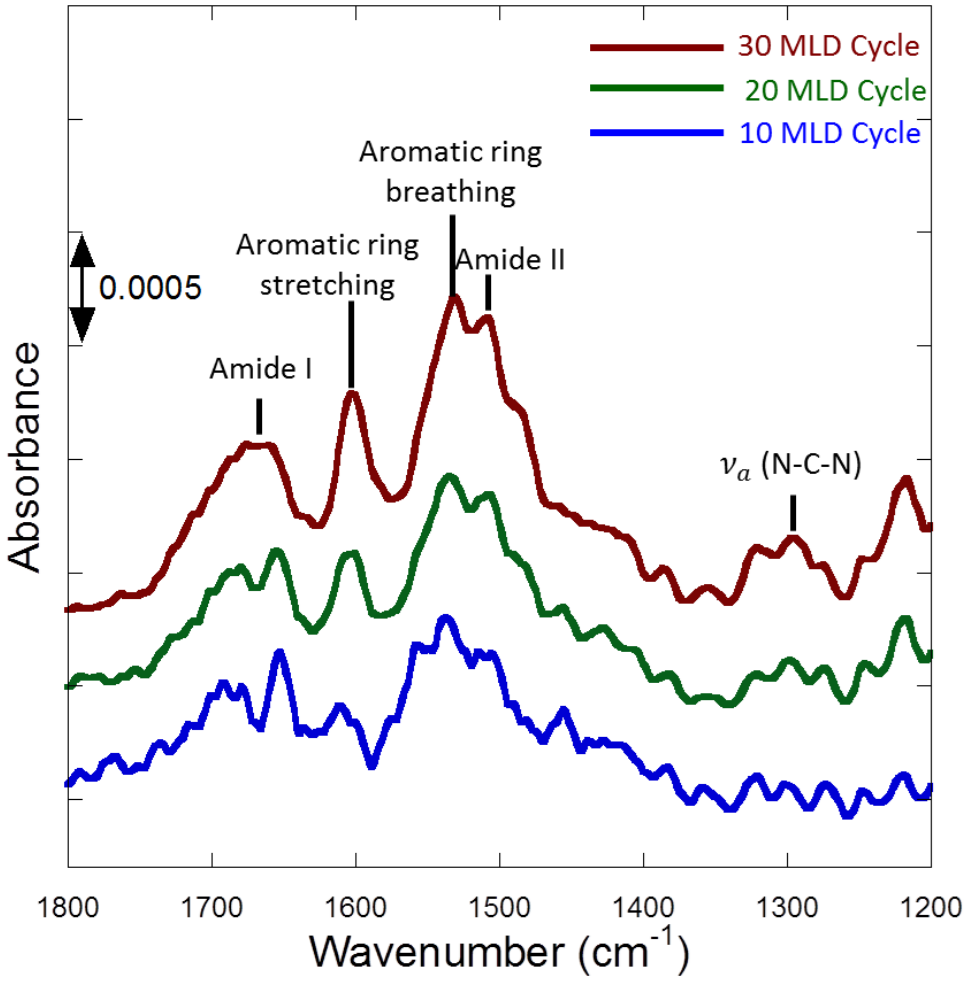

Figure 2.5. IR spectra of 10, 20, and 30 MLD cycle thin films in the infrared vibrational region for urea bonds. Spectra were measured under a nitrogen atmosphere.

Coleman and co-workers has been classified "ordered hydrogen bonded", "disordered hydrogen bonded" and "non-hydrogen bonded" urea, based on amide I characteristic infrared band for urea linkage. These bands were observed at 1630 cm^{-1}, 1650 cm^{-1} and 1690 cm^{-1} respectively.[40] Therefore from amide I band in IR spectra, can be conclude that fabricated polyurea networks were dominated with disordered

hydrogen bonded fashion.

Furthermore, in higher wavenumber region a broad ν(N-H) stretching band appeared at 3255 cm^{-1} (Figure 2.6), which is the evidence in the presence of wide distribution of hydrogen bonds (with different distances and geometries) that would be expected as disordered hydrogen bonded polyurea networks.[41,42]

It is expected to presence some unreacted isocyanate (-NCO groups), because of incomplete reaction with sequentially deposited TAPM monomers. This might happen because of steric hindrance or others. However, In this study, no peak was observed at 2270 cm^{-1}, indicates no unreacted isocyanate is present in polyurea thin films.[29] The probable reason is that the unreacted isocyanate groups are easily converted to amine by expose to humid air.[36] Spectra up to this region was not shown, because of high level of noise.

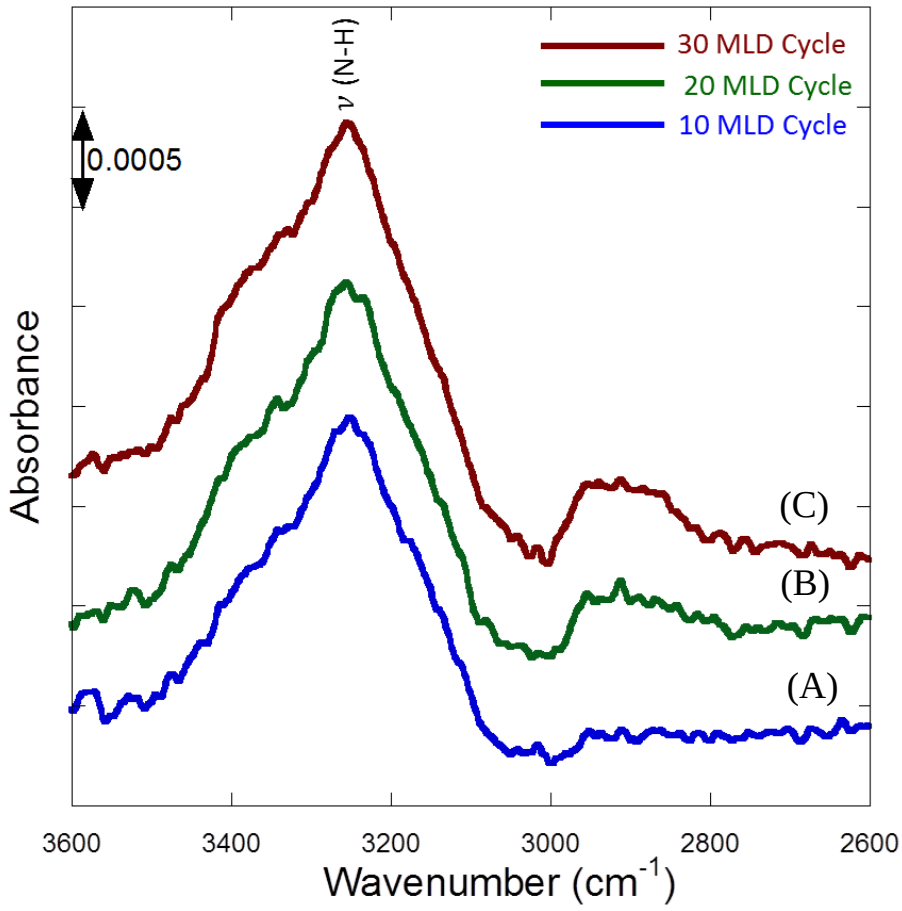

Figure 2.6. IR spectra of (A) 10 MLD cycle, (B) 20 MLD cycle, and (C) 30 MLD cycle thin films. Spectra were measured in the region 2600-3600 cm^{-1} under nitrogen atmosphere.

2.3.5 Investigation of Atomic Environments and Chemical Bonding using XPS

Along with infrared spectroscopy, X-ray photoelectron spectroscopy (XPS) can also be used to investigate the bonding to as-synthesized polyurea thin films. The atomic environments and chemical bonding in the thin films can be discussed using XPS fine scan spectra. Figure 2.7 and Figure 2.8 depict C 1s and N 1s XPS fine scan spectra of 10, 20, and 30 MLD cycle films, respectively.

The C 1s fine scan spectra showed three different types of carbon species in all MLD films. The lowest binding energy peak at 284.5 eV resulted from the electron-rich aromatic carbon. The highest binding energy peak near 288.6 eV resulted from the carbonyl carbon (C=O) from urea linkage. The intermediate peak at 285.9 eV resulted from the combination of alkyl carbon and substituted aromatic carbon linked with urea. These assignments of the C 1s fine scan spectra are consistent with other reports of the polyurea-based and thiourea-based MLD literature.[30,31] These assignments confirm the formation of urea into thin films. The IR results also reinforce urea bond formation, indicating that the reaction between amine and isocyanate functionalities form polyurea networks via a urea-coupling reaction.

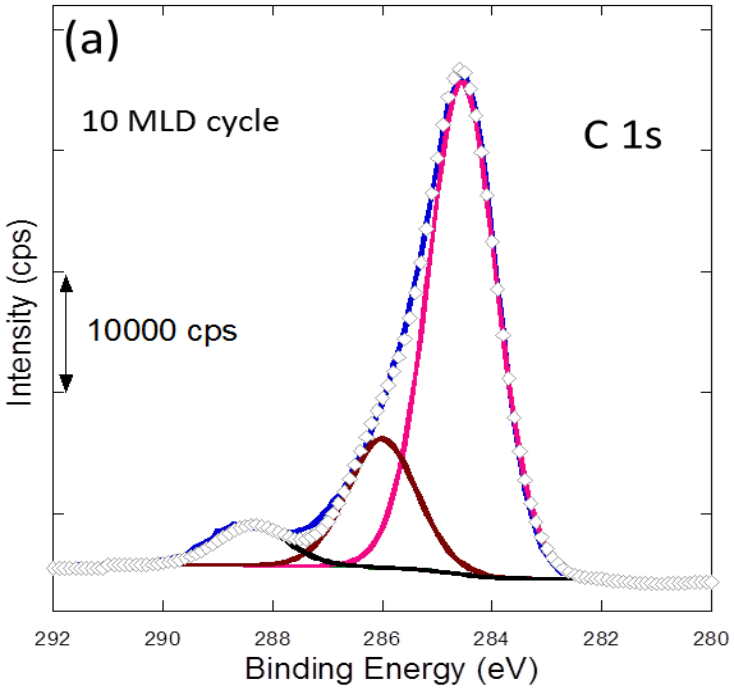
(a)
10 MLD cycle
C 1s
Intensity (cps)
10000 cps
292
290
288
286
284
282
280
Binding Energy (eV)

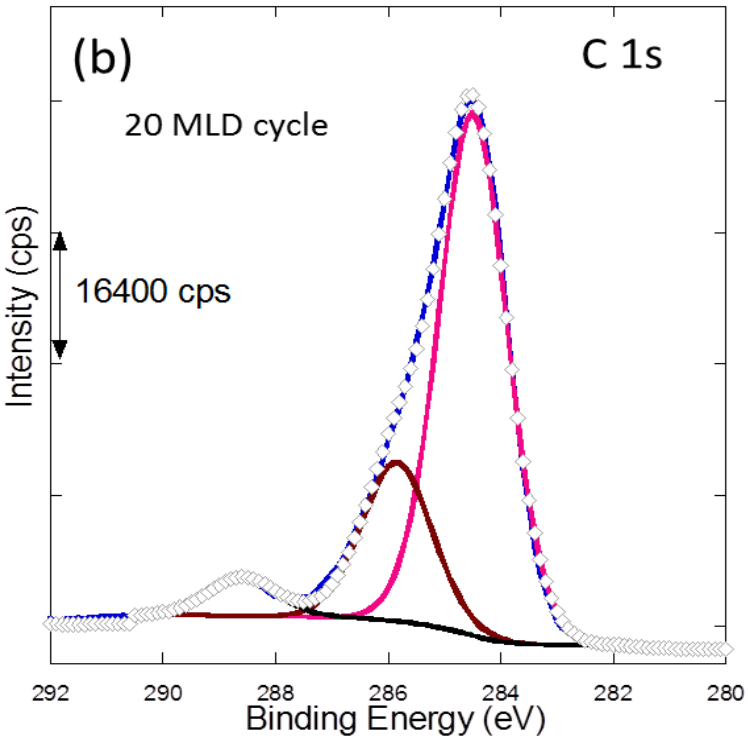
(b)
C 1s
20 MLD cycle
Intensity (cps)
16400 cps
292
290
288
286
284
282
280
Binding Energy (eV)

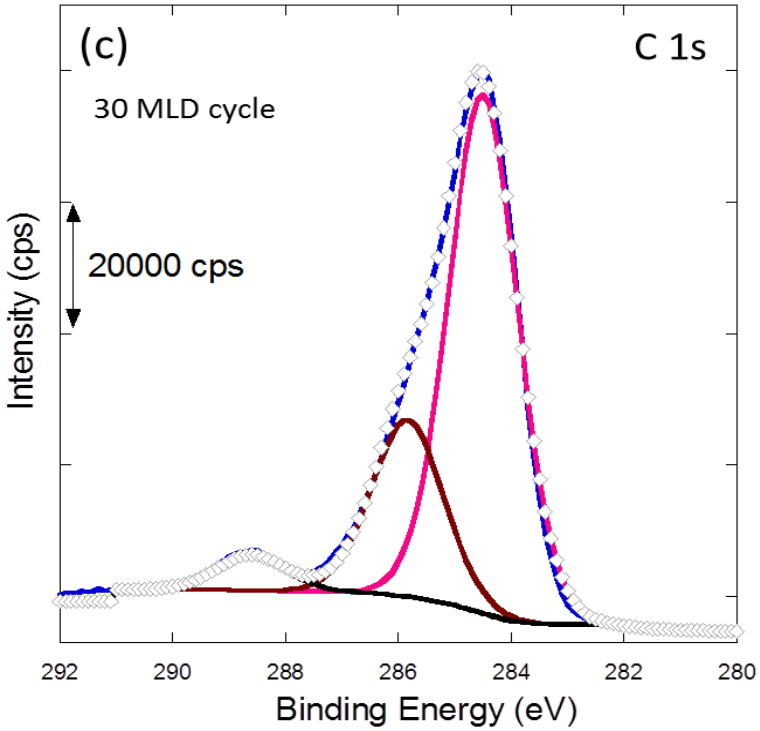

Figure 2.7. XPS fine scan spectra of C 1s at (a) 10, (b) 20, and (c) 30 MLD cycle films.

The N 1s fine scan spectra also contained three isolated peaks (Figure 2.8). The intermediate binding energy peak at 399.9 eV corresponds to urea groups.[30,36] The lower binding energy at 399.3 eV and higher binding energy at 401.3 eV are attributed to nonhydrogen-bonded and hydrogen-bonded free amine groups, respectively, in polyurea thin films.[37] N 1s for isocyanate was not detected because the unreacted isocyanate groups are converted easily to amine by exposure to humid air.[36] This results are consistent with FTIR results discussed above.

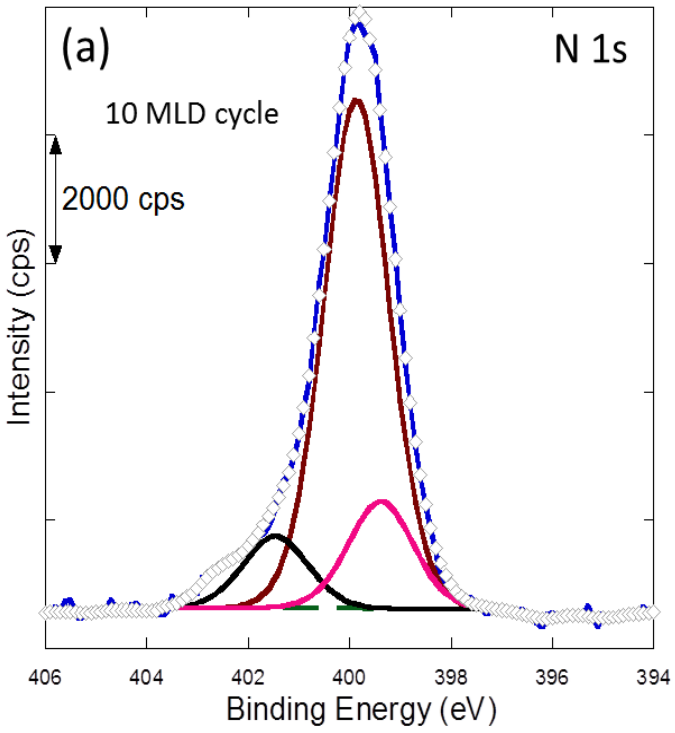
(a)
N 1s
10 MLD cycle
2000 cps
Intensity (cps)
406
404
402
400
398
396
394
Binding Energy (eV)

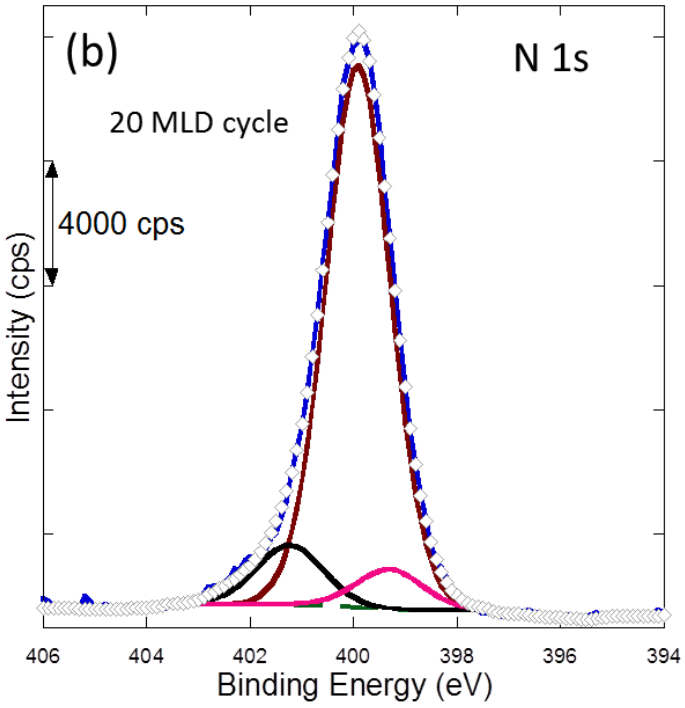
(b)
N 1s
20 MLD cycle
4000 cps
Intensity (cps)
406
404
402
400
398
396
394
Binding Energy (eV)

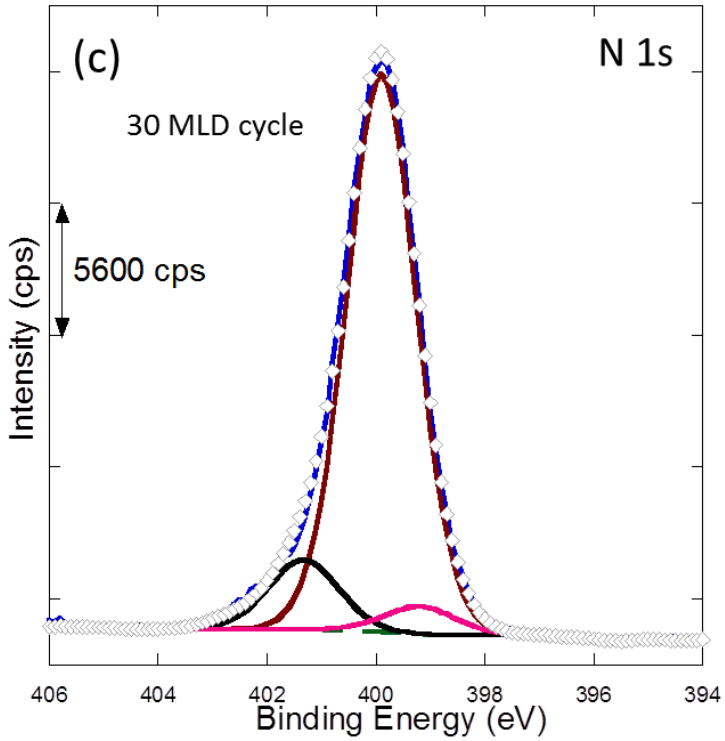

Figure 2.8. XPS fine scan spectra of N 1s at (a) 10, (b) 20, and (c) 30 MLD cycle films.

From Table 2.1, results show that the peak intensity percentage of N 1s for urea linkage increases from 74 to 85% with layer growth. The urea density apparently increased with layer growth. This revealed that different degrees of cross-linking were formed among layers proximate to the surface and extending away from the surface. This degree of cross-linking might also influence the mass density (g/cm^3) of 10, 20, and 30 MLD cycle films.

Table 2.1. Peak Widths and Intensity of the Deconvoluted N 1s in 10, 20, and 30 MLD Cycle Films

	N 1s in urea	N 1s in amine	N 1s in H-bonded amine
10 Cycles			
Binding Energy (eV)	399.9	399.3	401.4
FWHM (eV)	1.49	1.49	1.49
Peak area (%)	73.97	15.57	10.44
20 Cycles			
Binding Energy (eV)	399.9	399.3	401.3
FWHM (eV)	1.44	1.49	1.49
Peak area (%)	84.0	6.41	9.59
30 Cycles			
Binding Energy (eV)	399.9	399.2	401.3
FWHM (eV)	1.46	1.50	1.49
Peak area (%)	84.82	4.30	10.87

However, inspection of the peak intensity ratio of three carbon species is not applicable because of the presence of adventitious carbon in thin films. This adventitious carbon might influence the intensity ratio of carbon species.

Finally, UV-vis, IR, and XPS results revealed that sequential deposition of amine and isocyanate functionalities produces polyurea networks and demonstrates multilayer growth.

2.3.6 Examination of Surface Morphology by AFM

Molecular layer deposition (MLD) technique has an advantage to fabricate smooth films with minimal roughness.[34] Tapping mode atomic force microscopy (AFM) was carried out to investigate the surface morphology of the polyurea thin films in open atmosphere. Figure 2.9 represents AFM (height) image of 10, 20, and 30 MLD cycle films. Root mean square (RMS) roughness analysis revealed that a smooth film surface with a maximum roughness is 1.20 nm. This roughness result is quite consistent with estimated roughness by XRR (discussed in next). Narrow scan area analysis of 10 MLD cycle film show a grain like morphology with dense packed (Figure 2.10).

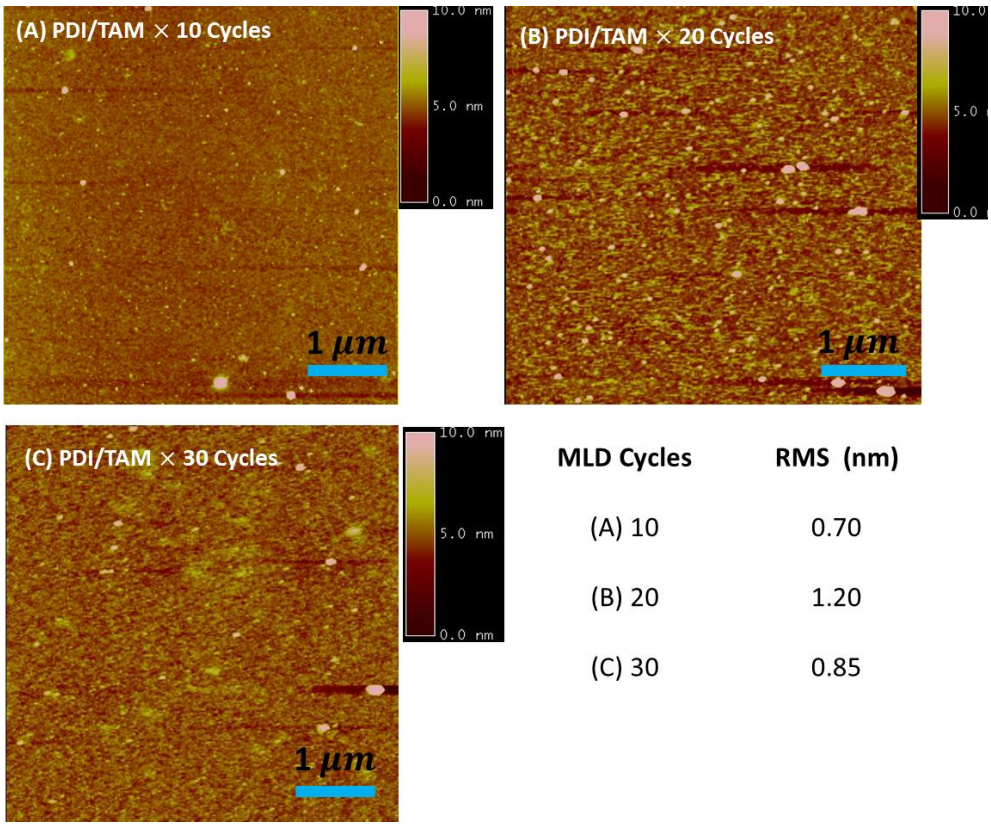

MLD Cycles	RMS (nm)
(A) 10	0.70
(B) 20	1.20
(C) 30	0.85

Figure 2.9. AFM (height) image for surface morphology (A) 10 MLD cycle, (B) 20 MLD cycle, and (C) 30 MLD cycle films (scan area 5 μm × 5 μm).

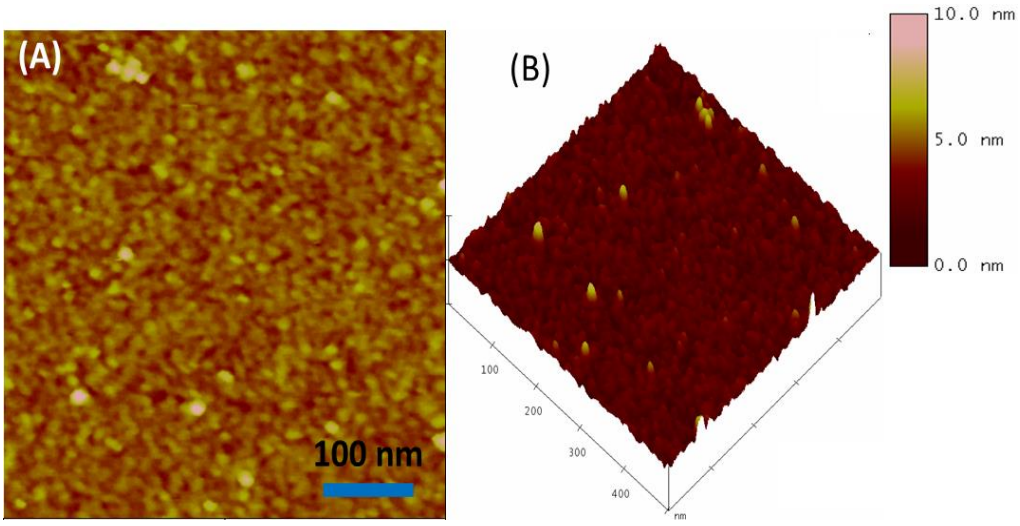

Figure 2.10. AFM image of 10 MLD cycle film (A) 2D (B) 3D (scan area 0.5 μm ×

0.5 μm).

2.3.7 Films Thickness, Mass Density and Roughness Analysis by XRR

In this research, the author performed a systematic study to evaluate films internal structure within layer growth. X-ray reflectometry (XRR) is ideally suited to investigate internal properties of multilayered film on solid surface, yielding data on sub-surface structure and polymer properties. Therefore, to evaluate the film thickness, film mass density, and interface roughness, XRR measurements were performed. XRR is a powerful tool for accurate measurement of multilayer thin film thickness, film mass density, and interface roughness.[43-45] Figure 2.11 shows XRR curves for 10, 20, and 30 MLD cycle films. From the XRR simulated fringes of Figure 2.11, film thickness, film mass density, and roughness of 10, 20, and 30 MLD cycle films were estimated.

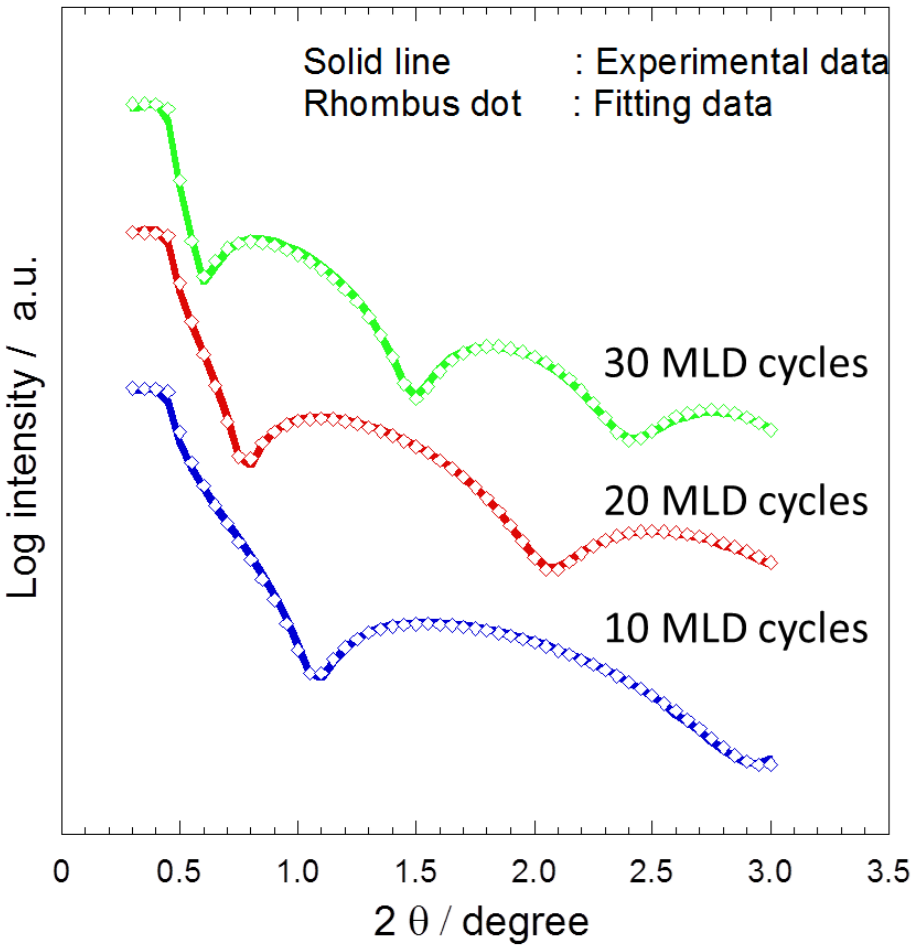

Figure 2.11. XRR profiles of different MLD cycles thin films. Solid lines and rhombus dots represent experimental and fitting data.

For XRR fitting curves, the simulated fringe satisfactorily fit with the experimental fringe profile in the case of 10 MLD cycles with a uniform density (Figure 2.12 (A)). In the case of 20 and 30 MLD cycle films, the results of satisfactory fit with a uniform density could not be obtained. More close fit has been tired with a bilayer model as shown in Figure 2.12 (B). The fit results were found to improve at the sufficiently satisfactory level. Figure 2.13 shows the comparison of bilayer and single layer fitting in 30 MLD cycle film. The statistical fitting variable χ^2 value reduced in bilayer fitting model in compare with single layer model, from 1.60 to 0.26. This result reflects the best fitting was observed in non-uniform density model rather than uniform density in thicker films case. However, the density around the boundary between the free interface layer and interfacial layer might intergrade. These results suggest the non-uniform density structure in the thicker film (20 and 30 MLD cycle films).

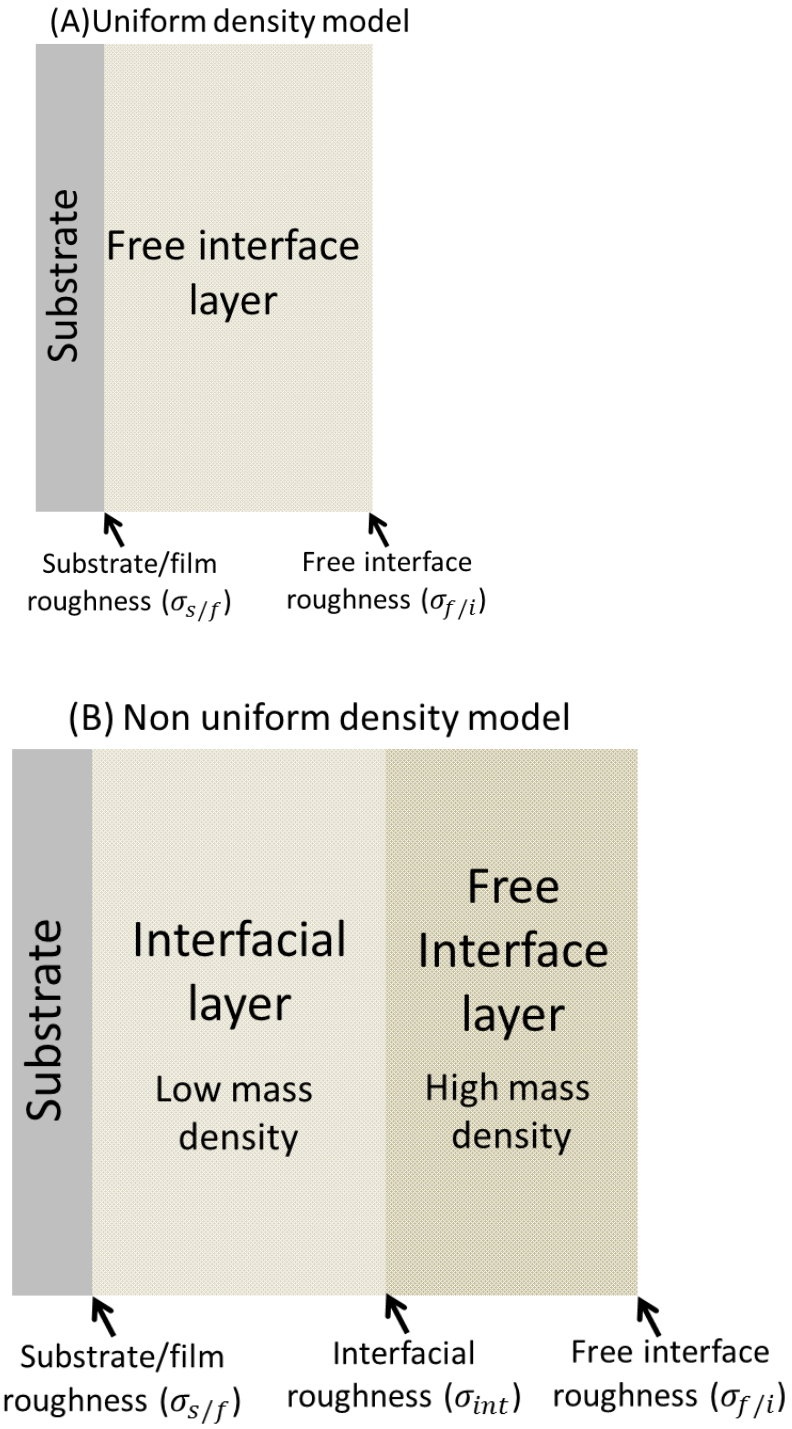

Figure 2.12. Schematic illustration of layer growth with (A) uniform density (B) non uniform densities.

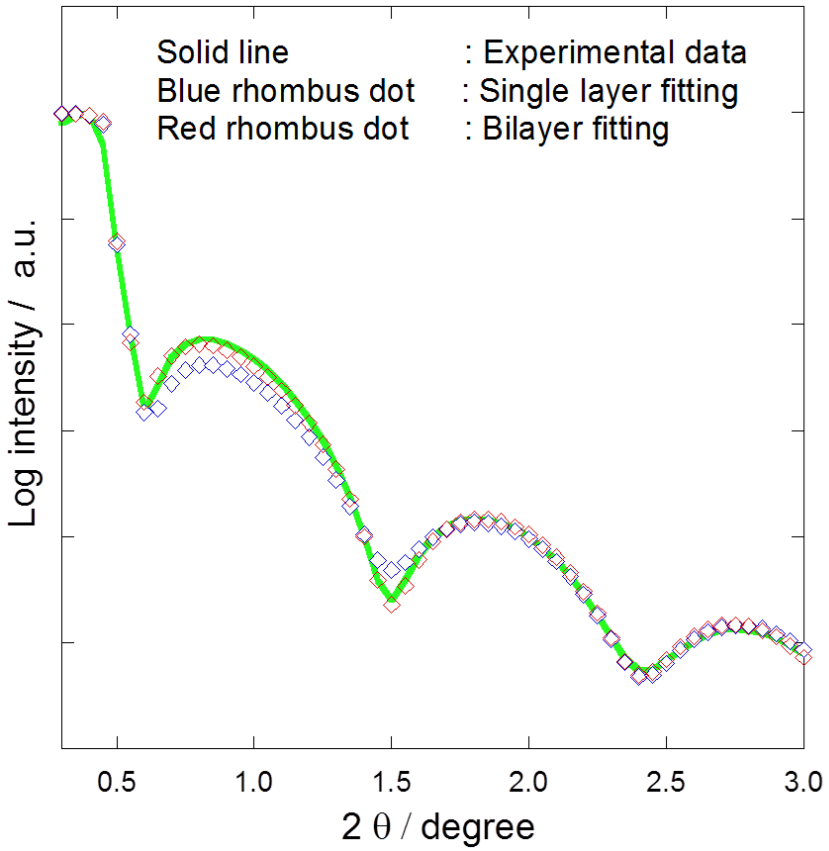

Figure 2.13. XRR comparison fitting profile of 30 MLD cycle film. Solid line represents experimental data and blue rhombus dot and red rhombus dot represent single layer and bilayer fitting, respectively.

From XRR measurements, the respective thicknesses of 10, 20, and 30 MLD cycle films were 4.55, 6.59, and 9.44 nm. This replies nonlinear thickness growth (in average) per cycle with respect to MLD cycles. AFM results support this nonlinear thickness growth as shown in Figure 2.4. Therefore, it is clear to say that the films density should vary with number of deposition cycles.

XRR density profiles (Figure 2.14) showed that the film mass density of 10 MLD cycle film is constant throughout the film depth. However, for 20 and 30 MLD cycle films, the mass density is not uniform throughout the range of film depths. The mass density of the free interface (f/i) region is ca. 16% higher than that of the interfacial layer (int.) region.

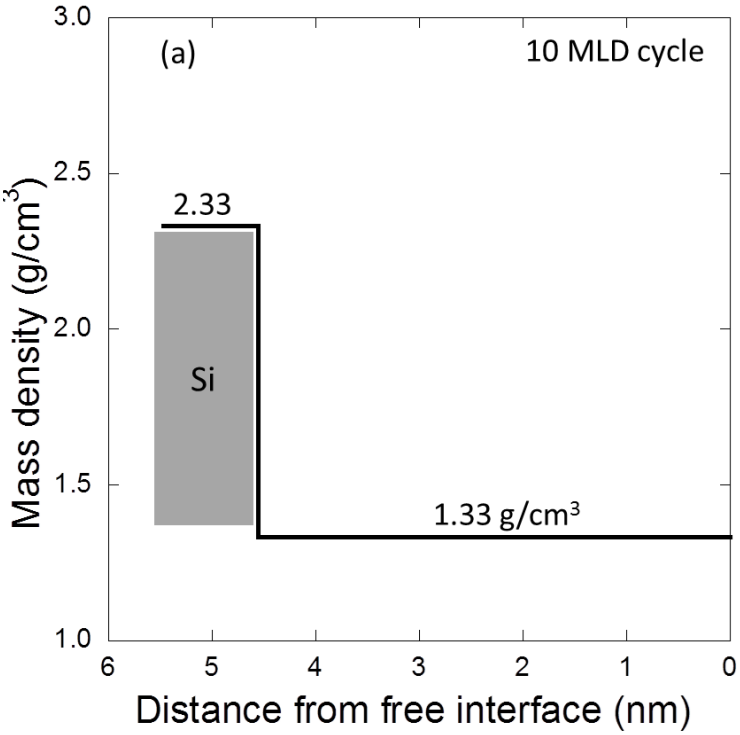

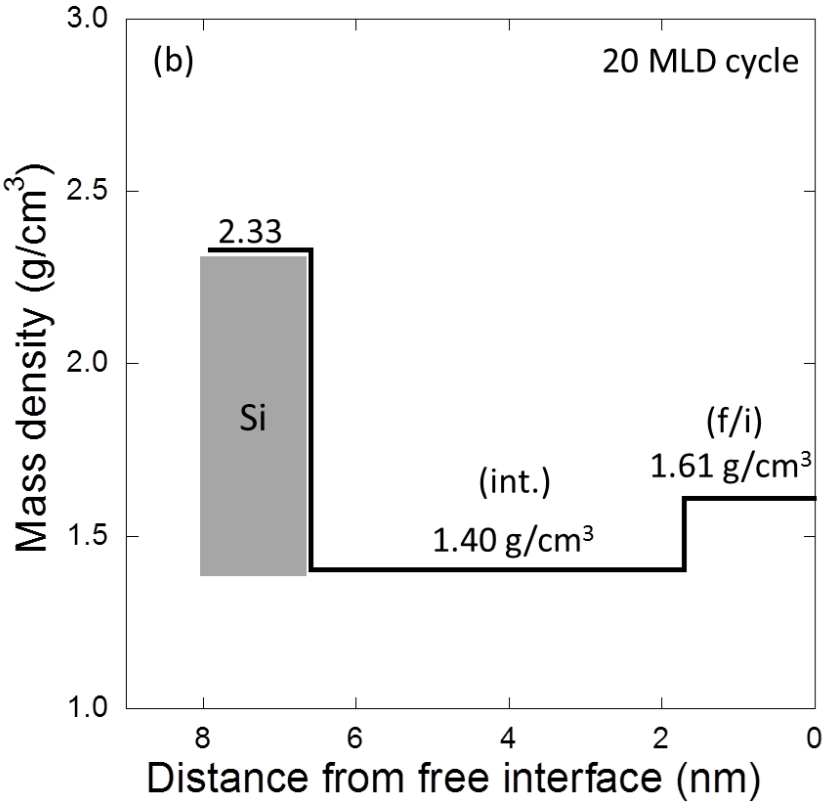
(b)
20 MLD cycle
2.33
Si
(int.)
1.40 g/cm3
(f/i)
1.61 g/cm3
Mass density (g/cm3)
Distance from free interface (nm)
3.0
2.5
2.0
1.5
1.0
8
6
4
2
0

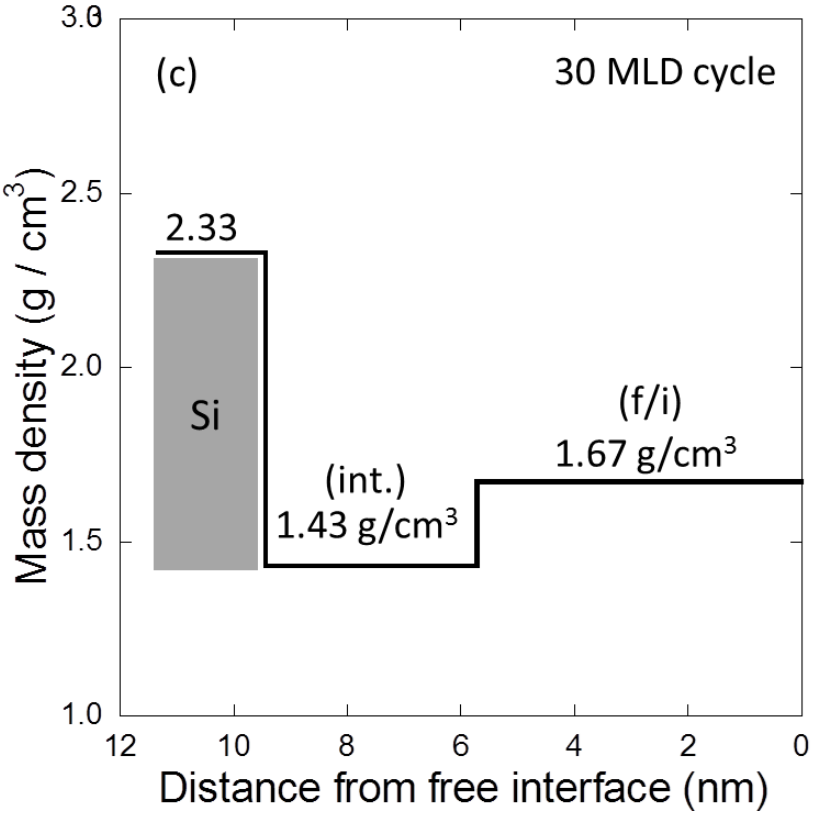

Figure 2.14. Film mass density (g/cm^3) profiles of simulated models for (a) 10 MLD cycle, (b) 20 MLD cycle, and (c) 30 MLD cycle thin films as a function of distance from the free interface.

Followed by films surface/interface roughness, 20 and 30 MLD cycle films was demonstrated three different roughness parameters; roughness between substrate and thin film ($\sigma_{s/f}$), roughness in free interface ($\sigma_{f/i}$) and interfacial roughness of different densities adjacent layers (σ_{int}) (Figure 2.12 (B)). In this present work, the roughness between substrate and thin film ($\sigma_{s/f}$) was considered as constant, $\sigma_{s/f} = \sigma_{Si} =$ 0.5 nm, which was determined by XRR measurement of a blank silicon wafer.

The statistical deviations between experimental and fitting XRR results for 10, 20, and 30 MLD cycle films was extracted from XRR oscillation fringes profile (Figure 2.11). From statistical deviations value (Table 2.2), it was found that the deviation is not so large. Therefore, it is considerable that the estimated density, thickness and roughness from XRR simulation are acceptable.

Table 2.2. Thickness, *d*, mass density, ρ, and roughness, σ of reported layers of 10, 20, and 30 MLD cycle thin films was extracted from the XRR profile shown in Figure 2.11. The statistical errors are shown in each value.

No. of MLD cycles	Layer name	Thickness, *d* (nm)	Mass density, ρ (g/cm^3)	Roughness, σ (nm)
10	Si wafer	0.00	2.33	0.5 ($\sigma_{s/f}$)
	Film	4.55 $\pm$ 0.03	1.33 $\pm$ 0.01	0.57 $\pm$ 0.03 ($\sigma_{f/i}$)
20	Si wafer	0.00	2.33	0.5 ($\sigma_{s/f}$)
	Film	4.89 $\pm$ 0.06 (int.)	1.40 $\pm$ 0.02 (int.)	0.85$\pm$ 0.3 (σ_{int})
		1.70 $\pm$ 0.06 (f/i)	1.61 $\pm$ 0.05 (f/i)	0.74 $\pm$ 0.04 ($\sigma_{f/i}$)
30	Si wafer	0.00	2.33	0.5 ($\sigma_{s/f}$)
	Film	3.73 $\pm$ 0.14 (int.)	1.43 $\pm$ 0.03 (int.)	0.68 $\pm$ 0.27 (σ_{int})
		5.71 $\pm$ 0.15 (f/i)	1.67 $\pm$ 0.04 (f/i)	0.60 $\pm$ 0.07 ($\sigma_{f/i}$)

$\boldsymbol{\sigma}_{s/f}$ denotes roughness of substrate/film interface, $\boldsymbol{\sigma}_{f/i}$ denotes roughness of free interface and $\boldsymbol{\sigma}_{int}$ represent interfacial roughness of different densities layers into thin films.

In 20 and 30 MLD cycle films, the non-linear densities phenomena might occur because of different packing densities among proximate to the surface (up to 3.5–5 nm thickness) and extending away from the surface (thicker than 3.5–5 nm). The XPS results support this hypothesis. Author assumes that these density changes might be observed according to the different degrees of interpenetration among organic molecular networks or different degrees of cross-linking. Because cross-linking introduces denser film[1] and the XPS results suggest that urea density increases with layer growth, this suggests that different degrees of cross-linking occurred among the layers near to the surface and extending away from the surface.

The propensity of cross-linking among molecular networks proximate to the substrate surface and extending away from the substrate surface can be considered with corresponding molecule–molecule interaction. Molecule–molecule interaction in layers extending away from the substrate surface might be considerably higher than that of near the substrate surface. Thereby, it is possible to change the degree of cross-linking proximate to the surface and extending away from the surface. This different degree of cross-linking can also be examined with changes in molecular volume ($Å^3$) in a single repeating unit within-layer deposition. Reportedly cross-linking increases the film density corresponding to the decrease in the molecular volume of each repeating unit.[1]

The repeating unit can be defined as the reactivity of four amine functional groups as one TAPM molecule with four isocyanate groups as two 1,3-PDI molecules. The molecular volume of each repeating unit can be extracted approximately by the mass-to-density ratio using the molecular mass of the single repeating unit and the film density obtained from XRR density profiles. This analysis revealed that the molecular volume in the free interface (f/i) region of 20 and 30 MLD cycle films decreases compared with that in the interfacial (int.) region (Table 2.3). The molecular volumes of the single repeating unit in the free interface (f/i) regions of 20 and 30 MLD cycle films are 722 and 696 $Å^3$, respectively. In contrast, the molecular volumes of the single repeating unit in the interfacial layers (int.) region of 20 and 30 MLD cycle films are 830 and 813 $Å^3$, respectively. This result reflects the presence of different degrees of cross-linking into thin films. This phenomenon is responsible for introducing nonlinear mass densities into thin films.

Table 2.3. Molecular volume of single repeated unit in 10, 20, and 30 MLD cycle films

MLD cycles	Total Thickness (nm)	Thickness (nm)	Mass density (g/cm^3)	Molecular volume ($Å^3$)
10	4.55	4.55	1.33	874
20	6.59	4.89 (int.) 1.70 (f/i)	1.40 (int.) 1.61 (f/i)	830 (int.) 722 (f/i)
30	9.44	3.73 (int.) 5.71 (f/i)	1.43 (int.) 1.67 (f/i)	813 (int.) 696 (f/i)

2.3.8 Investigation of Structural Ordering

To increase the film mass density with deposition cycles, structural change might occur. The molecular ordering of the thin film within layer growth has been investigated with grazing incidence small angle X-ray scattering (GI-SAXS) analysis. From GI-SAXS investigation, it was observed that the molecular ordering seems to be improved within number of deposition cycles or film thickness. Figure 2.15 represent 2D and 1D GI-SAXS profiles for the 10 MLD cycle film on Si wafer. No diffraction was observed neither in-plane (surface parallel) nor out-of-plane (surface normal) direction indicates random molecular arrangement. However, a clear diffraction was observed in the 30 MLD cycle film in 2D imaging plate at the out-of-plane direction at $2\theta_z = 12.5°$ (Figure 2.16) with a corresponding *d*-spacing value of 0.7 nm. This result indicates that the threshold thickness should be considered for molecular ordering of the thin films. In addition, it may conclude that molecular ordering seems to be improved in the surface normal direction of the substrate with a certain number of deposited layers. In the in-plane direction, no diffraction peak was observed in 10, 20, or 30 MLD cycle films, which indicates that the MLD thin film exhibits less molecular ordering in the in-plane direction.

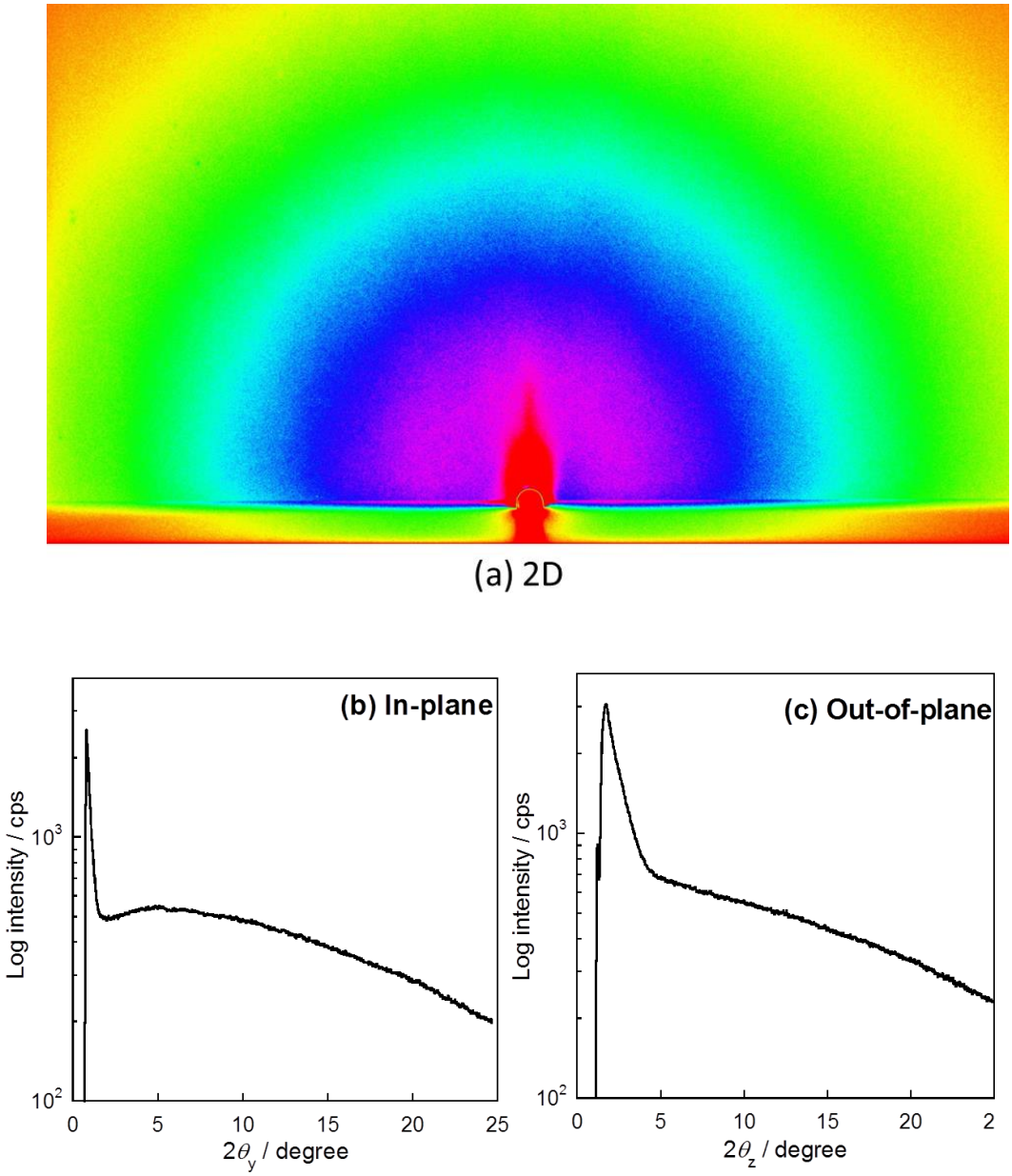

Figure 2.15. (a) 2D GI-SAXS imaging plate pattern of the 10 MLD cycle film on a Si surface. 1D profile in the (b) in-plane (c) out-of-plane direction extracted from the 2D GI-SAXS pattern.

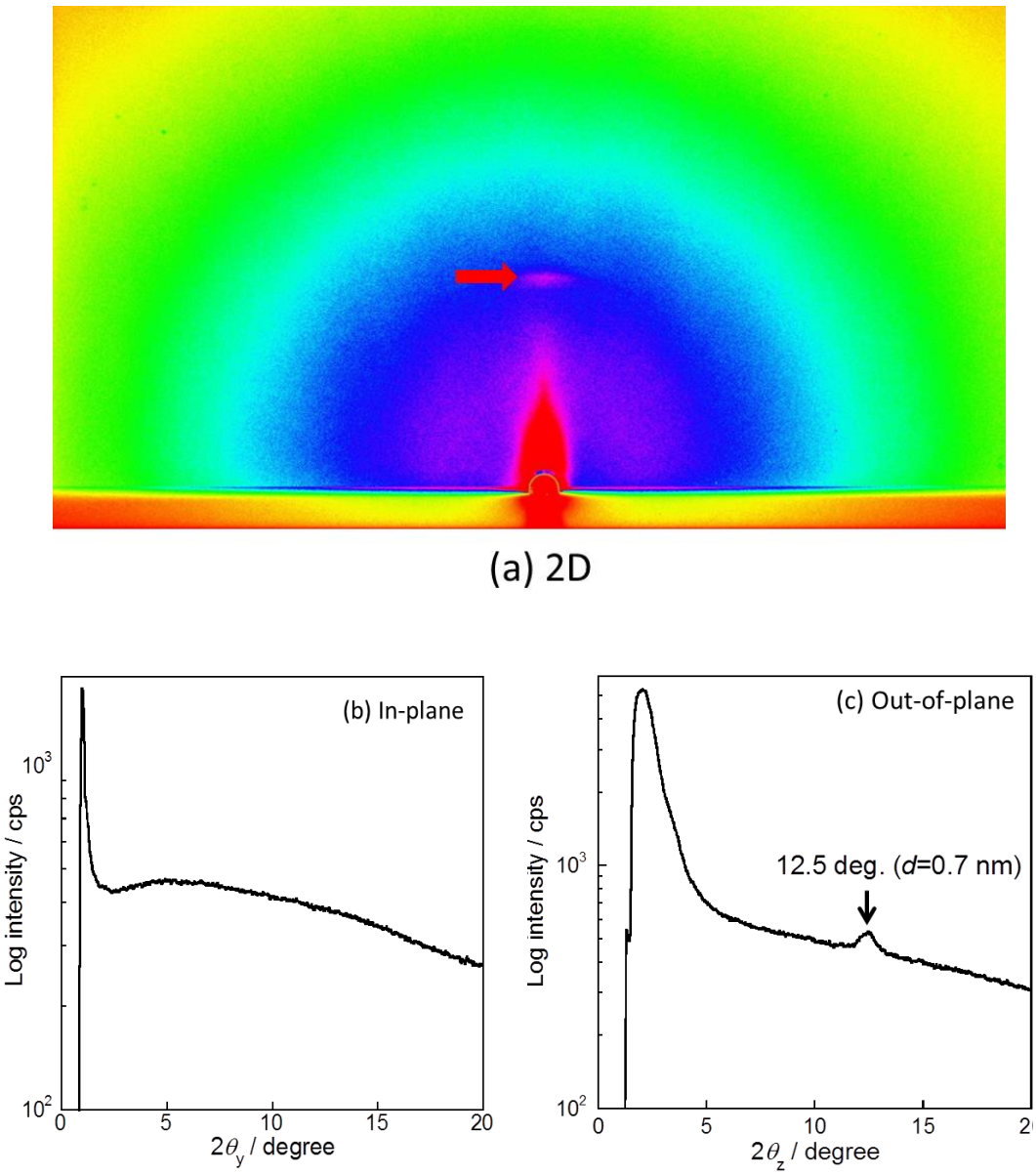

Figure 2.16. (a) 2D GI-SAXS imaging plate pattern of the 30 MLD cycle film on a Si surface. 1D profile in the (b) in-plane (c) out-of-plane direction extracted from the 2D GI-SAXS pattern.

2.4 CONCLUSIONS

Using solution-based MLD technique in ambient conditions, author synthesized 3D covalent bonded organic thin films with variable densities from sequential exposure of bifunctional 1,3-PDI and tetrafunctional TAPM precursors. This layer-assembled thin films exhibited multilayer growth. Fabricated thin films included three characteristic infrared vibrational bands for urea linkage, confirming the existence of polyurea networks' in the thin films. Furthermore, in the XPS study, peak splitting within N 1s and C 1s corresponded to the values expected for polyurea films. Results showed that structural periodicity and mass density (g/cm^3) of the thin films increased concomitantly with the number of MLD cycles. These unusual changes might result from different degrees of cross-linking of organic molecular networks proximate to the substrate surface and extending away from the substrate surface. This approach of synthesizing organic molecular networks with higher degrees of cross-linking can be extended to porous substrates that can be used for ion separation membranes.

REFERENCES

(1) Zhou, H.; Toney, M. F.; Bent, S. F. Cross-Linked Ultrathin Polyurea Films via Molecular Layer Deposition. *Macromolecules* **2013**, *46*, 5638-5643.

(2) Richert, L.; Engler, A. J.; Discher, D. E.; Picart, C. Elasticity of Native and Cross-Linked Polyelectrolyte Multilayer Films. *Biomacromolecules* **2004**, *5*, 1908-1916.

(3) Such, G. K.; Quinn, J. F.; Quinn, A.; Tjipto, E.; Caruso, F. Assembly of Ultrathin Polymer Multilayer Film by Click Chemistry. *J. Am. Chem. Soc.* **2006**, *128*, 9318-9319.

(4) Quinn, J. F.; Johnston, A. P. R.; Such, G. K.; Zelikin, A. N.; Caruso, F. Next Generation, Sequentially Assembled Ultrathin Films: Beyond Electrostatics. *Chem. Soc. Rev.* **2007**, *36*, 707-718.

(5) Wang, C.; Lee, W-Y.; Nakajima, R.; Mei, J.; Kim, D. H.; Bao, Z. Thiol–Ene Cross-Linked Polymer Gate Dielectrics for Low-Voltage Organic Thin-Film Transistor. *Chem. Mater.* **2013**, *25*, 4806-4812.

(6) Wang, Y.; Kim, Y.; Lee, E.; Kim, H. Fabrication of Organic Thin-Film Transistors Based on Cross-Linked Hybrid Dielectric Materials. *Jpn. J. Appl. Phys.* **2012**, *51*, 09MJ02 (1-5).

(7) Geise, G. M.; Lee, H. S.; Miller, D. J.; Freeman, B. D.; Mcgrath, J. E.; Paul, D. R. Water Purification by Membranes: The Role of Polymer Science. *J. Polym. Sci. Part B: Polym. Phys.* **2010**, *48*, 1685-1718.

(8) Yimsiri, P.; Mackley, M. R. Spin and Dip Coating of Light Emitting Polymer Solution: Matching Experiment with Modeling. *Chem. Eng. Sci*. **2006**, *61*, 3496-3505.

(9) Ulman, A. *An Introduction to Ultrathin Organic Films from Langmuir–Blodgett to Self-Assembly*; Academic Press: San Diego, CA, 1991.

(10) George, S. M.; Yoon, B.; Dameron, A. A. Surface Chemistry for Molecular Layer Deposition of Organic and Hybrid Organic-Inorganic polymers. *Acc. Chem. Res.* **2009**, *42*, 498-508.

(11) Zhou, H.; Bent, S. F. Fabrication of Organic Interfacial Layers by Molecular Layer Deposition: Present Status and Future Opportunities. *J. Vac. Sci. Technol., A* **2013**, *31*, 040801-040818.

(12) Sundberg, P.; Karppine, M. Inorganic–Organic Thin Film Structures by Molecular Layer Deposition: A review. *Beilstein J. Nanotechnol.* **2014**, *5*, 1104-1136.

(13) Seo, J.; Schattling, P.; Lang, T.; Jochum, F.; Nilles, K.; Theato, P.; Char, K. Covalently Bonded Layer-by-Layer Assembly of Multifunctional Thin Films

Based on Activated Esters. *Langmuir* **2010**, *26*, 1830-1836.

(14) Guin, T.; Cho, J. H.; Xiang, F.; Ellison, C. J.; Grunlan, J. C. Water-Based Melanin Multilayer Thin Films with Broadband UV Absorption. *ACS Macro Lett.* **2015**, *4*, 335-338.

(15) Chan, R.; Bent, S. F. Chemistry for Positive Pattern Transfer Using Area-Selective Atomic Layer Deposition. *Adv. Mater.* **2006**, *18*, 1086-1090

(16) Chan, R.; Bent, S. F. Highly Stable Monolayer Resists for Atomic Layer Deposition on Germanium and Silicon, *Chem. Mater.* **2006**, *18*, 3733-3741.

(17) Jiang, X.; Huang, H.; Prinz, F. B.; Bent, S. F. Application of Atomic Layer Deposition of Platinum to Solid Oxide Fuel Cells. *Chem. Mater.* **2008**, *20*, 3897-3905.

(18) Adamczyk, N. M.; Dameron, A. A.; George, S. M. Molecular Layer Deposition of Poly(p-phenyleneterephthalamide) Films Using Terephthaloyl Chloride and p-Phenylenediamine. *Langmuir* **2008**, *24*, 2081-2089.

(19) Du, Y.; George, S. M. Molecular Layer Deposition of Nylon 66 Films Examined Using in situ FTIR Spectroscopy. *J. Phys. Chem. C* **2007**, *111*, 8509-8517.

(20) Peng, Q.; Efimenko, K.; Genzer, J.; Pardsons, G. N. Oligomer Orientation in

Vapor-Molecular-Layer-Deposited Alkyl-Aromatic Polyamide films. *Langmuir* **2012**, *28*, 10464-10470.

(21) Bizer, T.; Richardson, N. V. Demonstration of an Imide Coupling Reaction on a Si(100) -2 ×1 Surface by Molecular Layer Deposition. *Appl. Phys. Lett.* **1997**, *71*, 662-664.

(22) Yoshimura, T.; Tatsuura, S.; Sotoyama, W. Polymer Films Formed with Monolayer Growth Steps by Molecular Layer Deposition. *Appl. Phys. Lett.* **1991**, *59*, 482-484.

(23) Yoshida, S.; Ono, T.; Esashi, M. Deposition of Conductivity-Switching Polyimide Film by Molecular Layer Deposition and Electrical Modification using Scanning Probe Microscope. *Micro. Nano Lett.* **2010**, *5*, 321-323.

(24)Yoshida, S.; Ono, T.; Esashi, M. Local Electrical Modification of a Conductivity-Switching Polyimide Film Formed by Molecular Layer Deposition. *Nanotechnology* **2011**, *22*, 335302.

(25) Haq, S.; Richardson N. V. Organic Beam Epitaxy Using Controlled PMDA−ODA Coupling Reactions on Cu{110}. *J. Phys. Chem. B* **1999**, *71*, 5256-5265.

(26) Lee, J. S.; Lee, Y. J.; Tae, E. L.; Park, Y. S.; Yoon, K. B. Synthesis of Zeolite as Ordered Multicrystal Arrays. *Science* **2003**, *301*, 818-821.

(27) Prasittichai, C.; Zhou, H.; Bent, S. F. Area Selective Molecular Layer Deposition of

Polyurea Films. *ACS Appl. Mater. Interfaces* **2013**, *5*, 13391-13396.

(28) Zhou, H.; Bent. S. F. Molecular Layer Deposition of Functional Thin Films for Advanced Lithographic Patterning. *ACS Appl. Mater. Interfaces* **2011**, *3*, 505-511.

(29) Kim, A.; Filler, M. A.; Kim, S.; Bent, S. F. Layer-by-Layer Growth on Ge (100) via Spontaneous Urea Coupling Reactions. *J. Am. Chem. Soc.* **2005**, *127*, 6123-6132.

(30) Loscutoff, P. W.; Zhou, H.; Clendenning, S. B.; Bent, S. F. Formation of Organic Nanoscale Laminates and Blends by Molecular Layer Deposition. *ACS Nano* **2010**, *4*, 331-341.

(31) Loscutoff, P. W.; Lee, H. B. R.; Bent S. F. Deposition of Ultrathin Polythiourea Films by Molecular Layer Deposition. *Chem. Mater*. **2010**, *22*, 5563-5569.

(32) Ivanova, Y. V.; Maydannik, P. S.; Cameron, D. C. Molecular Layer Deposition of Polyethylene Terephthalate Thin Film. *J. Vac. Sci. Technol., A* **2012**, *30*, 01A121 (1-5).

(33) Qian, H.; Li, S.; Zheng, J.; Zhang, S. Ultrathin Films of Organic Networks as Nanofiltration Membranes via Solution-Based Molecular Layer Deposition. *Langmuir* **2012**, *28*, 17803-17810.

(34) Johnson, P. M.; Yoon, J.; Kelly, J. Y.; Howarter, J. A.; Stafford, C. M. Molecular Layer-by-Layer Deposition of Highly Crosslinked Polyamide Films. *J. Polym. Sci.*

Part B: Polym. Phys. **2012**, *50*, 168-173.

(35) Chan, E. P.; Lee, J-H.; Chung, J. Y.; Stafford, C. M. An Automatic Spin-Assisted Approach for Molecular Layer-by-Layer Assembly of Crosslinked Polymer Thin Films. *Rev. Sci. Instrum.* **2012**, *83*, 114102 (1-6).

(36) Kim, M.; Byeon, M.; Bae, J-S.; Moon, S. Y.; Yu, G.; Shin. K.; Basarir, F.; Yoon, T. H.; Park, J-W. Preparation of Ultrathin Films of Molecular Networks through Layer-by-Layer Cross-Linking Polymerization of Tetrafunctional Monomers. *Macromolecules* **2011**, *44*, 7092-7095.

(37) Graf, N.; Yegen, E.; Gross, T.; Lippitz, A.; Weigel, W.; Krakert, S.; Terfort, A.; Unger, W. E. S. XPS and NEXAFS Studies of Aliphatic and Aromatic Amine Species on Functionalized Surfaces. *Surf. Sci.* **2009**, *603*, 2849-2860.

(38) Ulman, A. Formation and Structure of Self-Assembled Monolayer, *Chem. Rev.* **1996**, *96*, 1533-1554.

(39) Kohli, P.; Blanchard, G. J. Applying Polymer Chemistry to Interfaces: Layer-by-Layer and Spontaneous Growth of Covalently Bound Multilayers. *Langmuir* **2000**, *16*, 4655-4661.

(40) Coleman, M. M.; Sobkowiak, M.; Pehlert, G. J.; Painter, P. C.; Iqbal, T. Infrared Temperature Studies of a Simple Polyurea. *Macromol. Chem. Phys.* **1997**, *198*,

117-136.

(41) Coleman, M. M.; Skrovanek, D. J.; Howe, S. E.; Painter, P. C. On the Validity of a Commonly Employed Infrared Procedure used to Determine Thermodynamic Parameters Associated with Hydrogen Bonding in Polymers. *Macromolecules* **1985,** *18*, 299-301.

(42) Coleman, M. M.; Lee, K. H.; Skrovanek, D. J.; Painter, P. C. Hydrogen Bonding in Polymers. 4. Infrared Temperature Studies of a Simple Polyurethane. *Macromolecules* **1986,** *19*, 2149-2157.

(43) Haque, H. A.; Hara, M.; Nagano, S.; Seki, T. Photoinduced In-Plane Motions of Azobenzene Mesogens Affected by the Flexibility of Underlying Amorphous Chains. *Macromolecules* **2013**, *46*, 8275-8283.

(44) Chason, E.; Mayer, T. M. Thin Film and Surface Characterization by Specular X-ray Reflectivity. *Critical Rev. Solid State Mat. Sci.* **1997**, *22*, 1-67.

(45) Stove, K.; Sakurai, K. Recent Theoretical Models in Grazing Incidence X-ray Reflectometry. *The Rigaku J.* **1997**, *14*, 22-37.

Chapter 3

Investigation of Surface Effect on Cross-linked Organic Multilayer Thin Film

In the previous chapter (chapter 2), the author has discussed the synthesis of 3D covalent bonded organic thin films using layer-by-layer deposition approach on propanol washed Si wafer. From the previous study, the non-linear mass density of the thin films was observed within layer deposition along with the improvement of molecular ordering after a certain number of layers depositions. This phenomenon might be achieved by varying the degree of cross-linking in molecular networks sited among near and extending away from the substrate surface. However, removing the native oxide layer from Si surface by Buffered Oxide Etch (BOE) as well as replaced the H-terminated Si to –OH terminated using short time O_2 plasma, demonstrated a significant change of multilayer films properties, especially, in film mass density. This may happen due to the formation of dense packed self-assembled monolayer (SAM), which is formed prior to the layer deposition. The polyurea networks in thin films are investigated by Fourier transform infrared spectroscopy (FTIR) and X-ray photoelectron spectroscopy (XPS) techniques. From IR spectra, three characteristics infrared bands of Amide I, Amide II and asymmetric ν_a(N-C-N) stretching band confirmed the formation of polyurea networks by alternate dipping into a solution of amine and isocyanate

functionality monomers. The deconvoluted component of the C 1s and N 1s spectra from XPS shows clear evidence of stable polyurea networks. Film mass density was inspected using X-ray reflectivity (XRR) analysis. This finding is crucially important to explore the surface phenomena of the multilayer films growth in MLD technique.

3.1 INTRODUCTION

Organic precursors deposited on semiconductor surface are a promising research arena of surface science which played a major role in the fabrication and development of molecular-based semiconductor devices. The deposition of organic molecules with precise functionalities at the semiconductor interface introduced novel properties to biological, chemical, and electronic device. However, the semiconductors' electronic and chemical natures influenced the deposition of precursors onto the surface. A number of studies of the covalent attachment of organic molecules to semiconductor surface have been conducted to comprehend the structure, reactivity, and interfacial properties of such hybrid inorganic/organic systems in gas phase condition.[1-5] By following the trend, one of the major research goals is to control the deposition of multiple organic layers to prepare precisely tailored surfaces.

To synthesize molecular-level controlled organic thin films on semiconductor surface, currently a number of deposition techniques are available such as Langmuir-Blodgett[6-7] film deposition and self-assembled monolayer formation.[8-9] Recently, a vacuum-based organic thin film deposition techniques, namely, molecular layer deposition (MLD),[10-12] an analogy of atomic layer deposition (ALD),[13-15] is growing interest for its versatility and simplicity. MLD process deposits conformal

ultrathin film based on sequential, self-limiting surface reaction. Since the introduction in the 1990s, a plenty of research have been reported based on molecular layer deposition techniques, where organic polymer are achieved using polymerization reaction. Polymeric films have been reported including reaction of acyl dichlorid with diamine to form polyamides,[16-19] reaction of dianhydrides and diamine to form polyimides,[20-23] reaction of diisocyanate and diamine to form polyurea,[24-29] reaction of diisothiocyanate and diamine to form polythiourea,[30] among others.[31-34]

However, this vacuum-based MLD technique for multilayer deposition faced several limitations, particularly, synthesis of organic thin films with multifunctional or bulky organic precursors. In contrast, solution-based MLD can offer an exclusive route to overcome this problem.[35-36]

In the previous chapter, the author has discussed the synthesis of 3D covalent bonded multilayer thin films based on sequentially deposited of bifunctional 1,3-phenylene diisocyanate (1,3-PDI) and tetrafunctional tetrakis(4-aminophenyl)methane (TAPM) monomers combination. In where, non-linear mass density phenomena were observed within layer deposition. It may happen due to the different degree of cross-linking properties among layers near to the substrate surface and extending away from the substrate surface. However, the role of substrate

surface properties and applied monomers was not certainly clear with this study. Therefore, in the present study the author has focused to synthesize thin films with same monomers combination and identical synthesis condition, on buffered oxide etch (BOE) followed by O_2 plasma treated Si surface using solution based MLD technique. Prior to the film formation a self-assembled monolayer was formed by using an amine-terminated silane-coupling agent.

In general, buffered oxide etch (BOE) followed by O_2 plasma treatment increased OH surface concentration on the substrate. It is considered that this change of OH surface concentration influenced the self-assembled monolayer property, which successively affects the film property. In ALD process, it has been proved that difference in the surface characteristics of the substrate can cause difference in ALD film growth, even though the experiment was carried out at the same reactant and experimental condition.[37-38] It is expected that, the hydrophilic property of the Si surface was enhanced by the O_2 plasma treatment through the conversion of H-terminated surface to OH surface. These provided more active sites to react with the H_3C-O-(methoxy) groups of APTMS i.e. increase organosilane nucleation density, introduces disorder and film defects in self-assembled monolayer.[8] This phenomenon may influence films properties by forming a significant numbers of double reaction between

initial deposited bifunctional isocyanate groups and surface attached amine groups (Figure 3.1).

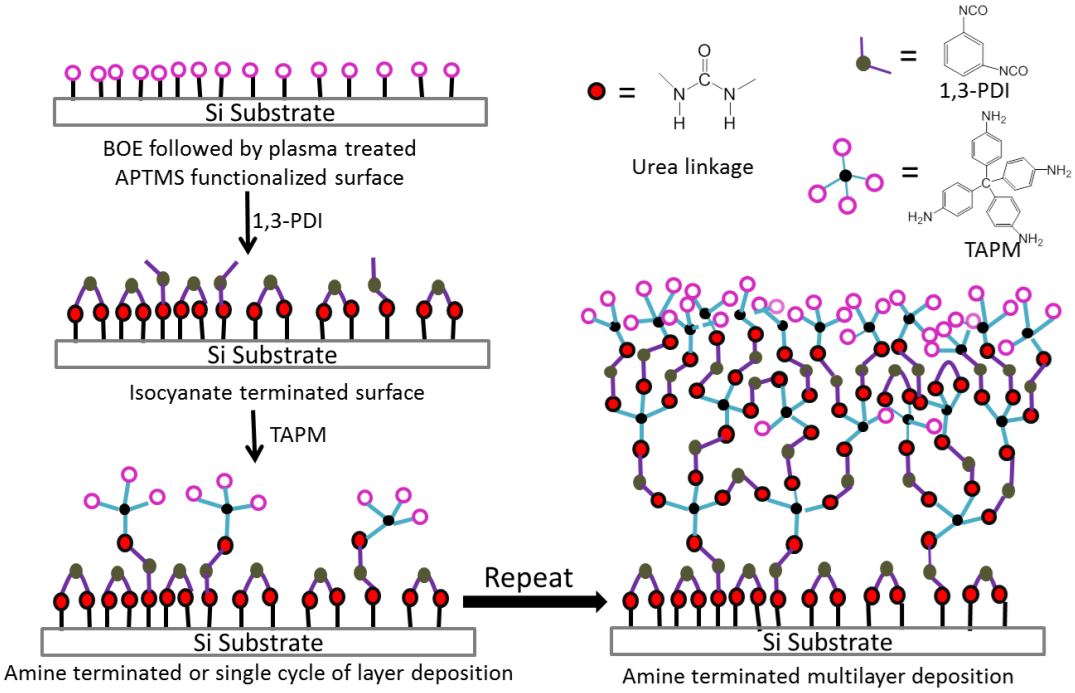

Figure 3.1. Schematic illustration of molecular layer deposition (MLD) process on a buffered oxide etch (BOE) followed by O_2 plasma treated Si surface and chemical structure of 1,3-PDI and TAPM monomers.

This work demonstrates spontaneous layer-by-layer surface reaction between isocyanate and amine functional moieties under solution processable MLD technique to get cross-linked polyurea thin films. Polyurea networks were confirmed using Fourier-transform infrared (FT-IR) spectroscopy and X-ray photoelectron spectroscopy (XPS) techniques. The thickness of the thin films was measured using atomic force

microscopy (AFM) technique, and films mass density is inspected with X-ray reflectivity (XRR) analysis. Prior to the film deposition the surface morphology and chemical/electronic state of self-assembled monolayer investigated using XPS and AFM techniques.

3.2 EXPERIMENTAL SECTION

3.2.1 Materials

As molecular building blocks, tetrakis(4-aminophenyl)methane (TAPM) and 1,3-phenylene diisocyanate (PDI) were purchased, respectively, from Manchester Organics, UK and Tokyo Chemical Industry Co. Ltd., Japan. Using recrystallization technique, 98% pure commercial PDI was purified further. 3-Aminopropyltrimethoxysilane (APTMS, >96%) was purchased from Tokyo Chemical Industry Co. Ltd., Japan, and was used as received. All solvents (super-dehydrated and AR grade) were purchased from Wako Pure Chemical Industries Ltd., Japan and were used without further purification.

3.2.2 Surface Cleaning

Si wafers of p-type silicon (p−Si(100), 5 − 20 Ω−cm), boron doped were used in this study. The silicon wafers were cut with a diamond (40 × 20 mm^2, t = 0.5 mm) and the substrates were cleaned using 2−propanol with ultrasonic bath (three times each 15 min duration), and finally, dried and kept in a clean bench. The propanol washed substrates were then treated with an aqueous NH_4HF_2 buffer (2.9 %) (STELLA CHEMIFA, Singapore) to remove the native oxide layer from Si surface. Finally, substrates were washed with deionized water, dried under an argon stream and

immediately, put in O_2 plasma chamber (CUTE-MP, Femto Science Inc. Korea) and treated with O_2 Plasma (10 sec, p = 50 pa). These plasma treated substrates were kept in ethanol solution to protect it from air contract. Maximum curation was taken to protect the Si substrates to avoid from air contact.

3.2.3 Self-assembled Monolayer (SAM) Formation

The BOE followed by O_2 plasma treated substrates were immersed into 10 mM amine-functionalized 3-aminopropyltrimethoxysilane (APTMS) in ethanol solution at room temperature for 1 h under Ar atmosphere with constant stirring. After taking out from the APTMS solution, substrates were cleaned using ethanol (twice) and 2-propanol (twice) consecutively with sonication and finally rinsed with 2-propanol and dried. Finally, APTMS modified substrates kept in a clean bench for multilayer film formation within 24 hours.

3.2.4 Multilayer Thin Film Formation

These amine-terminated substrates were used for multilayer thin film formation using an automatic LbL system. Layer deposition was carried out in the previous chapter described procedures: (i) amine-functionalized substrate was immersed into 17.6 mM 1,3-PDI in 1,4-dioxane and toluene (3:1, v/v) solution for 5 min. Then, the substrate was rinsed in five separate containers with organic solvent, 1,4-dioxane and

toluene mixture, THF and chloroform, respectively. (ii) After washing, the isocyanate-terminated substrate was immersed into 3.78 mM TAPM in 1,4-dioxane and toluene (3:1, v/v) solution for 5 min, followed by rinsing successively in four separate containers with 1, 4-dioxane and toluene mixture, and THF. The deposited substrate was dried under Ar atmosphere. This bilayer deposition process described above [steps (i) and (ii)] was designated as a single cycle of molecular layer deposition (MLD). Multilayer thin films were formed by repeating the procedure described above in a desired number of cycles. In every cycle, the amine-terminated surface is regarded as a top surface.

3.2.5 Instrumentation and Analysis Condition

3.2.5.1 X-ray Photoelectron Spectroscopy (XPS)

XPS study was performed using a Shimadzu Kratos Axis−Ultra (Kratos Analytical Ltd.) DLS high performance XPS system. Photoelectron was excited by monochromated Al Kα radiation source (1486.6 eV). Spectra were taken at 90° normal to the specimen surface. A neutralizer gun used to reduce charging of the samples. Energy calibration and component separation were conducted using the bundled software with pure Gaussian profile and a Shirley background. C 1s at binding energy 284.5 eV was used as standard calibration condition.

3.2.5.2 Atomic Force Microscopy (AFM)

Surface morphology of bare Si wafer and APTMS modified Si wafer was investigated by AFM, under following experimental conditions. For surface morphology investigation, atomic force microscopy (AFM, Nanoscope IIIa; Veeco Instruments) with tapping mode was used. Silicon cantilevers (SI-DF3FM; Nanosensors Corp.) with a spring constant between 2.8 and 4.4 Nm^{-1} and a resonance frequency of 79–89 kHz were used. The measurements were taken under an air atmosphere with a scan rate of 0.4 Hz and scan size of $5 \times 5\ \mu m^2$.

Thickness of multilayer films was measured using an AFM (VN–8000;

Keyence Co.) equipped with a DFM/SS mode cantilever (OP−75041; Keyence Co.). During thickness measurement, films were partly scratched with sharp blade and height difference was evaluated for film thickness. Thickness was measured at least six different positions of each sample and got an average value.

3.2.5.3 IR Spectra

Fourier-transform infrared (FTIR) spectroscopy was used to investigate the formation of a urea bond of the thin films on the substrate. Infrared spectra were collected using an FTIR spectrometer (Nicolet 6700; Thermo Fisher Scientific Inc.) equipped with a mercury cadmium telluride (MCT) detector. An APTMS-modified Si wafer was used as a background. Spectra were taken at 8° from the surface normal. The measurement was taken at nitrogen atmosphere. The signal to noise ratio has been improved by a smoothing process.

3.2.5.4 X-ray reflectivity (XRR)

X-ray reflectivity (XRR) analysis was performed using a high-resolution diffractometer (ATX/G; Rigaku Corp.; Japan) with an R-AXIS IV two-dimensional (2D) detector. The diffractometer was equipped with Cu Kα radiation (λ= 0.1542 nm) and divergence of 0.01°. The reflective oscillation curves were fitted using software (GIXRR; Rigaku Corp.; Japan). Curve fitting areas were chosen between 0.2° to 3.0°.

3.3 RESULTS AND DISCUSSION

3.3.1 Investigation of Self-assembled Monolayer

Oxidation treatment of hydrogen terminated (NH_4HF_4 treated) Si surface is necessary for the surface modification with silane coupling agent.[39] Generally piranha solution was used for oxidation of Si surface to form silicon oxide layer for that purpose.[40-42] However, piranha can form tens of nanometer thick oxide surfaces, which may affect some of device applications need electrical conductivity.[39] Therefore, in this work the author has examined a simple alternative to a short time (10 sec) plasma oxidation after NH_4HF_4 buffered Oxide Etch (BOE) of Si surface.

Self−assembled monolayer was formed using amine-terminated silane coupling agent (APTMS) on the propanol washed surface and BOE followed by O_2 plasma treated surface with the same modification condition. To investigate the changes of chemical property, a comparison study was done using XPS. In Si 2p XPS fine scan spectra, an aminosilane peak was observed in APTMS modified Si surface near 101.8 eV in both samples (Figure 3.2 C and 3.2 D). However, the peaks of Si-bulk (Si $2p_{3/2}$ and Si $2p_{1/2}$) was shifted towards negative binding energies within the formation of an oxide layer in compare with buffered oxide etch Si surface (Figure 3.2 (A−D)). The highest shifting was occurred in BOE followed by O_2 plasma treated APTMS modified

sample. This shifting might be observed due to the presence of relatively thick/dense oxide layer in BOE followed by O_2 plasma treated APTMS modified sample in compare with propanol washed APTMS modified sample. This phenomenon can also be investigated by calculating the atomic concentration (%) of nitrogen spices among propanol washed and BOE followed by O_2 plasma treated APTMS modified samples. The atomic concentration (%) of nitrogen in BOE followed by O_2 plasma treated sample is increased appx. 70 % (avg.) in compare with the propanol washed Si sample, in respectively, 2.20 and 1.30 %. This result suggests higher SAM density appears in BOE followed by O_2 plasma treated sample compared with propanol washed sample.

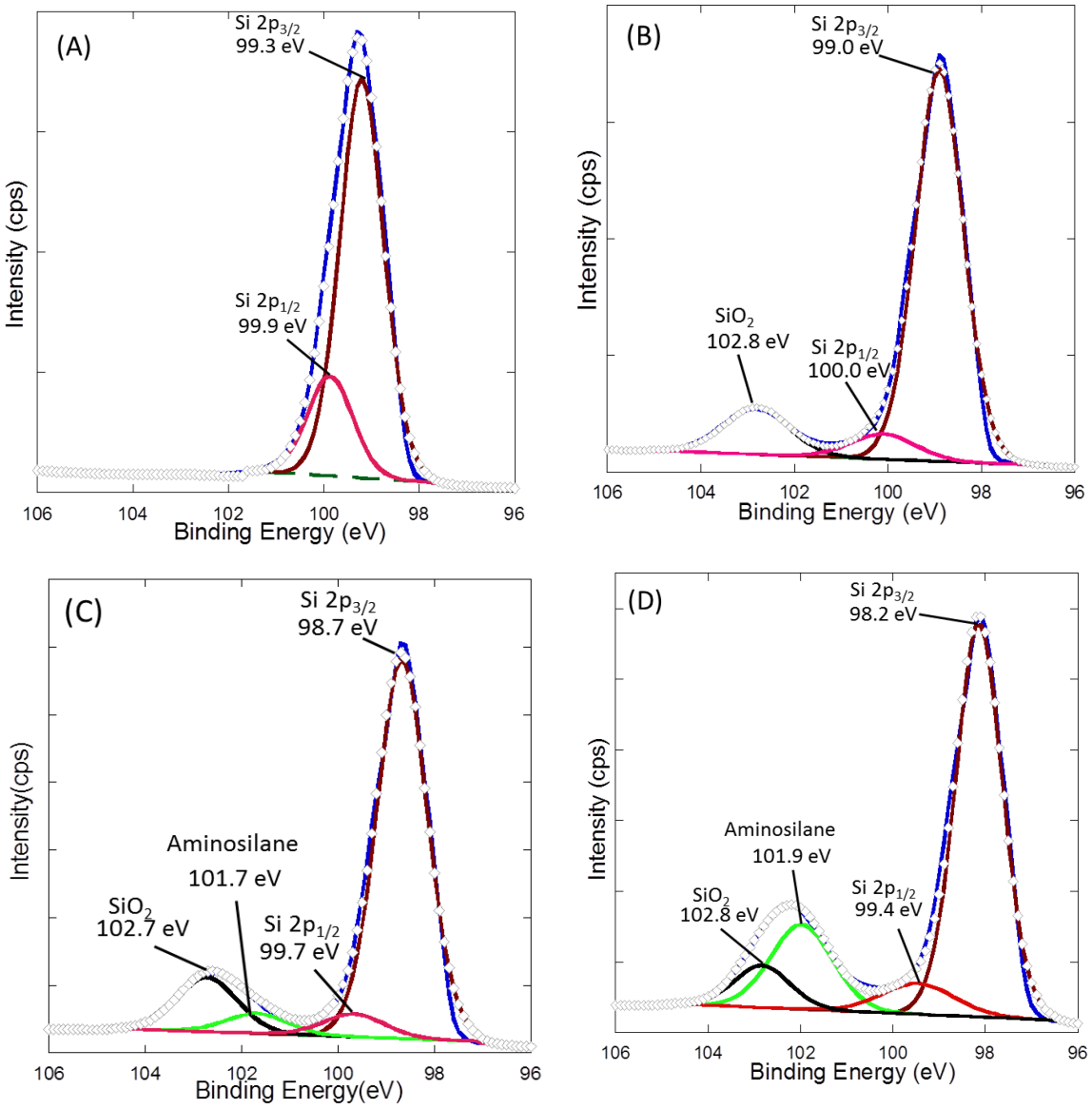

Figure 3.2. XPS fine scan spectra of Si 2p; (A) Buffered oxide etched Si surface (B) Propanol washed Si surface (C) Propanol washed APTMS modified surface (D) BOE followed by O_2 plasma treated APTMS modified Si surface.

3.3.2 Surface Morphology Investigation by AFM

To check the BOE followed by O_2 plasma process does not affect the silicon surface morphology rather than increases self-assembly monolayer density, AFM scans were recorded on 5 × 5 μm^2 area of samples. Figure 3.3 shows the AFM (height) image of propanol washed bare Si surface (control), BOE followed by O_2 plasma treated bare Si surface as well as the comparison of APTMS modified surface in both cases. No significant roughness variation was observed after BOE followed by O_2 plasma treatment of Si surface, indicating constant surface morphology. However, the surface roughness change was observed among propanol washed, and BOE followed by O_2 plasma treated APTMS modified surface, Figure 3.3 (B) and 3.3 (D), respectively.

It is well-established that the plasma-mediated enhancement of hydrophilic behavior on the silicon surface with the formation of OH groups (Si−OH). [43-44] Therefore it is rational to consider that this silanol groups (−OH) can enhance the nucleation density of self-assembled monolayer (APTMS) and increased the surface roughness. This hypothesis is consistent with XPS results discussed above.

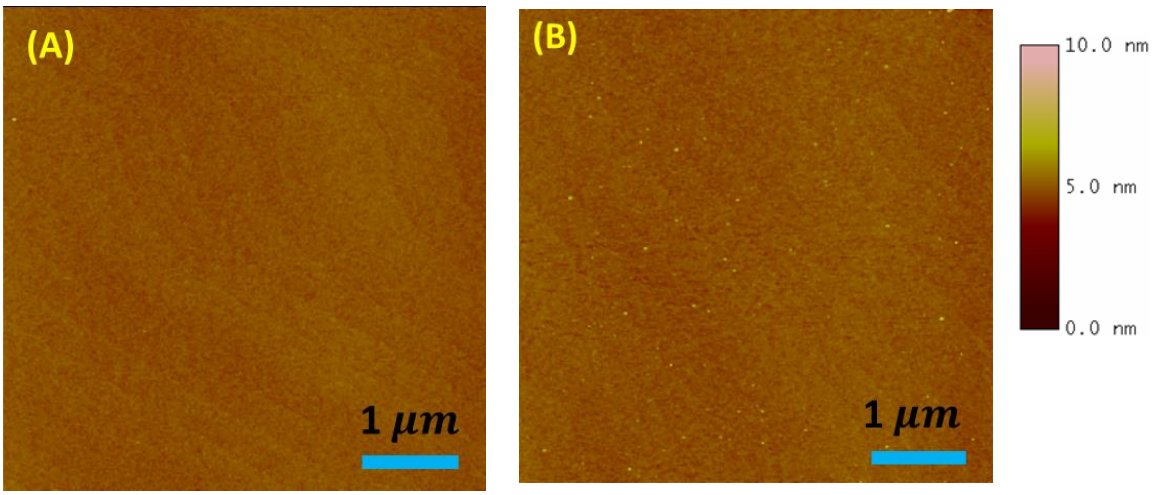

Ra = 1.5 Å, RMS = 1.97 Å

Ra = 1.7 Å, RMS = 2.4 Å

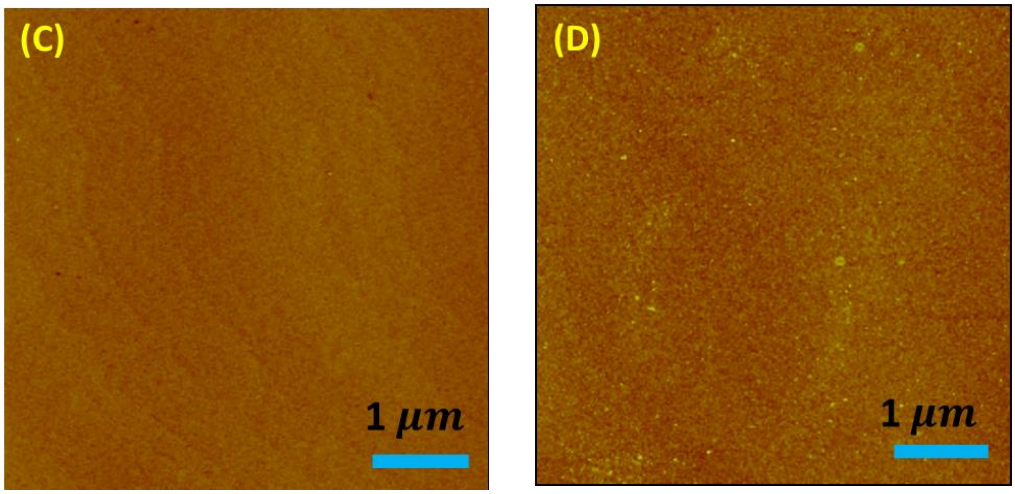

Ra = 1.5 Å, RMS = 1.84 Å

Ra = 2.5 Å, RMS = 3.7 Å

Figure 3.3. AFM image for surface morphology (Top) propanol washed Si (A) bare surface (B) APTMS modified Si surface. (Bottom) BOE followed by O_2 plasma treated Si (C) bare surface (D) APTMS modified Si surface.

3.3.3 Investigation of wetting property of APTMS Modified Surface

From wetting property investigation, it was observed that BOE followed by O_2 plasma treated APTMS modified surface provides higher contact angle ($63 \pm 2°$) in compare with propanol washed APTMS modified surface ($51 \pm 2°$) (Figure 3.4). This suggests the higher nucleation density of APTMS monolayer on BOE followed by O_2 plasma treated Si surface compared with propanol washed Si.

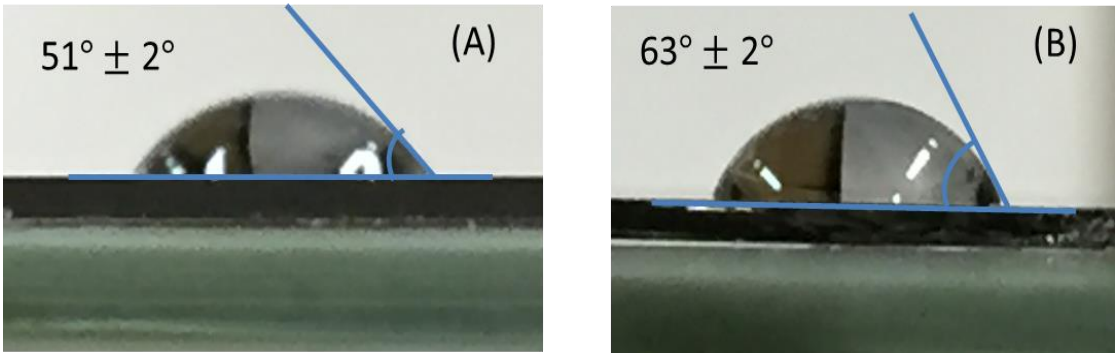

Figure 3.4. Contract angle measurement of (A) propanol washed APTMS modified surface (B) BOE followed by O_2 plasma treated APTMS modified surface, with 10 μl distilled water as an indicator.

Finally, XPS, AFM and contract angle results confirmed the enhancement of APTMS nucleation density in BOE followed by O_2 plasma treated Si surface compared with propanol washed Si surface. The author assumes that APTMS nucleation density was increased due to the enhancement of surface –OH concentration using plasma

mediation.

3.3.4 Investigation of Multilayer Growth

Cross-linked multilayer polyurea thin film deposition was carried out using MLD process by alternating dipping of isocyanate and amine functionalized precursors, starting with an amine terminated surface after APTMS functionalized. Figure 1 demonstrated the chemical structure of the monomers employed in this study as well as schematic drawing of MLD process.

To demonstrate the MLD growth behavior, the thickness of the polyurea films was measured in different number of MLD cycles (Figure 3.5). Film thickness was investigated using AFM techniques. Films were partially scratched and the height difference was evaluated for the film thickness. Thickness was measured at least six different positions of each samples and got an average value. The observed thicknesses of the 10, 20 and 30 MLD cycle films were 4.55 $\pm$ 0.76, 7.06 $\pm$ 0.81 and 9.85 $\pm$ 0.98 nm, respectively (error bars based on standard deviation). This thickness value is nearly matched with the previous study (chapter 2), representing non-uniform growth rate per cycle deposition (average). Even though the non-uniform film growth, film thickness increased with deposition cycles, indicating multilayer deposition was carried out within MLD cycles.

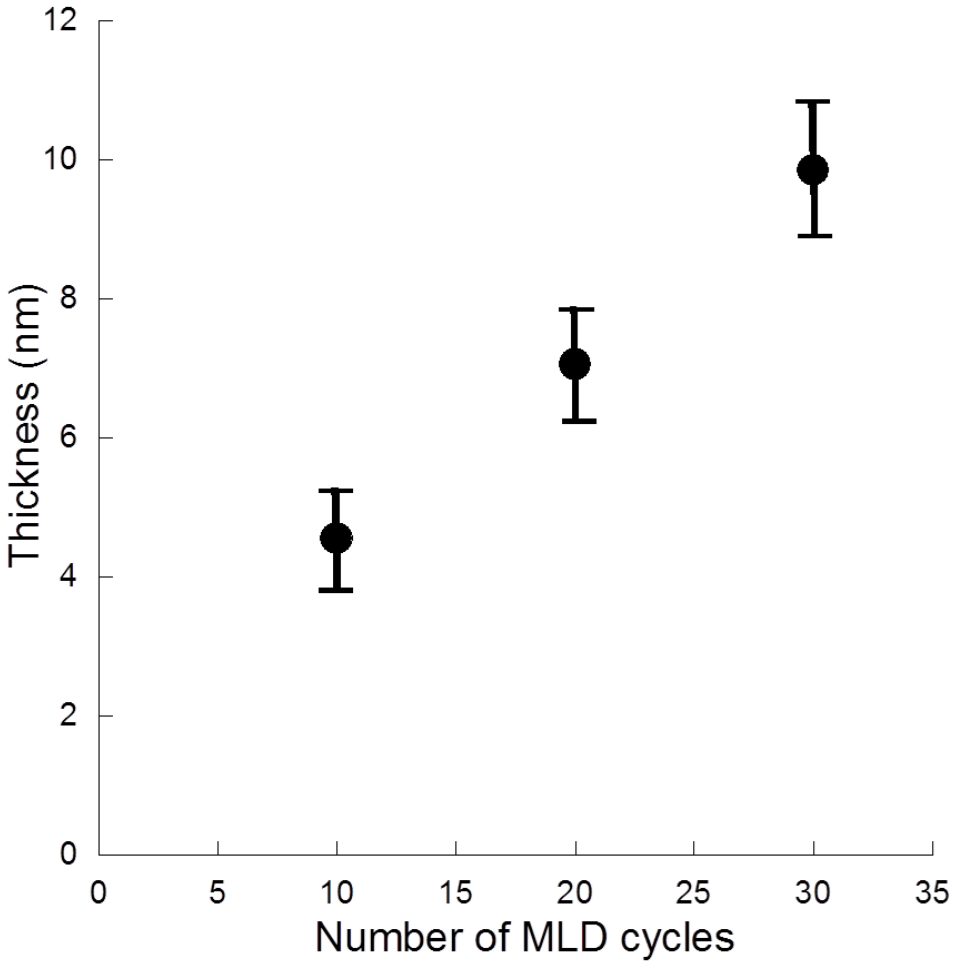

Figure 3.5. Film thickness with error bar as a function of number of MLD cycles for polyurea thin film.

3.3.5 Investigate the Chemical Bond in MLD Thin Films using FT-IR

Polymerization reaction of amine and isocyanate functionalities produced polyurea networks, which is inspected with infrared (IR) spectroscopy. Figure 3.6 presents IR spectra of 10, and 30 MLD cycle films. Characteristic peaks amide I, amide II and asymmetric ν_a(N-C-N) stretching band confirmed the presence of urea linkage into the thin films. Peaks around 1650-1690 cm^{-1} can be assigned as amide I; (C=O) for the urea groups. The band at 1510 cm^{-1} can be assigned to the amide II band with (N–H) bending vibration and the ν_a(N-C-N) asymmetric stretching band attributed at 1300 cm^{-1}. The wavenumbers of these characteristic peaks are consistent with others reported literature of polyurea linkage,[28,29,45,46] and assist to confirm polyurea networks in as-synthesized thin films. In addition, a shoulder-type band near 1535 cm^{-1} and a band near 1603 cm^{-1} are attributable to aromatic ring breathing and aromatic ring stretching, respectively. No isocyanate peak was observed at 2270 cm^{-1}.[28]

Interestingly, a new shoulder-type band at 1713 cm^{-1} for 10 MLD cycles and 1733 cm^{-1} for 30 MLD cycles were appeared in the spectra of the polyurea films. These bands cannot be assigned to the urea linkage because of higher frequency position than the amide I stretching band for urea.[47,48] This band may be attributed due to conversion of isocyanate to trace amount of carbamic acid as an unstable intermediate product which finally decomposed to produce amine and carbon-di-oxide.[45,49]

Another interesting feature was observed in the IR spectra the presence of a very weak band at ~1775 cm^{-1} for 30 MLD cycle film. This peak is resulted due to anhydride formation by the reaction between two intermediate carbamic acids. Blanchard and co-workers have been reported this kind of phenomena in polyurea thin films.[45]

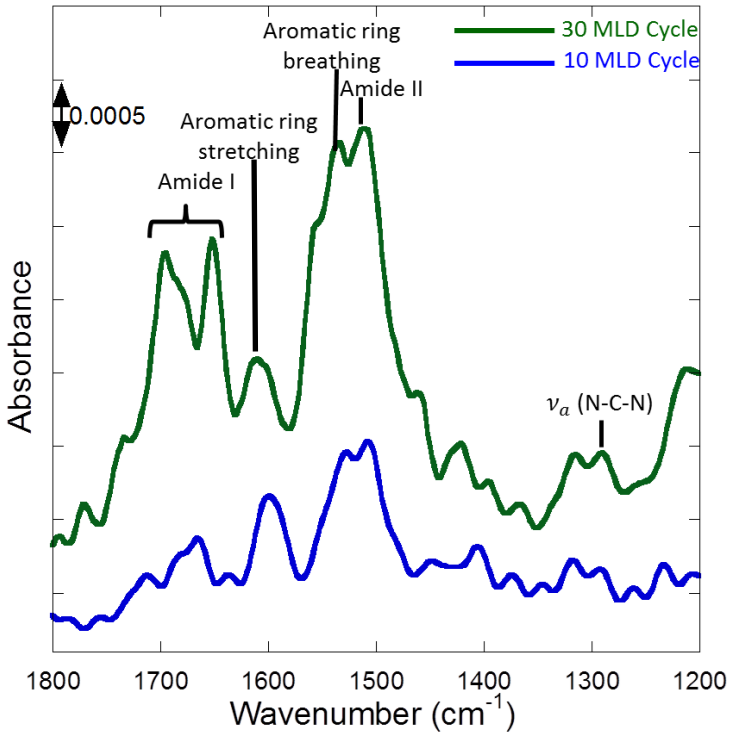

Figure 3.6. IR spectra of 10 and 30 MLD cycle thin films in the IR vibrational region for urea bonds. Spectra were measured under nitrogen atmosphere.

Furthermore, in higher wavenumber region a broad ν(N-H) stretching band appeared at 3270 cm^{-1} (Figure 3.7), which is the evidence in the presence of wide distribution of hydrogen bonds.[50,51]

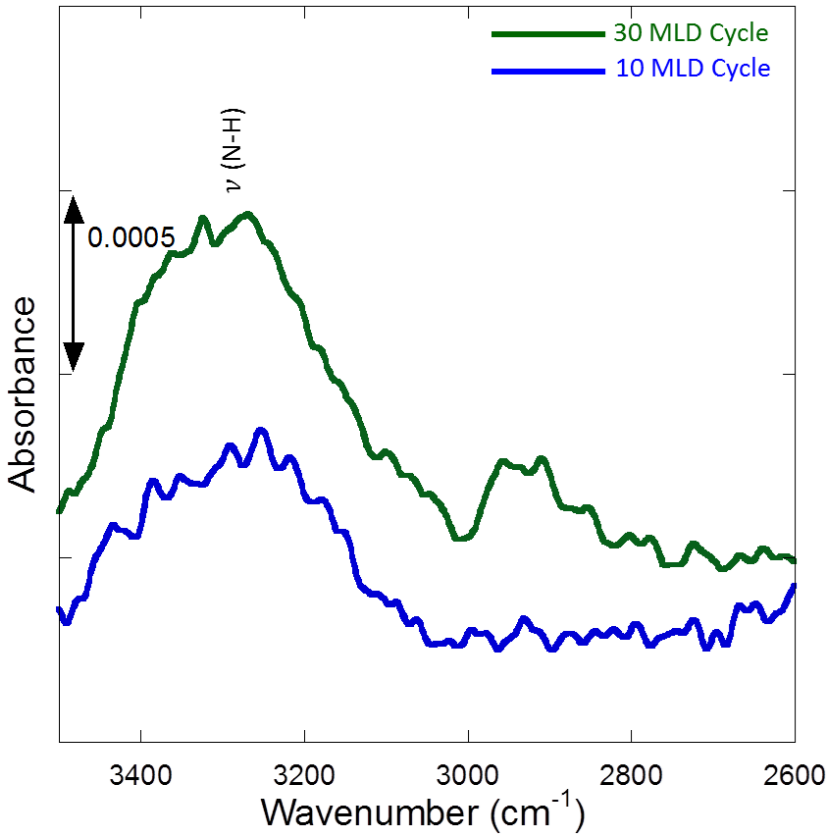

Figure 3.7. IR spectra of 10 and 30 MLD cycle thin films. Spectra were measured in the region 2600-3500 cm^{-1} under nitrogen atmosphere.

3.3.6 Investigation of Atomic Environments and Chemical Bonding using XPS

The atomic environments and chemical bonding into thin films can be discussed using XPS fine scan spectra. Figure 3.8 shows the elemental fine scan spectra of C 1s for 10 and 30 MLD cycle films. At least three peaks are noticeable: peaks at 284.5, 285.9, and 288.6 eV. Because of the binding energy makes an inverse relationship with electron density. Therefore, the peak at 288.6 eV is assigned to the carbonyl carbon of urea linkage; peak at 285.9 eV is corresponded to the combination of alkyl carbon and substituted aromatic carbon linked with urea; the lowest binding energy peak at 284.5 eV resulted from electron-rich aromatic carbon. These assignments of the C 1s fine scan spectra are consistent with other reports of the polyurea and thiourea based literature.[29,30] These assignments confirm the formation of urea bond into thin films. The IR results also reinforce urea bond formation, indicating that the reaction between amine and isocyanate functionalities form polyurea networks via a urea-coupling reaction.

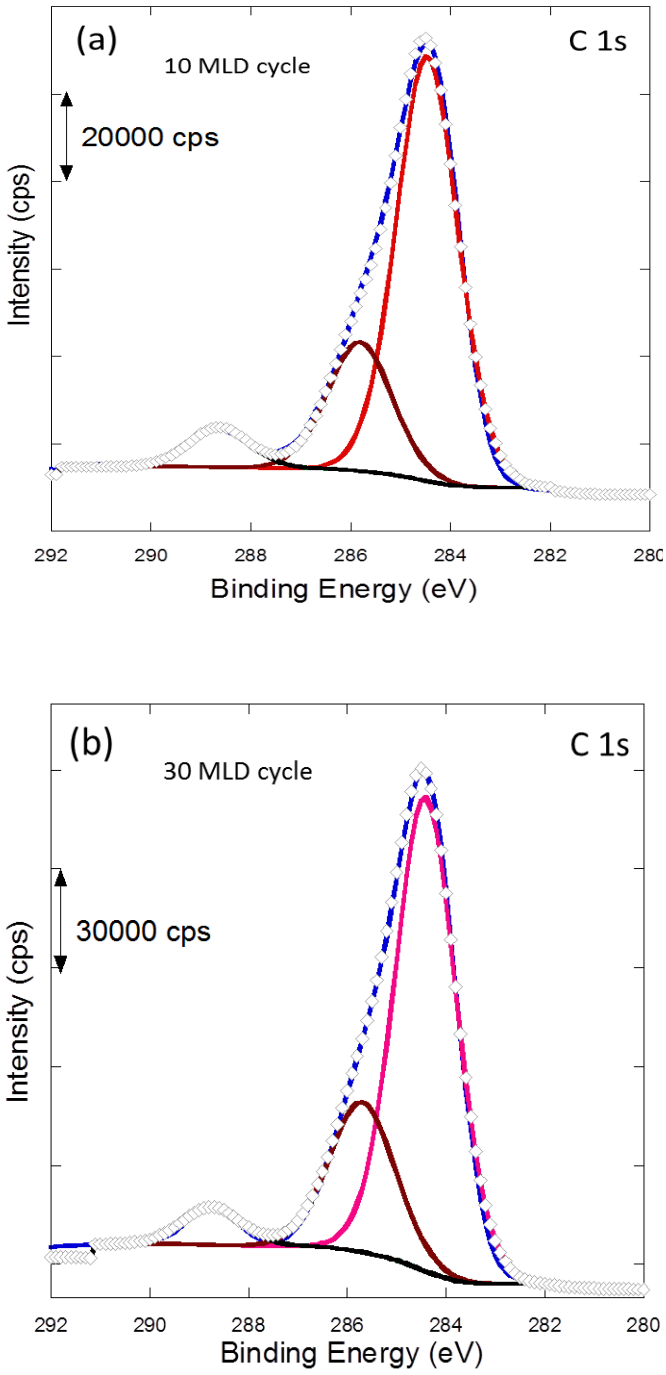

Figure 3.8. XPS fine scan spectra of C 1s (a) 10 and (b) 30 MLD cycle films.

Figure 3.9 depicts N 1s XPS fine scan spectra for 10 and 30 MLD cycle films. The N 1s fine scan also contained three isolated peaks. The major Peak at 399.9 eV corresponds to urea groups,[29,35] peaks near 399.2 eV and 401.3 eV are attributed to nonhydrogen-bonded and hydrogen-bonded free amine groups in polyurea thin films respectively.[52] N 1s for isocyanate was not detected because in presence of any unreacted isocyanate groups are converted easily to amine by exposure to humid air.[35]

Inspection of peak intensity ratio of these three nitrogen species did not provide any significant information. In both films case, it might be happened due to the reaction of maximum number of amine groups with isocyanate groups including the surface double reaction. However, XPS can depth only a few nanometers from the film surface and does not provide total films quantitative information.[53] To get more details about the film internal properties X-ray reflectivity analysis (XRR) was carried out, will be discussed in next.

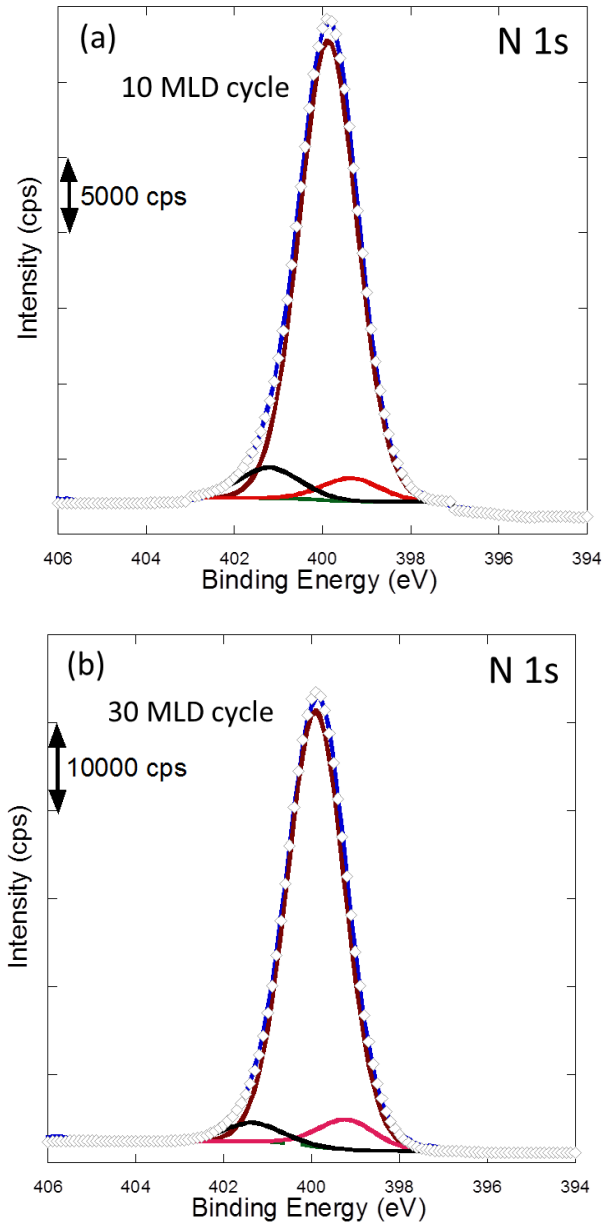

Figure 3.9. XPS fine scan spectra of N 1s in (a) 10, and (b) 30 MLD cycle polyurea thin films.

Finally, FT-IR and XPS studies revealed that sequential deposition of amine and isocyanate functionalities produced polyurea networks as well as thickness profile confirmed the multilayer growth within number of deposition cycles.

3.3.7 Films Mass Density Analysis by XRR

Films internal structural properties within layer growth were investigated using X-ray reflectivity analysis. X-ray reflectivity is a nondestructive probe of surface morphology and structure. XRR has dual advantages of being able to measure electron density variations as well as determine overall layer structure at the surface and inside the film.[54] Figure 3.10 shows the XRR experimental (solid line) and simulation (dotted line) fringes profile of 10 and 30 MLD cycle films. It was observed that the simulation fringe is satisfactory fitted with experimental fringe in case of 10 MLD cycles with a uniform density. However, for 30 MLD cycles film case, the result of satisfactory fit with a uniform density could not be obtained. The best fitting result was observed in non-linear density model rather than linear density model throughout the film depth (Figure 3.11). However, the density around the boundary between the free interface layer and interfacial layer might intergrade. These XRR profile suggest the non-uniform density structure in the thicker film case.

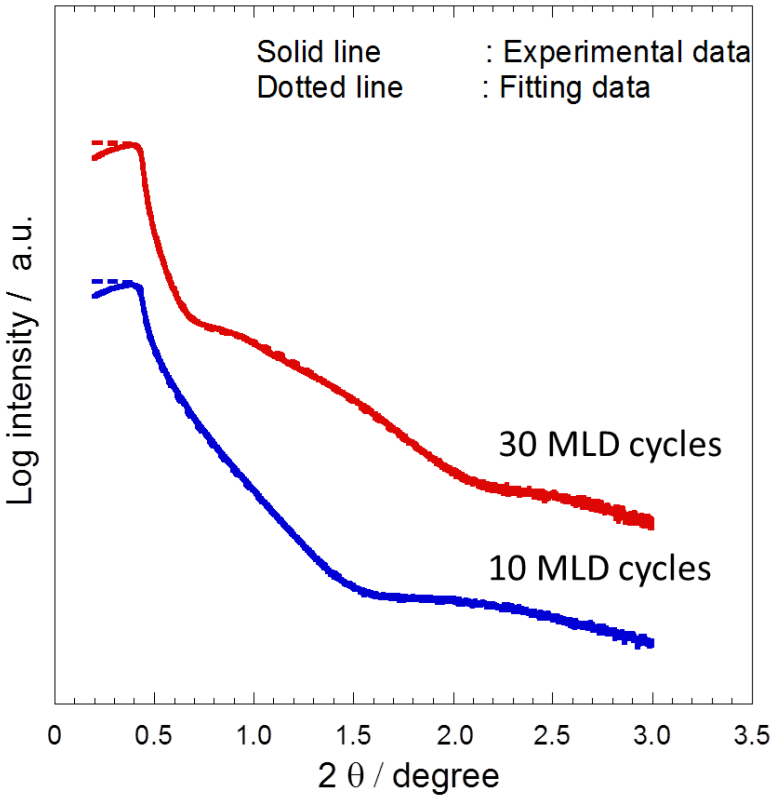

Figure 3.10. XRR profile of 10 and 30 MLD cycle thin films. Solid lines and dotted lines represent experimental and fitting data.

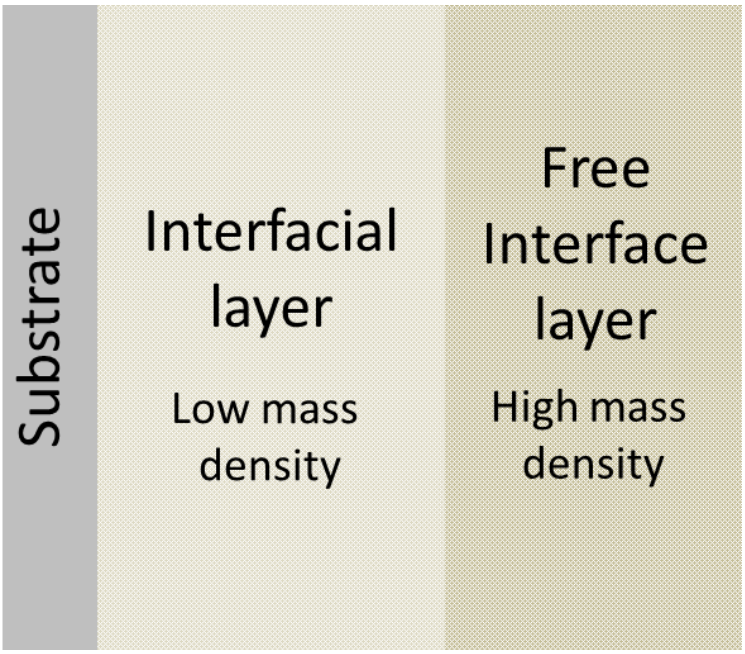

Figure 3.11. Schematic illustration of layer growth with non-linear mass density.

From XRR simulation profile (Figure 3.10), the estimated thickness of 10 and 30 MLD cycle films were found 2.93 and 5.69 nm, respectively. This estimated thickness is lower than the thickness was obtained from AFM measurement (Figure 3.5). This might happen due to the high surface/interface roughness in thin films. Table 3.1 demonstrates the thickness, roughness and mass density values with error bar extracted form XRR profile shown in Figure 3.10.

Table 3.1. Thickness, *d*, mass density, ρ, and roughness, σ of reported layers of 10, and 30 MLD cycle thin films was extracted from the XRR profile shown in Figure 3.10 The statistical errors are shown in each value.

No. of MLD cycles	Layer name	Thickness, *d* (nm)	Mass density, ρ (g/cm^3)	Roughness, σ (nm)
10	Si wafer	0.00	2.33	0.5 ($\sigma_{s/f}$)
	Film	2.93 $\pm$ 0.01	0.84 $\pm$ 0.02	0.76 $\pm$ 0.03 ($\sigma_{f/i}$)
30	Si wafer	0.00	2.33	0.5 ($\sigma_{s/f}$)
	Film	4.10 $\pm$ 0.02 (int.)	0.98 $\pm$ 0.007 (int.)	0.94 $\pm$ 0.21 (σ_{int})
		1.58 $\pm$ 0.06 (f/i)	1.58 $\pm$ 0.02 (f/i)	2.6 $\pm$ 0.04 ($\sigma_{f/i}$)

$\boldsymbol{\sigma}_{s/f}$ denotes roughness of substrate/film interface, $\boldsymbol{\sigma}_{f/i}$ denotes roughness of free interface and $\boldsymbol{\sigma}_{int}$ represent interfacial roughness of different densities layers into thin films.

Films mass density extracted from the XRR simulation fringe profiles (Figure 3.10). XRR mass density profile (Figure 3.12) showed that the estimated film mass density of 10 MLD cycle film is constant throughout the film depth. However, for 30 MLD cycles, the mass density is not uniform throughout the range of film depth. The mass density of film proximate to the surface (interfacial layer (int.)) is ca. 60% lower than the mass density of film extending away from the surface (free interface (f/i) region), 0.98 g/cm^3 to 1.58 g/cm^3.

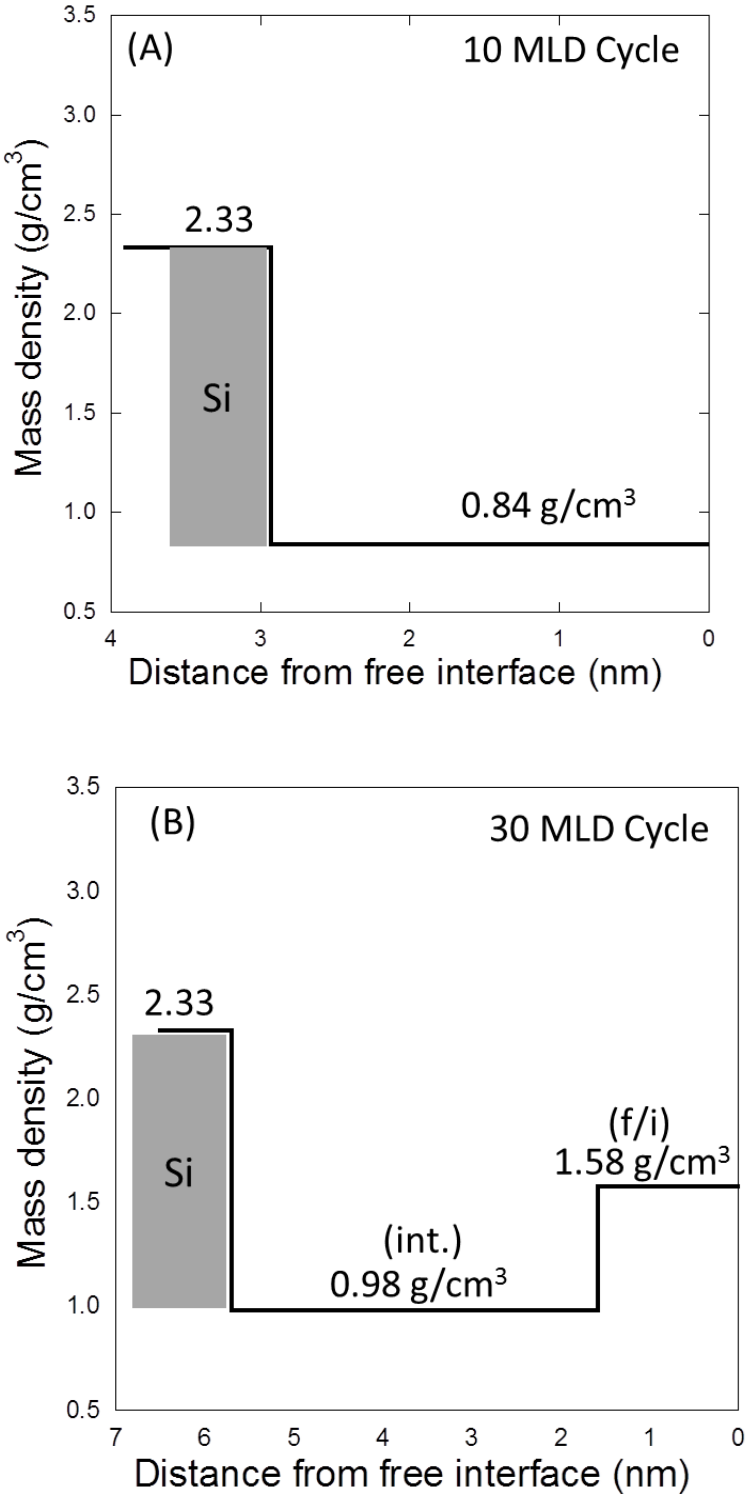

Figure 3.12. Film mass density (g/cm^3) profile of simulated model for (A) 10 MLD cycle, and (B) 30 MLD MLD cycle films as a function of distance from the free

interface.

This large variation of mass densities among layers proximate to the surface and extending away to the surface might be observed due to the influence of surface activation after plasma treatment. This plasma treatment enhanced the hydrophilic behavior of the silicon surface with the formation of silanol groups (Si-OH). This high concentration of surface silanol groups (Si-OH) increased the surface attachment of the forming siloxane group, in term of self-assembled monolayer formation (APTMS monolayer).[8] In this case, the distance between two amine active sites in self-assembled monolayer might be too closed to each other. This conjugated active sites proceed a significant numbers of double reaction between initial deposited one 1,3-PDI molecules and two surface attached amine groups of APTMS species (Figure 3.1).[17] This "double" reaction would eliminate active isocyanate functionalities and hinder further coupling reaction with amine functionalized TAPM molecules, ultimately reduced the film packing density. In addition, the significant number of these double reactions increased the distance between the isocyanate active sites for extending molecular networks with further deposited TAPM monomers. However, it was observed that film mass density increased with increasing number of deposition cycles. This phenomenon resulted due to the presence of multiple reactive sites of multifunctional building block (TAPM),

which provide reactive sites and laterally extended the molecular networks and directed closer to each other. Due to the closer approach of the molecular networks, the intermolecular interactions, as well as the cross-linking properties were increased. This result suggests that not only the degree of cross-linking but also the particular monomers combination are responsible for non-linear mass densities into cross-linked multilayer thin film.

3.4 CONCLUSIONS

Thin film with polyurea molecular networks was synthesized using solution processable MLD techniques over chemical etch followed by O_2 plasma-mediated silicon surface. This plasma-mediated process enhanced surface hydrophilicity with increasing surface OH concentration. XPS, AFM and contact angle analysis revealed that enhancement of surface OH group (Si−OH) make dense packed self-assembled monolayers (SAMs), which are formed prior to layer deposition. The formation of polyurea networks in multilayer thin films was confirmed using FT-IR and XPS investigations. However, a larger density variation was observed among layers sited near to the substrate surface and extending away to the substrate surface. This variation might results due to the formation of large number of double reaction between initial deposited bifunctional isocyanate monomer and APTMS modified NH_2-terminated surface.

REFERENCES

(1) Wolkow, R. A. Controlled Molecular Adsorption on Silicon: Laying a Foundation for Molecular Devices. *Annu. Rev. Phys. Chem.* **1999**, *50*, 413-441.

(2) Hamers, R. J.; Coulter, S. K.; Ellison, M. D.; Hovis, J. S.; Padowitz, D. F.; Schwartz, M. P.; Greenlief, C. M.; Russell, J. N. Cycloaddition Chemistry of Organic Molecules with Semiconductor Surfaces. *Acc. Chem. Res.* **2000**, *33*, 617-624.

(3) Bent, S. F. Organic Functionalization of Group IV Semiconductor Surfaces: Principles, Examples, Applications, and Prospects. *Surf. Sci.* **2002**, *500*, 879-903.

(4) Bent, S. F. Attaching Organic Layers to Semiconductor Surfaces. *J. Phys. Chem. B* **2002**, *106*, 2830-2842.

(5) Kim, A.; Choi, D. S.; Lee, J. Y.; Kim, S. Adsorption and Thermal Stability of Ethylene on Ge(100). *J. Phys. Chem. B* **2004**, *108*, 3256-3261.

(6) Blodgett. K. B. Films Built by Depositing Successive Monomolecular Layers on a Solid Surface. *J. Am. Chem. Soc.* **1935**, *57*, 1007-1022.

(7) Langmuir, I.; Schaefer, V. J. Monolayers and Multilayers of Chlorophyll. *J. Am. Chem. Soc.* **1937**, *59*, 2075-2076.

(8) Ulman, A. Formation and Structure of Self-Assembled Monolayer, *Chem. Rev.* 1996, *96*, 1533-1554.

(9) Ulman, A. *An Introduction to Ultrathin Organic Films from Langmuir–Blodgett to Self-Assembly*; Academic Press: San Diego, CA, **1991**.

(10) Kubono, A.; Yuasa, N; Shao, H.-L.; Umemoto, S.; Okui, N. In-situ Study on Alternating Vapor Deposition Polymerization of Alkyl Polyamide with Normal Molecular Orientation. *Thin Solid Films* **1996**, *289*, 107-111.

(11) Du, Y.; George, S. M. Molecular Layer Deposition of Nylon 66 Films Examined Using in situ FTIR Spectroscopy. *J. Phys. Chem. C* **2007**, *111*, 8509-8517.

(12) Kim, A.; Filler, M. A.; Kim, S.; Bent, S. F. Layer-by-Layer Growth on Ge (100) via Spontaneous Urea Coupling Reactions. *J. Am. Chem. Soc.* **2005**, *127*, 6123-6132.

(13) George, S. M. Atomic Layer Deposition: An Overview. *Chem. Rev*. **2009**, *110*, 111-131.

(14) Ritala, M.; Leskela, M. Atomic Layer Deposition. In Handbook of Thin Film Materials. Nalwa, H. S., Ed.; Academic Press; San Diego, **2002**; Vol.1.

(15) Johnson, R. W.; Hultqvist, A.; Bent, S. F. A Brief Review of Atomic Layer Deposition: from Fundamental to Applications. *Mater. Today*, **2014**, *17 (5)*, 236-246.

(16) Shao, H.; Umemoto, S.; Kikutani, T. Okui, N. Layer-by-Layer Polycondensation of Nylon 66 by Alternating Vapour Deposition Polymerization. *Polymer* **1997**, *38*, 459-462.

(17) Adamczyk, N. M.; Dameron, A. A.; George, S. M. Molecular Layer Deposition of Poly(p-phenyleneterephthalamide) Films Using Terephthaloyl Chloride and p-Phenylenediamine. *Langmuir* **2008**, *24*, 2081-2089.

(18) Nagai, A.; Shao, H.; Umemoto, S.; Kikutani, T. Okui, N. Quadruple Aliphatic Polyamide Systems Prepared by a Layer-by-Layer Alternating Vapor Deposition Method, *High perform. Polym.* **2001**, *13*, S169-S179.

(19) Peng, Q.; Efimenko, K.; Genzer, J.; Parsons, G. N. Oligomer Orientation in Vapor-Molecular-Layer-Deposited Alkyl Aromatic Polyamide Films, *Langmuir* **2013**, *28*, 10468-10470.

(20) Yoshimura, T.; Tatsuura, S.; Sotoyama, W. Polymer Films Formed with Monolayer Growth Steps by Molecular Layer Deposition. *Appl. Phys. Lett.* **1991**, *59*, 482-484.

(21) Bizer, T.; Richardson, N. V. Demonstration of an Imide Coupling Reaction on a Si(100)-2 × 1 Surface by Molecular Layer Deposition, *Appl. Phys. Lett.* **1997**, *71*, 662-664.

(22) Haq, S.; Richardson N. V. Organic Beam Epitaxy Using Controlled PMDA−ODA Coupling Reactions on Cu{110}. *J. Phys. Chem. B* **1999**, *71*, 5256-5265.

(23) Yoshida, S.; Ono, T.; Esashi, M. Local Electrical Modification of a Conductivity-Switching Polyimide Film Formed by Molecular Layer Deposition. *Nanotechnology* **2011**, *22*, 335302.

(24) Prasittichai, C.; Zhou, H.; Bent, S. F. Area Selective Molecular Layer Deposition of Polyurea Films. *ACS Appl. Mater. Interfaces* **2013**, *5*, 13391-13396.

(25) Zhou, H.; Blackwell, J. M.; Lee, H.-B.-R., Bent, S. F. Highly Sensetive, Patternable Organic Films at the Nanoscale made by Bottom-Up Assembly, *ACS Appl. Mater. Interfaces* **2013**, *5*, 3691-3696.

(26) Zhou, H.; Bent. S. F. Molecular Layer Deposition of Functional Thin Films for Advanced Lithographic Patterning. *ACS Appl. Mater. Interfaces* **2011**, *3*, 505-511.

(27) Zhou, H.; Toney, M. F.; Bent, S. F. Cross-Linked Ultrathin Polyurea Films via Molecular Layer Deposition. *Macromolecules* **2013**, *46*, 5638-5643.

(28) Kim, A.; Filler, M. A.; Kim, S.; Bent, S. F. Layer-by-Layer Growth on Ge (100) via Spontaneous Urea Coupling Reactions. *J. Am. Chem. Soc.* **2005**, *127*, 6123-6132.

(29) Loscutoff, P. W.; Zhou, H.; Clendenning, S. B.; Bent, S. F. Formation of Organic Nanoscale Laminates and Blends by Molecular Layer Deposition. *ACS Nano* **2010**, *4*, 331-341.

(30) Loscutoff, P. W.; Lee, H. B. R.; Bent S. F. Deposition of Ultrathin Polythiourea Films by Molecular Layer Deposition. *Chem. Mater*. **2010**, *22*, 5563-5569.

(31) Ivanova, Y. V.; Maydannik, P. S.; Cameron, D. C. Molecular Layer Deposition of Polyethylene Terephthalate Thin Film. *J. Vac. Sci. Technol., A* **2012**, *30*, 01A121 (1-5).

(32) Yoshimura, T.; Kudo, Y. Monomolecular-Step Polymer Wire Growth from Seed Core Molecules by the Carrier-Gas-Type Molecular Layer Deposition, *Appl. Phys. Express*. **2009**, *2*, 015502 (1-3).

(33) Yoshimura, T.; Ito, S.; Nakayama, T.; Matsumoto, K. Orientation-controlled Molecule-by-Molecule Polymer Wire Growth by the Carrier-gas Type Organic Chemical Vapor Deposition and the Molecular Layer Deposition, *Appl. Phys. Lett.***2007**, *91*, 033103 (1-3).

(34) Miyamae, T.; Tsukagoshi, K.; Matsuoka, O.; Yamamoto, S.; Nozoye, H. Preparation of Polyimide-Polyamide Random-Copolymer Thin Film by Sequential Vapor Deposition Polymerization. *Jpn. J. Appl. Phys., Part 1*, **2002**, *41*, 746-748.

(35) Kim, M.; Byeon, M.; Bae, J-S.; Moon, S. Y.; Yu, G.; Shin. K.; Basarir, F.; Yoon, T. H.; Park, J-W. Preparation of Ultrathin Films of Molecular Networks through Layer-by-Layer Cross-Linking Polymerization of Tetrafunctional Monomers. *Macromolecules* **2011**, *44*, 7092-7095.

(36) Qian, H.; Li, S.; Zheng, J.; Zhang, S. Ultrathin Films of Organic Networks as Nanofiltration Membranes via Solution-Based Molecular Layer Deposition. *Langmuir* **2012**, *28*, 17803-17810.

(37) Puuruuen, R. L. Correlation between the Growth-per-cycle and the Surface Hydroxyl Group Concentration in the Atomic Layer Deposition of Aluminum Oxide from Trimethylaluminum and Water. *Appl. Sur. Sci.* **2005**, *245*, 6-10.

(38) Puuruuen, R. L. Surface Chemistry of Atomic Layer Deposition: A case Study for the Trimethylaluminum/Water Process. *J. Appl. Phys.* **2005**, *97*, 121301-121352.

(39) Tanaka, M.; Sawaguchi, T.; Kuwahara, M.; Niwa, O. Surface Modification of Silicon Oxide with Trialkoxysilanes towards Close-Packed Monolayer Formation. *Langmuir* **2013**, *29*, 6361-6368.

(40) Zhang, F.; Srinivasan, M. P. Self-Assembled Molecular Films of Aminosilanes and Their Immobilization Capacities. *Langmuir* **2004**, *20*, 2309-2341.

(41) Howarter, J. A.; Youngblood, J. P. Optimization of Silica Silanization by 3-Aminopropyltriethoxysilane, *Langmuir* **2006**, *22*, 11142-11147.

(42) Pasternack, R. M. Amy, S. R.; Chabal, Y. J. Attachment of 3-(aminopropyl)trietoxysilane on Silicon Oxide Surface: Dependence on Solution Temperature. *Langmuir* **2008**, *24*, 12963-12971.

(43) Kaya, S.; Rajan, P.; Dasari, H.; Ingram, D. C.; Jadwisienczak, W.; Rahman, F. A Systematic Study of Plasma Activation of Silicon Surfaces for Self Assembly. *ACS appl. Mater. Interfaces* **2015**, *7*, 25024-25031.

(44) Alam, A. U.; Howlader, M. M. R.; Deen, M. J. Oxygen Plasma and Humidity Dependent Surface Analysis of Silicon, Silicon Dioxide and Glass for Direct Wafer Bonding. *ECS J. Solid State Sci. Technol.* **2013**, *2(12)*, 515-523.

(45) Kohli, P.; Blanchard, G. J. Applying Polymer Chemistry to Interfaces: Layer-by-Layer and Spontaneous Growth of Covalently Bound Multilayers. *Langmuir* **2000**, *16*, 4655-4661.

(46) Coleman, M. M.; Sobkowiak, M.; Pehlert, G. J.; Painter, P. C.; Iqbal, T. Infrared Temperature Studies of a Simple Polyurea. *Macromol. Chem. Phys.* **1997**, *198*, 117-136.

(47) Vien, D. L.; Colthup, N. B.; Fateley, W. G.; Grasselli, J. G. The Handbook of Infrared and Raman Characteristic Frequencies for Organic Molecules, Academic Press; London. **1991**.

(48) Pouchert, C. J. The Aldrich Library for Infrared Spectra; The Aldrich Chemical Co.; Milwaukee, WI, **1970**.

(49) Ege, S. N. Organic Chemistry, Heath, D. C. and Co.: Lexington, **1989**.

(50) Coleman, M. M.; Skrovanek, D. J.; Howe, S. E.; Painter, P. C. On the Validity of a Commonly Employed Infrared Procedure used to Determine Thermodynamic Parameters Associated with Hydrogen Bonding in Polymers. *Macromolecules* **1985,** *18*, 299-301.

(51) Coleman, M. M.; Lee, K. H.; Skrovanek, D. J.; Painter, P. C. Hydrogen Bonding in Polymers. 4. Infrared Temperature Studies of a Simple Polyurethane. *Macromolecules* **1986,** *19*, 2149-2157.

(52) Graf, N.; Yegen, E.; Gross, T.; Lippitz, A.; Weigel, W.; Krakert, S.; Terfort, A.; Unger, W. E. S. XPS and NEXAFS Studies of Aliphatic and Aromatic Amine Species on Functionalized Surfaces. *Surf. Sci.* **2009**, *603*, 2849-2860.

(53) Riviere, J. C.; Myhra, S. Handbook of Surface and Interface Analysis Methods for Problem-Solving, CRC press, 2nd Ed. **2009**.

(54) Brian, C.; Yushan, S.; Satyendra, K. X-Ray Reflectivity Study of Interface Roughness, Structure, and Morphology of Alignment Layers and Thin Liquid-Crystal Films. *Phys. Rev. E* **1995**, *51(1)*, 526-535.

Chapter 4

CONCLUSIONS AND PROSPECTS

Molecular layer deposition (MLD) has been shown to be a powerful technique for fine-tuning film properties by depositing on demand monomers combination. Optical and mechanical properties have been successfully tuned by varying the numbers of the deposition cycle. Moreover, post-modification treatments of films using residing organic functionalities within the multilayer nanostructure enable the design and fabrication of tailored multifunctional assembly and to expand the application range of MLD thin films. Therefore, to develop thin film with MLD technique is need to deal with several factors such as substrate surface properties, self-assembled monolayer, monomers symmetrical combination, as well as optimized reaction condition and so on.

This present study was conducted to develop a new class of layer assembled nanoscale organic multilayer thin film using MLD technique. In this research, I focused to fabricate 3D molecular networks based functional organic thin films on a smooth surface of silicon wafer using solution based molecular layer deposition technique. Several characteristics techniques have been employed to confirm the multilayer growth, expected covalent networks as well as explored the film physical and chemical properties. These results showed that MLD technique provided relatively dense-packed

multilayer thin film in propanol washed Si surface (chapter 2). However, a linear mass density was not observed within number of layers deposition. This may happen due to the different cross-linking state of molecular networks in different distance from the substrate surface. This propensity of cross-linking among molecular networks proximate to the substrate surface and extending away from the substrate surface can be considered with variable intermolecular interactions. However, with increasing the deposition cycles, improvement of molecular ordering was observed. I assume that the improvement of film mass density may relate to the improvement of the structural periodicity.

In contrast, deposition of organic thin film with same monomers combination, and identical synthesis condition on buffered oxide etch and followed by oxygen plasma treated Si surface, also demonstrated variable mass densities behavior (chapter 3). However, a larger density variation was observed among layers near to the surface and extending away from the surface. This phenomenon might be related to the enhancement of hydrophilic nature of Si surface (Si−OH) after plasma-mediation. Prior to the MLD film growth, the substrate surface was chemically modified using organosilane precursors. The high concentration of surface OH groups increased the surface attachments of the forming siloxane (Si−O−Si) groups, in terms of

self-assembled monolayer formation; introduced dense-packed self-assembled monolayer. It is considered that this high nucleation density of self-assembled monolayer influenced layer assembled multilayer film properties.

This variable mass densities phenomenon may provide an opportunity to develop ion separation membrane with a wide range of ion selectivity using only one monomers combination. In conventional case, it is not possible. Furthermore, by utilizing multi-functionalities in molecular networks, it may possible to conduct the post-modification step by using different organic and inorganic species and make application diversity.

In conventional or vacuum based MLD technique rely on limited numbers of linking chemistry and the number of applied precursors is inadequate. Taking the advantage of solvent media, this solution based MLD can offer a wide range of linking chemistry as well as may apply an unprecedented number of organic precursors. Therefore, it is expected that this research will be encouraged for further investigation to the development of different types of molecular networks based organic thin films using solution based molecular layer deposition technique.

Since this solution based MLD technique is an infancy stage that still faces several problems. One of the major problem the “capped” reaction on the surface which

is generally formed by using homo-bifunctional monomers; eliminated the necessary surface active sites for MLD growth. This problem might overcome by using mask functionality. Thus one end of the precursor can react with surface and the other functional group remaining unchanged. After this self-saturation reaction, the masked functional groups will be unmasked or activated using a chemical reaction, thermal annealing or light exposure. Once the hidden functionality has been exposed, this new functionality is ready to react with the next incoming organic precursor. This approach of mask functionalities may improve the implementation of solution based MLD.

Finally, I anticipate that molecular networks based nanoscale MLD thin films have very encouragement prospects and enable to use a wide range of applications. I hope that this present finding will make a significant contribution to surface and interface science and to the development of varieties of molecular scale functional multilayer thin films for diverse application fields.

Acknowledgments

This presented thesis is author's studies for doctoral program, School of Material Science, Japan Advanced Institute of Science and Technology from October' 2013 to September' 2016.

This study could not able to be completed without the help and contribution of many peoples. I wish to express my earnest thanks to my PhD supervisor Associate Professor Dr. Yuki Nagao, Japan Advanced Institute of Science and Technology for his valuable discussions, appropriate advices, and encouragement to lead me ahead with my research. I learned from him, how to pursue a world class research as well as how to face difficulties in scientific research.

I also deeply acknowledge Prof. Noriyoshi Matsumi, School of Material Science, Japan Advanced Institute of Science and Technology for being my second supervisor, I learned from him many helpful things for my research.

I express my thanks to Dr. Tsutomu Hamada, Associated professor, School of Material Science, Japan Advanced Institute of Science and Technology for considering me in my minor research project in his lab. His suggestive discussion and encouragement helped me to get knowledge about a wonderful arena of science bio-physics.

I am grateful to Dr. Shusaku Nagano, Associated professor and Dr. Mitsuo Hara, Assistant Professor in Nagoya University for their kind cooperation and discussion in technical issues for X-ray reflectivity and grazing incidence small angle X-ray scattering (GI-SAXS) measurements.

I express my sincere gratitude to the former and current members of Nagao laboratory for their support and sharing with me studying time in the lab as well as try to make my Japan life easier and comfortable.

Finally, I would like to thank my family members for their endless love, sacrificing and encouragement.

Md. Abu Rashed

September’2016

ACHIEVEMENTS

Paper Published

1. **Md. A. Rashed**, Salinthip Laokroekkiat, Mitsuo Hara, Shusaku Nagano and Yuki Nagao "Fabrication and Characterization of Cross-Linked Organic Thin Films with Non-linear Mass Densities" *Langmuir*, Vol. 32, pp. 5917-5924, **2016**.
2. Mohammad A. Hasnat, Jamil A. Safwan, **M. A. Rashed**, Zidnia Rahman, Mohammad A. Rahman, Yuki Nagao, M. Abdullah Asiri "Inverse Effects of Supporting Electrolytes on the Electrocatalytic Nitrate Reduction Activities in a Pt|Nafion|Pt-Cu-type Reactor Assembly" *RSC Advances*, Vol. 6, pp. 11609-11617, **2016**.

Selected Conference Presentations

1. Md. Abu RASHED, Mitsuo HARA, Shusaku NAGANO and Yuki NAGAO "Synthesis and Characterization of Ultrathin Films of 3-D Molecular Networks through Molecular Layer Deposition" 96 CSJ Annual Meeting, 24-27 March, **2016**, Kyoto, Japan.
2. Md. Abu RASHED, Mitsuo HARA, Shusaku NAGANO and Yuki NAGAO "Synthesis of Multilayer Organic Thin Film with Variable Densities by Layer-by-Layer (LbL) Deposition Technique" 251st ACS National Meeting & Exposition, 13-17 March' **2016**, San Diego, CA, USA.
3. M. A. Rashed, M. Hara, S. Nagano and Y. Nagao "Synthesis of Polyurea Thin Film with Non-linear Densities Using Sequential Layer Wet Deposition Technique" 25th Annual Meeting of MRS-Japan 2015, 8-10 December' **2015**, Yokohama, Japan.

4. Md. A. Rashed, Salinthip Laokroekkiat, Matsuo Hara, Shusaku Nagano and Yuki Nagao "Synthesis of Surface Bound 3-D Organic Network using Layer-by-Layer (LBL) Assembled Techniques" The 65th Japan Society of Co-ordination Chemistry Symposium (JSCC), 21-23 September' **2015**, Nara, Japan.
5. M. Abu RASHED, Mitsuo HARA, Shusaku NAGANO and Yuki NAGAO "Synthesis of Covalent Bonded Multilayer Thin Film with Non-linear Densities" 5th Molecular Materials Meeting (M3) @Singapore **2015**, 3-5 August, 2015, Singapore.
6. M. A. Rashed, S. Laokroekkiat, M. Hara, S. Nagano and Y. Nagao "Fabrication of Covalently Bonded Multilayer Organic Thin Film by Molecular Layer Deposition" 64th Society of Polymer Science Japan Annual Meeting, 2015, 27-29 May' **2015**, Sapporo, Japan.

Abstract of Subtheme Research

Ion channels have many district features that make them interest for biophysical and physiological applications. Prussian blue (PB) nanoparticles covered with long alkyl chain oleylamine are capable of forming nano-pores in a lipid bilayer membrane. Using fluorescence sensitive dye, “pyranine” we observed a dramatic change of fluorescence spectra at 511 nm emission wavelength along with changes pH in PB embedded lipid bilayer suspension and control DOPC suspension. The fluorescence intensity difference between control DOPC and PB embedded DOPC was carried out might due to transportation of proton from the inner aqueous volume to the outer aqueous volume across lipid bilayer membrane using PB nanopores.

Keywords: ion channel, lipid bilayer, Pyranine, Fluorescence, nano-channels